Zootaxa 3364: 1–78 (2012)
www.mapress.com/zootaxa/

Monograph

ISSN 1175-5326 (print edition)
ZOOTAXA
ISSN 1175-5334 (online edition)

ZOOTAXA

3364

Molecular phylogenetics of stream treefrogs of the *Hyloscirtus larinopygion* group (Anura: Hylidae), and description of two new species from Ecuador

LUIS A. COLOMA[1], SOFÍA CARVAJAL-ENDARA[1], JUAN F. DUEÑAS[1], ARTURO PAREDES-RECALDE[2], MANUEL MORALES-MITE[3], DIEGO ALMEIDA-REINOSO[1], ELICIO E. TAPIA[1], CARL R. HUTTER[4], EDUARDO TORAL[1], & JUAN M. GUAYASAMIN[5]

[1]*Centro Jambatu de Investigación y Conservación de Anfibios, Fundación Otonga, Geovanni Farina 566 y Baltra, San Rafael, Quito, Ecuador. lcoloma@otonga.org, sofia.carvajal@gmail.com, juanferdu@yahoo.com, diegoalmeida@otonga.org, eliciotapia@otonga.org, eduardotoral@yahoo.com*

[2]*Universidad San Francisco de Quito, Colegio de Ciencias Biológicas y Ambientales, Laboratorio de Zoología Terrestre. Campus Cumbayá USFQ, Vía Interoceánica y Diego de Robles. Casilla Postal 17-1200-841. Quito, Ecuador. aparedes@usfq.edu.ec*

[3]*Museo Ecuatoriano de Ciencias Naturales, División de Herpetología, calle Rumipamba 341 y Av. de Los Shyris. Casilla Postal 17-07-8976, Quito, Ecuador. manuelmoralesmite@yahoo.com.mx*

[4]*Department of Ecology and Evolution, Stony Brook University, Stony Brook, NY 11794-5245, USA. carl.hutter@gmail.com*

[5]*Centro de Investigación de la Biodiversidad y Cambio Climático, Universidad Tecnológica Indoamérica, Av. Machala y Sabanilla, Quito, Ecuador. jmguayasamin@gmail.com*

Magnolia Press
Auckland, New Zealand

Accepted by S. Castroviejo-Fisher: 20 Jun. 2012; published: 4 Jul. 2012

LUIS A. COLOMA, SOFÍA CARVAJAL-ENDARA, JUAN F. DUEÑAS, ARTURO PAREDES-RECALDE, MANUEL MORALES-MITE, DIEGO ALMEIDA-REINOSO, ELICIO E. TAPIA, CARL R. HUTTER, EDUARDO TORAL, & JUAN M. GUAYASAMIN

Molecular phylogenetics of stream treefrogs of the *Hyloscirtus larinopygion* group (Anura: Hylidae), and description of two new species from Ecuador

(*Zootaxa* 3364)

78 pp.; 30 cm.

4 Jul. 2012

ISBN 978-1-86977-927-6 (paperback)

ISBN 978-1-86977-928-3 (Online edition)

FIRST PUBLISHED IN 2012 BY

Magnolia Press

P.O. Box 41-383

Auckland 1346

New Zealand

e-mail: zootaxa@mapress.com

http://www.mapress.com/zootaxa/

ISSN 1175-5326 (Print edition)

ISSN 1175-5334 (Online edition)

Table of contents

Abstract

We review the systematics of frogs of the *Hyloscirtus larinopygion* group. A new phylogenetic tree inferred from mitochondrial DNA (partial sequences of 12S rRNA, valine-tRNA, and 16S rRNA genes; ~2.3 kb) of eleven species of the *H. larinopygion* group is provided, based on maximum parsimony, maximum likelihood, and Bayesian analyses. Our phylogeny confirms the close relationship of members of the *H. larinopygion* group with Andean relatives of the *H. armatus* group, which also occurs in the Andes. *Hyloscirtus tapichalaca* is placed as sister species to the rest of the *H. larinopygion* group, in which two clades (A+B) are evident. Although ingroup relationships are well supported, the monophyly of the *H. larinopygion* group and placement of *H. tapichalaca* require additional testing. Genetic divergences among species of the *H. larinopygion* group are shallow compared to those observed in many other anurans, with genetic distance among sister species (*H. princecharlesi* and *H. ptychodactylus*) as low as 1.31%. However, this pattern is concordant with radiations in other highland Andean lineages of anurans that show marked morphological or behavioral differentiation, but low divergence in mitochondrial markers. Divergence-time analyses (using BEAST) indicate that the *Hyloscirtus* clade is a relatively ancient lineage that appeared in the Eocene, at a minimum age of 51.2 million years ago (MYA), while the *H. larinopygion* group originated in the Middle-Late Eocene at a minimum age of 40.9 MYA. Our results might suggest a rapid radiation of *Hyloscirtus* starting in the Miocene into the Pliocene, from at least 14.2 MYA to the most recent divergence between sister taxa at ~2.6 MYA. We also describe two sympatric new species of *Hyloscirtus* from northwestern Ecuador: *H. criptico* sp. nov. and *H. princecharlesi* sp. nov. We diagnose them by their phylogenetic position (they are not sister to each other), genetic divergence, and a unique combination of color patterns, and other morphological features. Additionally, we describe the suctorial tadpoles and the extreme ontogenic color changes in *H. larinopygion, H. lindae, H. pantostictus, H. princecharlesi*, *H. psarolaimus*, and *H. tigrinus*. Furthermore, we describe the osteology of *H. criptico*, *H. lindae, H. pacha, H. pantostictus, H. princecharlesi*, *H. psarolaimus, H. ptychodactylus,* and *H. staufferorum*. We describe vocalizations of *H. lindae*, *H. pacha*, *H. pantostictus*, *H. pasarolaimus*, *H. staufferorum*, and *H. tapichalaca*. *Hyloscirtus tigrinus* is recorded for the first time in Ecuador and its range is extended 62.4 km (airline distance), from its southernmost locality record in Departamento de Nariño, Colombia. Most species of the *H. larinopygion* group are currently severely threatened by extinction, after surviving the catastrophic extinctions in the 1980s and 1990s that led to the disappearance of many other sympatric anurans that bred in swiftly flowing water and had lotic water tadpoles in the Andean highlands. Research and conservation actions are urgently needed for these species. In order to better call attention to these conservation issues, we name one of the new species in honor of Prince Charles of Wales, who is contributing significantly to the growth of awareness in the battle against tropical deforestation, climate change, and the catastrophic extinction of rainforest amphibians.

Key words: Anura; Ecuador; Calls; Conservation; Extinction; Hylidae; *Hyloscirtus criptico* sp. nov.; *Hyloscirtus larinopygion; Hyloscirtus lindae; Hyloscirtus pantostictus; Hyloscirtus princecharlesi* sp. nov.; *Hyloscirtus psarolaimus; Hyloscirtus ptychodactylus; Hyloscirtus staufferorum; Hyloscirtus tigrinus;* Morphology; New species; Osteology; Phylogeny; Systematics; Tadpoles

Resumen

Se revisa la sistemática de las ranas del grupo *Hyloscirtus larinopygion.* Se provee un nuevo árbol filogenético basado en el ADN mitocondrial (secuencias parciales de genes 12S rRNA, tRNA valina, y 16S rRNA; ~2.3 kb) de once especies del grupo *H. larinopygion*, el cual se basa en análisis de máxima parsimonia, máxima verosimilitud, y Bayesiano. Nuestra filogenia confirma la estrecha relación de los miembros del grupo *H. larinopygion* con parientes andinos del grupo *H. armatus. Hyloscirtus tapichalaca* se ubica como la especie hermana del resto de especies del grupo *H. larinopygion,* en el cual dos clados (A+B) son evidentes. Aunque las relaciones intragrupales tienen fuerte soporte estadístico, la monofilia del group *H. larinopygion* y la posición de *H. tapichalaca* requieren pruebas adicionales. Las divergencias genéticas entre las especies del grupo *H. larinopygion* son pequeñas al compararlas con aquellas observadas en muchos otros anuros, con una distancia genética entre especies hermanas (*H. princecharlesi* e *H. ptychodactylus*) tan baja como el 1.3%. Sin embargo, este patrón concuerda con las radiaciones de otros linajes de anuros de las zonas Altoandinas que muestran notoria diferenciación morfológica o comportamental a pesar de la baja diferenciación genética en marcadores mitocondriales. Análisis de tiempos de divergencia (usando BEAST) señalan que el clado de *Hyloscirtus* es un linaje relativamente antiguo pues habría surgido en el Eoceno, hace cerca de al menos 51.2 millones de años, mientras que el grupo *H. larinopygion* se habría originado en el Eoceno Medio-Tardío hace al menos 40.9 millones de años. Nuestros resultados sugerirían una rápida radiación de *Hyloscirtus* desde el Mioceno hasta el Plioceno desde al menos 14.2 millones de años hasta la más reciente diversificación de taxa hermanos que ocurrió hace al menos ~2.6 millones de años. También describimos dos especies nuevas simpátricas de *Hyloscirtus* del noroccidente de Ecuador: *H. criptico* sp. nov. e *H. princecharlesi* sp. nov. Las diagnosticamos por su posición filogenética (no son taxa hermanos), divergencia genética y una combinación única de patrones de color, y otras características morfológicas. Adicionalmente describimos los renacuajos suctoriales y los excepcionales cambios de color ontogénicos de *H. larinopygion, H. lindae, H. pantostictus, H. princecharlesi, H. psarolaimus*, e *H. tigrinus*. Además describimos la osteología de *H. criptico, H. lindae, H. pacha, H. pantostictus, H. princecharlesi*, *H. psarolaimus, H. ptychodactylus*, e *H. staufferorum*. Describimos las vocalizaciones de *H. lindae, H. pacha, H. pantostictus, H. psarolaimus, H. staufferorum*, e *H. tapichalaca.* Registramos a *Hyloscirtus tigrinus* por primera vez en Ecuador ampliando en 62.4 km su rango (en línea recta) hacia el sur desde su registro previo de una localidad en el Departamento de Nariño, Colombia. La mayoría de las especies del grupo *H. larinopygion* están hoy severamente amenazadas de extinción, después de sobrevivir a las extinciones catastróficas ocurridas en las décadas de los 80–90, las cuales produjeron la desaparición de muchos otros anuros simpátricos que se reproducían en aguas torrentosas y tenían renacuajos lóticos en zonas Altoandinas. Se requieren acciones urgentes de investigación y conservación de estas especies. Para llamar la atención sobre estos aspectos de conservación, nombramos a una de las especies nuevas en honor al Príncipe Carlos de Gales, quien está contribuyendo de manera significativa al crecimiento de la conciencia en la lucha contra la deforestación tropical, el cambio climático, y la extinción catastrófica de los anfibios de los bosques lluviosos.

Palabras claves: Anura*;* Ecuador; Cantos; Conservación; Especies Nuevas; Extinción; Filogenia; Hylidae; *Hyloscirtus criptico* sp. nov.; *Hyloscirtus larinopygion; Hyloscirtus lindae; Hyloscirtus pantostictus; Hyloscirtus princecharlesi* sp. nov.; *Hyloscirtus psarolaimus; Hyloscirtus ptychodactylus; Hyloscirtus staufferorum*; *Hyloscirtus tigrinus;* Morfología; Osteología; Renacuajos; Sistemática

Introduction

The Neotropical Andean stream-breeding frogs of the genus *Hyloscirtus* (Peters 1882) were recognized by Faivovich *et al.* (2005) as a monophyletic group (currently containing 32 species; updated from Frost, 2011) on the basis of 56 molecular (nuclear, mitochondrial, and ribosomal genes) and one morphological (wide dermal fringes on fingers and toes) synapomorphies. Within this genus, three previously proposed (see Duellman *et al.* 1997 and references cited therein) and putative monophyletic groups were also recognized by Faivovich *et al.* (2005), pending evaluation of their status: the *Hyloscirtus armatus, H. bogotensis,* and the *H. larinopygion* groups. Wiens *et al.* (2005) accommodated these three groups in the genus *Boana*, cautioning that their placement "should not be taken as a sign of confidence in the monophyly of the species groups". Wiens *et al.* (2006) adopted the

nomenclature of Faivovich *et al.* (2005) and Wiens *et al.* (2010) found strong support for the monophyly of *Hyloscirtus.* Additionally, Sánchez (2010) delimited two species groups within *Hyloscirtus* based on larval morphology.

Frogs of the *Hyloscirtus larinopygion* group are relatively large and some species could be considered as some of the most colorful and beautiful frogs on Earth (e.g., *H. tigrinus* Mueses-Cisneros and Anganoy-Criollo 2008, *H. pantostictus* Duellman and Berger 1982, *H. princecharlesi* this paper). Despite these morphological traits, individuals of the *H. larinopygion* group are remarkably elusive and are therefore difficult to detect. Perhaps this is why the first known species of this group was described less than 40 years ago (*H. larinopygion* Duellman 1973). Since then, eight species were described by the end of the 20th century, and four more were described only in the last decade. It is clear that a combination of their restricted elevational ranges in habitats difficult to access (undisturbed cascading montane streams), and their nocturnal and apparently seasonal activity have hindered our understanding of their diversity and ecology. Basic knowledge of their natural history is still lacking because most aspects of their reproductive mode and/or behaviors have not been observed. Frogs of the *H. larynopygion* group are survivors of mass extinctions that affected species living in the same habitats and having similar natural history features (e.g., tadpoles developing in lotic streams of *Atelopus* and *Hyloxalus,* in the northern Andes of Ecuador; *Atelopus* and *Telmatobius* in the south; La Marca *et al.* [2005], Bustamante *et al.* [2005], Merino *et al.* [2005], Coloma *et al.* [2007, 2010])

The Andean *Hyloscirtus larinopygion* group was initially defined by Duellman and Hillis (1990) and included eight species originally described in the genus *Hyla* (*H. caucana* [cited as *H.* sp. A.] Ardila-Robayo, Ruiz-Carranza and Roa-Trujillo 1993, *H. larinopygion, H. lindae* Duellman and Altig 1978, *H. pacha* Duellman and Hillis 1990, *H. pantosticta, H. psarolaima* Duellman and Hillis 1990, *H. ptychodactyla* Duellman and Hillis 1990, and *H. sarampiona* Ruiz-Carranza and Lynch 1982). Duellman and Hillis performed a cladistic analysis of allozymes that included five species (*Hyloscirtus larinopygion, H. lindae, H. pacha, H. pantostictus, H. psarolaimus*) and provided a phylogenetic hypothesis of their relationships. Subsequently, *Hyla staufferorum* Duellman and Coloma 1993 was described and placed in the group, and *Hyla tapichalaca* Kizirian, Coloma, and Paredes-Recalde 2003 was described. The allocation of the later to the *Hyla* groups recognized at that time was considered problematic. Faivovich *et al.* (2005) diagnosed the group by 32 molecular features of three species (*Hyloscirtus tapichalaca, H. pantostictus, H. pacha*), resurrected the name *Hyloscirtus* from its synonym with *Hyla* (Duellman 1970), and included ten species in the group (*H. caucanus, H. larinopygion, H. lindae, H. pacha, H. pantostictus, H. psarolaimus, H. ptychodactylus, H. sarampiona, H. staufferorum, H. tapichalaca*), founded on a previous morphology-based taxonomy. More recently, one new species (*H. tigrinus*) was added to the group by Mueses-Cisneros (2008). Wiens *et al.* (2010) included four species of the group (*H. lindae, H. tapichalaca, H. pantostictus, H. pacha*) in molecular analyses based on mitochondrial and nuclear sequence data. Since no morphological features have been identified as unambiguous synapomorphies to diagnose the *H. larinopygion* group, placement of species that lacked molecular data at the time of description (e. g., *H. tapichalaca*, *H. tigrinus*) was tentative and problematic. Furthermore, Paredes-Recalde (1999) and Kizirian *et al.* (2003) suggested that the *H. armata* group *sensu* Duellman *et al.* (1997) was nested in the *H. larinopygion* group. The latter hypothesis was not supported by Faivovich *et al.* (2005), but it was congruent with two groups proposed by Sánchez (2010) based on larval morphology.

The osteology, calls, and tadpoles have been been described for only some species in the *Hyloscirtus larinopygion* group. A complete osteological description for *H. tapichalaca* (Kizirian *et al.* 2003), whereas descriptions of cranial osteology have been published for *H. caucana, H. lindae,* and *H. sarampiona* (Duellman and Altig 1978, Ruíz-Carranza and Lynch 1982, Ardila-Robayo *et al.* 1993). Calls are only known for *H. staufferorum* and *H. tapichalaca* (Duellman and Coloma 1993, Kizirian *et al.* 2003). Tadpoles of only four species are known: *H. caucana, H. lindae, H. ptychodactylus,* and *H. staufferorum* (Duellman and Altig 1978, Duellman and Hillis 1990, Ardila-Robayo *et al.* 1993, Duellman and Coloma 1993). Furthermore, these tadpoles are only tentatively assigned to these taxa.

Herein, we: (1) test the monophyly of the *Hyloscirtus larinopygion* group, (2) provide an expanded phylogenetic hypothesis that includes eleven species of the *Hyloscirtus larinopygion* group based on mitochondrial sequence data, (3) describe two new species, (4) describe the osteology, tadpoles, and calls of most species, (5) describe ontogenic variation in coloration for several species, and (6) report *H. tigrinus* as a new addition to the Ecuadorian fauna.

Materials and methods

The phylogeny is based on mitochondrial DNA sequence data, and we provide data on various phenotypic traits (e.g., tadpoles, coloration, osteology, calls) that could be informative in future taxonomy and phylogenetic hypotheses based on all the available data. Herein, we use an integrative approach to taxonomy and avoid uncertain boundaries by providing discrete molecular and morphological characters. Nonetheless, we acknowledge that delimitation of species is an active area of research (Wiens 2007, Jarrín-V and Kunz 2008, Padial *et al.* 2010). The recognition of species is enhanced by genetic data and a phylogeny-based delimitation of species boundaries (see Discussion). Institutional abbreviations follow Leviton *et al.* (1985) as updated by Frost (2011), with the addition of Centro Jambatu de Investigación y Conservación de Anfibios, Quito, Ecuador (CJ). Specimens examined are housed at CJ, Museum of Natural History of The University of Kansas (KU), Museo de Zoología, Pontificia Universidad Católica del Ecuador (QCAZ), and Museo de Zoología, Universidad Tecnológica Indoamérica (MZUTI).

Author contributions. LAC conceived and designed research. LAC, SCE, JFD, APR, and MMM analyzed data and wrote the paper. DAR reared tadpoles and metamorphs. LAC, SCE, JFD, APR, MMM, DAR, EET, CRH, ET, and JMG collected specimens, data, and reviewed the paper.

DNA sampling. Phylogenetic relationships of the *Hyloscirtus larinopygion* group were analyzed using a dataset of ~2.3 kb of mitochondrial DNA that include 18 species of *Hyloscirtus*. Muscle and liver tissue samples were collected from 18 populations of *Hyloscirtus* and stored in 95% ethanol. Ingroup taxon sampling included eleven species (*H. criptico*, *H. larinopygion, H. lindae, H. pacha, H. pantostictus, H. princecharlesi, H. psarolaimus, H. ptychodactylus, H. staufferorum, H. tapichalaca,* and *H. tigrinus*) depicted in Figure 1. The sequences of *H. pacha* and *H. tapichalaca,* published by Darst and Cannatella (2004) and Faivovich *et al.* (2004) respectively, were obtained from GenBank (www.ncbi.nlm.nih.gov). Tissue samples of the Colombian *H. caucanus* and *H. sarampiona* were unavailable. As outgroups, we included *Myersiohyla inparquesi* (Ayarzagüena and Señaris 1994) and five species representing the two remaining species groups recognized in *Hyloscirtus* (groups defined by Duellman *et al.* 1997): (1) *H. armatus* (Boulenger 1902) and *H. charazani* (Vellard 1970) from the *H. armatus* group, (2) *H. alytolylax* (Duellman 1972), *H. colymba* (Dunn 1931), *H. palmeri* (Boulenger 1908), and *H. phyllognathus* (Melin 1941) from the *H. bogotensis* group. The sequences of *H. armatus,* produced by Faivovich *et al.* (2004), as well as the sequences of *H. charazani*, *H. colymba*, *H. palmeri*, and *Myersiohyla inparquesi,* produced by Faivovich *et al.* (2005) were obtained from GenBank. Information on voucher specimens, associated locality data, and GenBank accession numbers are summarized in Table 1.

DNA amplification and sequencing. Genomic DNA was extracted from frozen and ethanol preserved tissues using standard phenol–chloroform extraction protocols (Sambrook *et al.* 1989). The polymerase chain reaction (PCR) was used to amplify independently three mtDNA overlapping fragments spanning to ~2.3 kb, which included partial sequences of 12S rRNA, valine-tRNA, and 16S rRNA genes. DNA amplification was completed using combinations of primers 12SH, MVZ50d, 12SM, 16Sa, 16Sc, and 16Sbr-H (Goebel *et al.* 1999; Table 2). Mitochondrial fragments were amplified with the following thermal cycle profile: 1 cycle of 2 min at 94˚C, 30 sec at 55˚C, 1 min at 72˚C; 5 cycles of 30 sec at 94˚C, 30 sec at 55˚C, 1 min at 72˚C; 22 cycles of 30 sec at 94˚C, 30 sec at 60˚C, 1 min at 72˚C; 1 cycle of 5 min at 72˚C. Single PCR products were visualized in 1% agarose gel by a horizontal electrophoresis and purified with ExoSap (ExoSap-iT, GE Healthcare). The PCR products were sequenced by the Macrogen Sequencing Team (Macrogen Inc., Seoul, Korea).

Sequence analysis. Data from six strands were assembled to construct contiguous consensus sequences for each sample, using Sequencher 4.8 (Gene Codes Corporation). We included data from 34 individuals. DNA sequences were aligned using CLUSTAL X 2.0.10 (Larkin *et al.* 2007), with default parameters. MESQUITE 2.73 (Maddison and Maddison 2010) was used to visualize the alignment and to make some manual alignment adjustments. Models from the Gutell Lab website (www.rna.ccbb.utexas.edu) of secondary structures were used to facilitate decisions about ambiguous regions. Alignment regions for which homology was ambiguous were excluded from analysis. The final matrix included 2256 characters, after exclusion of 105 ambiguously aligned characters. We excluded regions that presented more than one equally parsimonious alignments.

TABLE 1. Taxa included in the phylogenetic analysis, with corresponding museum numbers, collecting localities, and Genbank accession numbers.

Species	Museum number	Locality	Genbank Number
Outgroup taxa			
Myersiohyla inparquesi	RWM 17688	Venezuela: Amazonas, Cerro Neblina	AY843672 (Faivovich *et al.* 2005)
Hyloscirtus alytolylax	QCAZ 24377	Ecuador: Cotopaxi: ca. San Francisco de las Pampas, 1760 m	JX155798 JX155825 (this study)
Hyloscirtus alytolylax	QCAZ 24376	Ecuador: Cotopaxi: ca. San Francisco de las Pampas, 1760 m	JX155799 JX155826 (this study)
Hyloscirtus armatus	AMNH 1651632	Bolivia: Santacruz: Caballero: Canton San Juan: Amboro National Park	AY549321 (Faivovich *et al.* 2004)
Hyloscirtus charazani	AMNH-A165132	Bolivia: La Paz, Bautista Saavedra, Canton Charazani, Stream 2	AY843618 (Faivovich *et al.* 2005)
Hyloscirtus colymba	SIUC H-7079	Panama: Cocle, Parque Nacional El Cope	AY843620 (Faivovich *et al.* 2005)
Hyloscirtus palmeri	SIUC H-6924	Panama: El Cope, Parque Nacional Omar Torrijos	AY843650 (Faivovich *et al.* 2005)
Hyloscirtus phyllognathus	QCAZ 23938	Ecuador: Morona Santiago: 16 km N El Ideal, 1600 m	JX155800 JX155827 (this study)
Hyloscirtus phyllognathus	QCAZ 41032	Ecuador: Zamora Chinchipe: ca. Miazal Alto, 1250 m	JX155801 JX155828 (this study)
Hyloscirtus phyllognathus	QCAZ 32271	Ecuador: Morona Santiago: ca. Nueve de Octubre, 1527 m	JX155802 JX155829 (this study)
Ingroup taxa			
Hyloscirtus tapichalaca	QCAZ 15083	Ecuador: Zamora Chinchipe: Reserva Tapichalaca, 2625 m	JX155803 JX155830 (this study)
Hyloscirtus tapichalaca	QCAZ 16704	Ecuador: Zamora Chinchipe: Reserva Tapichalaca 4º29.049'S, 79º8.925'W, 2697 m	AY563625 (Faivovich *et al.* 2004)
Hyloscirtus ptychodactylus	QCAZ 46030	Ecuador: Cotopaxi: ca. Pilaló, 2500 m	JX155804 JX155831 (this study)
Hyloscirtus ptychodactylus	QCAZ 46031	Ecuador: Cotopaxi: ca. Pilaló, 2500 m	JX155805 JX155832 (this study)
Hyloscirtus princecharlesi	QCAZ 42165	Ecuador: Imbabura: ca. Cuellaje, 2720 m	JX155806 JX155833 (this study)
Hyloscirtus princecharlesi	QCAZ 43654	Ecuador: Imbabura: ca. Cuellaje, 2760 m	JX155807 JX155834 (this study)
Hyloscirtus psarolaimus	QCAZ 27049	Ecuador: Sucumbíos: ca. Santa Bárbara, 2600 m	JX155808 JX155835 (this study)

...continued on next page

TABLE 1. (Continued)

Species	Museum number	Locality	Genbank Number
Outgroup taxa			
Hyloscirtus psarolaimus	QCAZ 46095	Ecuador: Napo: 60 km E Salcedo, 2748 m	JX155809 JX155836 (this study)
Hyloscirtus tigrinus	QCAZ 41351	Ecuador: Sucumbíos: ca. Santa Bárbara, 2638 m	JX155810 JX155837 (this study)
Hyloscirtus tigrinus	QCAZ 31550	Ecuador: Napo: ca. Santa Bárbara, 2620 m	JX155811 JX155838 (this study)
Hyloscirtus criptico	QCAZ 43421	Ecuador: Imbabura: ca. Cuellaje, 2560 m	JX155812 JX155839 (this study)
Hyloscirtus criptico	QCAZ 45466	Ecuador: Carchi: Road Tulcán-Maldonado. Quebrada Centella, 2806 m	JX155813 JX155840 (this study)
Hyloscirtus criptico	QCAZ 43422	Ecuador: Imbabura: ca. Cuellaje 2560 m	JX155814 JX155841 (this study)
Hyloscirtus pacha	KU 202760	Ecuador: Azuay 2.0 km SSE Palmas, 2340 m	AY326057 (Darst and Cannatella, 2004)
Hyloscirtus staufferorum	QCAZ 45967	Ecuador: Pastaza: ca. Santa Clara, 2250 m	JX155815 JX155842 (this study)
Hyloscirtus staufferorum	QCAZ 45962	Ecuador: Pastaza: ca. Santa Clara 2250 m	JX155816 JX155843 (this study)
Hyloscirtus larinopygion	QCAZ 41826	Ecuador: Carchi: Morán, 2452 m	JX155817 JX155844 (this study)
Hyloscirtus larinopygion	QCAZ 45462	Ecuador: Carchi: Road Tulcán-Maldonado. Quebrada Centella, 2806 m	JX155818 JX155845 (this study)
Hyloscirtus pantostictus	QCAZ 45438	Ecuador: Sucumbíos: ca. Santa Bárbara, 2709 m	JX155819 JX155846 (this study)
Hyloscirtus pantostictus	QCAZ 45435	Ecuador: Sucumbíos: ca. Santa Bárbara, 2709 m	JX155820 JX155847 (this study)
Hyloscirtus lindae	QCAZ 41232	Ecuador: Napo: Parque Nacional Sumaco, Sumaco Lake, 2479 m	JX155821 JX155848 (this study)
Hyloscirtus lindae	QCAZ 45346	Ecuador: Napo: 11–12 km E Papallacta, 2600 m	JX155822 JX155849 (this study)
Hyloscirtus lindae	QCAZ 45463	Ecuador: Sucumbíos: ca. Santa Bárbara, 2341m	JX155823 JX155850 (this study)
Hyloscirtus lindae	QCAZ 45342	Ecuador: Napo: 11–12 km E Papallacta, 2700 m	JX155824 JX155851 (this study)

TABLE 2. Primers used for amplification and sequencing reactions.

Primer	Sequence (5'–3')	Gene	Source
12SH	AAAGGTTTGGTCCTAGCCTT	12S	Goebel, 1996; Cannatella, 1998
MVZ50d	TYTCGGTGTAAGYGARAKGCTT	tRNA-Val	Graybeal, 1997
12SM	GGCAAGTCGTAACATGGTAAG	12S	Darst and Cannatella, 2004
16SA	ATGTTTTTGGTAAACAGGCG	16S	Palumbi *et al.* 1991
16Sc	GTRGGCCTAAAAGCAGCCAC	16S	Moriarty and Cannatella, 2004
16Sbr-H	CCGGTCTGAACTCAGATCACGT	16S	Palumbi *et al.* 1991

Phylogenetic analysis. We analyzed the phylogenetic relationships of the *Hyloscirtus larinopygion* group using maximum parsimony, maximum likelihood, and Bayesian analyses. Maximum parsimony analyses were performed in PAUP* 4.0a109 (Swofford 2009), using heuristic searches with tree bisection and reconnection (TBR) branch swapping and 10,000 random addition sequences replicates. All characters were weighted equally and gaps were treated as missing data. To obtain estimates of support for each clade, bootstrapping was employed (100 replicates), with each bootstrap replicate using heuristic searches with 10,000 replicates and TBR branch swapping.

For Bayesian and likelihood analyses, the best-fitting evolutionary model was selected using jMODELTEST 0.1.1 (Posada 2008, Guindon and Gascuel 2003), under the Bayesian Information Criterion (BIC). The BIC has been suggested to have high accuracy and precision relative to other selection criteria (Luo *et al.* 2010). For ML analyses, we used GARLI 2.0 (Zwickle 2006). Two partitioning schemes were used: without a partition and with a two-partition scheme (12S rRNA + valine-tRNA; 16S rRNA). We used the best log-likelihood across the search replicates and number of parameters to calculate the AIC for each partition scheme to determine the preferred partition, which was the two-partition scheme. A total of 25 independent runs were performed to infer the best tree, using the model selected in jMODELTEST but with parameter values estimated from the data. Bootstrap support was assessed via 1000 pseudoreplicates under the same settings used during tree search to estimate support for the nodes.

Bayesian analyses were performed in MrBAYES 3.1.2 (Huelsenbeck and Ronquist 2001, Ronquist and Huelsenbeck 2003). In order to determine the best partition scheme, we performed a Bayes factor analysis (Kass & Raftery 1995, Brandley *et al.* 2005) without a partition and a two-partition scheme (12S rRNA + valine-tRNA; 16S rRNA). We used the harmonic means obtained to estimate the Bayesian factor. As a Bayes factor cut off we considered a 2ln Bayes factor > 5 as a strong evidence favoring a partitioning scheme. Subsequent analyses were performed with a two-partition scheme (12S rRNA + valine-tRNA; 16S rRNA), which resulted in the preferred partitioning scheme. To each partition, we assigned its best-fit model of evolution estimated in jMODELTEST. All parameters were unlinked between partitions, except topology and branch lengths. Bayesian phylogenetic analyses consisted of two independent runs of 10 million generations each and four Markov chains (temperature set to 0.20), with trees sampled every 1000 generations. Of the 10000 trees generated per run, the first 2500 were discarded as "burn in". After confirming that the two analyses reached stationarity at a similar likelihood score and that the topologies were similar, using TRACER 1.5 (Drummond and Rambaut 2007), the remaining 15000 trees were combined to calculate the posterior probabilities in a 50% majority-rule consensus tree. To address intra- and interspecies sequence divergence we used maximum-likelihood corrected pair-wise distances, calculated in PAUP* 4.0a115 (Swofford 2002), under the same model selection strategy used in the phylogenetic analyses.

Divergence time estimates. We estimated divergence times among species of *Hyloscirtus* using BEAST 1.7.1 (Drummond and Rambaut 2007). We used two methods of calibration: (1) the estimated rate of evolution for anuran mitochondrial 12S and 16S from *Pseudacris* (0.00277 substitutions per site per lineage per MYA; Lemmon *et al.* 2007), and (2) combined fossil and paleobiogeographic information (Salerno *et al.* 2012). Because there is no fossil information on species of *Hyloscirtus*, we used only external calibration points. Following Smith *et al.* (2005) we included the following minimum ages of clades based on the hylid fossil record: most recent common ancestor (MRCA) of *Acris–Pseudacris* clade (15 MYA), MRCA of European *Hyla* (10 MYA), MRCA of *H. squirella–H. cinerea* clade (15 MYA), MRCA of North American *Hyla* (33 MYA), and MRCA of the *Hyla gratiosa–H. versicolor* clade (15 MYA). Additionally, we added a calibration point corresponding to the common

ancestor of *Osteopilus* and *Phyllodytes auratus* based on the Aves Ridge landbridge hypothesis (GAARlandia; Iturralde-Vinent and MacPhee 1999). The substitution rate from *Pseudacris* was estimated based partially on hylid fossils (Lemmon *et al.* 2007), and, thus, these two calibration approaches are not fully independent.

For the analyses, we used a two partition scheme (12S rRNA + valine-tRNA; 16S rRNA), which included a single representative of each *Hyloscirtus* species from our dataset, complemented with 24 sequences of other hylid species (Table 3) that represent the clades used for calibration points (also used by Salerno *et al*. 2012). Analyses were conducted under the GTR + I + Γ model for each partition, with a Yule speciation prior. In the case of fossil calibration, we use a lognormal relaxed-clock and a lognormal distribution of branch lengths. Fossil calibration points were used as priors on clade ages. We used a lognormal prior distribution, where the minimum ages of clades was used as an offset, with an arbitrary mean close to the offset values (+ 2 million years) and a standard deviation of 1 million years. For the common ancestor of *Osteopilus* and *Phyllodytes auratus,* we used a normal distribution with a mean of 34 MYA and a standard deviation of 1 MYA (Iturralde-Vinent and MacPhee 1999). In order to achieve an Effective Sample Size (ESS) of at least 200 for all parameters, the length of chain used in these analyses was 35 million in the *Pseudacris* calibration and 50 million in the case of other fossil calibrations. Results were visualized in TRACER 1.5 and a summary tree was generated using TREEANNOTATOR under the maximum clade credibility in the target tree type option.

TABLE 3. Sequences used to estimate divergence times in *Hyloscirtus*.

Species	Genbank Number
Acris crepitans	EF566969
Hyla arborea	AY843601
Hyla arenicolor	EF566960
Hyla cinerea	AY680271
Hyla gratiosa	AY843630
Hyla meridionalis	EF566953
Hyla squirella	AY843678
Hyla versicolor	EF566951
Osteopilus crucialis	AY843710
Osteopilus dominicensis	AY843711
Osteopilus marianae	DQ380383
Osteopilus marianae	EU034086
Osteopilus pulchrilineatus	AY819436
Osteopilus pulchrilineatus	EU034087
Osteopilus septentrionalis	AY843712
Osteopilus vastus	AY843713
Osteopilus wilderi	DQ380385
Osteopilus wilderi	EU034092
Phyllodytes auratus	AY819383
Phyllodytes auratus	DQ403730
Phyllodytes auratus	DQ403728
Phyllodytes auratus	DQ403726
Phyllodytes auratus	AY819515
Pseudacris crucifer	AY291103

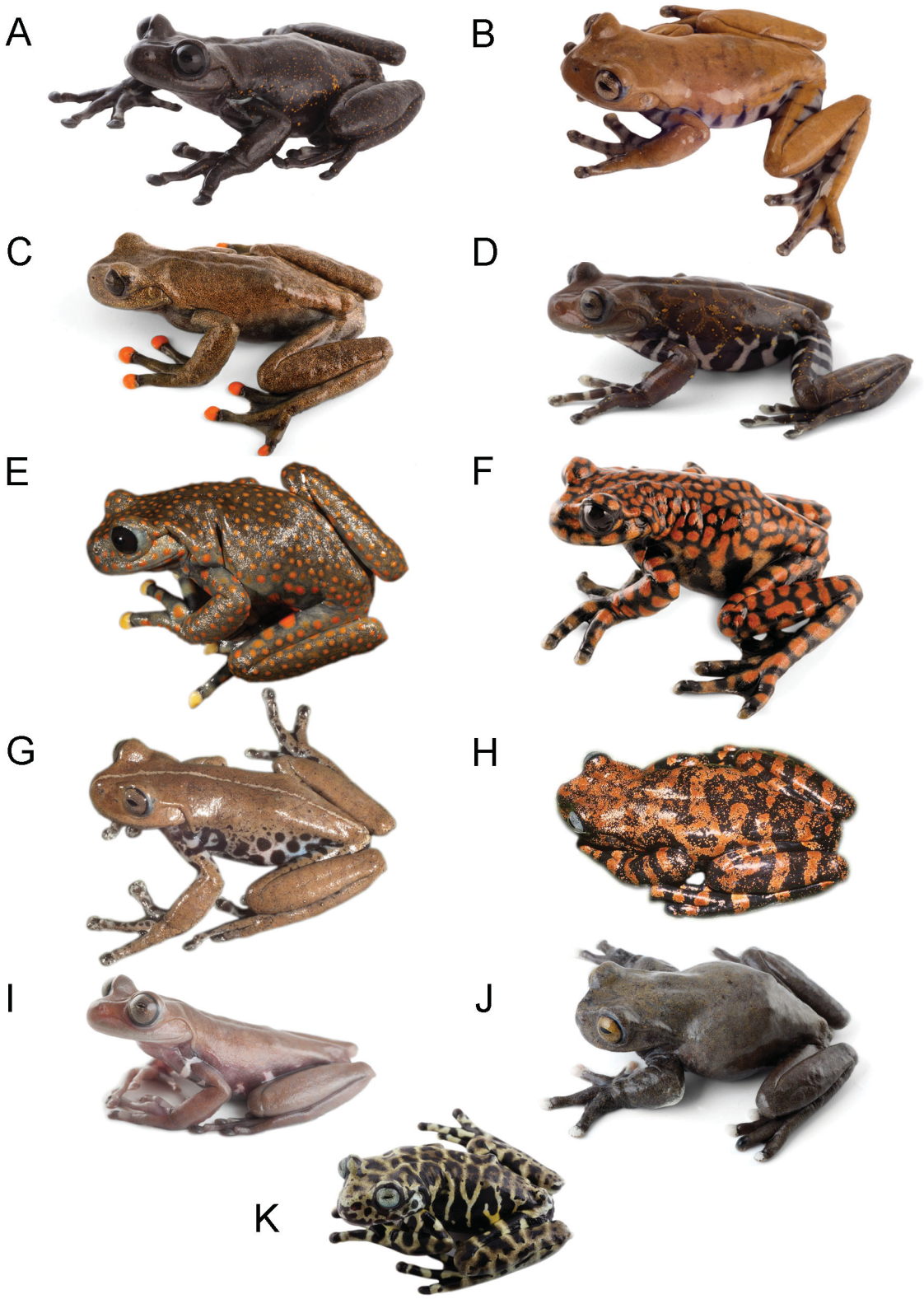

FIGURE 1.—Eleven species of frogs of the *Hyloscirtus larinopygion* group included in this study: (A) *H. criptico*, CJ 313, (B) *H. larinopygion,* QCAZ 41826, (C) *H. lindae,* QCAZ 41298, (D) *H. pacha,* QCAZ (sc 32420), (E) *H. pantostictus,* no number associated, (F) *H. princecharlesi*, QCAZ 44893, (G) *H. psarolaimus,* QCAZ 31671, (H) *H. ptychodactylus,* no number associated, (I) *H. staufferorum,* QCAZ 45962, (J) *H. tapichalaca,* QCAZ (sc 29217), and (K) *H. tigrinus,* QCAZ 40331. Not to scale. Photos by Luis A. Coloma.

TABLE 4. Species, specimen museum numbers, localities and coordinates included in the distribution map (Fig. 9) of *Hyloscirtus.*

Museum number	Species	Locality	Latitude	Longitude
QCAZ 4168	*Hyloscirtus criptico*	Ecuador: Carchi: 22 km E Maldonado	0.8200	-77.9600
CJ 312	*Hyloscirtus criptico*	Ecuador: Pichincha: Las Gralarias, 2175 m	-0.0252	-78.7030
CJ 311	*Hyloscirtus criptico*	Ecuador: Imbabura: ca. Cuellaje	0.4775	-78.5626
QCAZ 29211	*Hyloscirtus larinopygion*	Ecuador: Carchi: 24 km E Maldonado, 2664 m	0.8232	-78.0254
QCAZ 38418	*Hyloscirtus larinopygion*	Ecuador: Carchi: Cerro Centella, 2709 m	0.81436	-78.0150
QCAZ 41826	*Hyloscirtus larinopygion*	Ecuador: Carchi: Morán, 2462 m	0.7467	-78.1039
QCAZ 7593	*Hyloscirtus lindae*	Ecuador: Napo: 10 km E Oyacachi, 2510 m	-0.2322	-78.0072
QCAZ 10483	*Hyloscirtus lindae*	Ecuador: Napo: ca. Oyacachi	-0.2100	-78.0700
QCAZ 41232	*Hyloscirtus lindae*	Ecuador: Napo: Parque Nacional Sumaco. Sumaco Lake, 2479 m	-0.5696	-77.5941
QCAZ 41294	*Hyloscirtus lindae*	Ecuador: Napo: Parque Nacional Sumaco, 2775 m	-0.5640	-77.6155
QCAZ 45345	*Hyloscirtus lindae*	Ecuador: Napo: 11–12 km E Papallacta, 2600 m	-0.3870	-78.0600
QCAZ 45463	*Hyloscirtus lindae*	Ecuador: Sucumbíos: ca. Santa Bárbara	0.6159	-77.4879
QCAZ 10489	*Hyloscirtus pacha*	Ecuador: Morona Santiago: 25.6 km E limit between Azuay and Morona Santiago, 2120 m	-3.0000	-78.4500
QCAZ 48237	*Hyloscirtus pacha*	Ecuador: Morona Santiago ca. Plan de Milagro, 2152 m	-3.0011	-78.5052
QCAZ 48238	*Hyloscirtus pacha*	Ecuador: Morona Santiago: ca. Plan de Milagro, 2300 m	-3.0079	-78.5254
QCAZ 2721	*Hyloscirtus pantostictus*	Ecuador: Sucumbíos: ca. Santa Bárbara, 2760 m	0.6500	-77.4800
QCAZ 45440	*Hyloscirtus pantostictus*	Ecuador: Sucumbíos. ca. Santa Bárbara, 2586 m	0.6136	-77.5323
QCAZ 45449	*Hyloscirtus pantostictus*	Ecuador: Sucumbíos. ca. Santa Bárbara, 2341 m	0.6159	-77.4879
CJ 308	*Hyloscirtus princecharlesi*	Ecuador: Imbabura: ca. Cuellaje, 2760 m	0.4724	-78.5660
QCAZ 13252	*Hyloscirtus psarolaimus*	Ecuador: Napo: 11 km SE Papallacta, 2800 m	-0.3870	-78.0600
QCAZ 31671	*Hyloscirtus psarolaimus*	Morona Santiago: Parque Nacional Sangay, San Vicente, 2815 m	-2.2103	-78.4487
QCAZ 46890	*Hyloscirtus psarolaimus*	Ecuador: Napo: Km 60 road Salcedo–Tena, 2748 m	-0.9720	-78.2414
MCZ 109317	*Hyloscirtus psarolaimus*	Ecuador: Napo: La Alegría–Sibundoy, 2410 m	0.5800	-77.5100
QCAZ 27049	*Hyloscirtus psarolaimus*	Ecuador: Sucunbíos: ca. Santa Bárbara	0.6422	-77.5265
QCAZ 46023	*Hyloscirtus ptychodactylus*	Ecuador: Cotopaxi: ca. Pilaló, 2258 m	-0.9444	-79.0076
QCAZ 46024	*Hyloscirtus ptychodactylus*	Ecuador: Cotopaxi: ca. Pilaló, 2500 m	-0.9425	-78.9957
QCAZ 3701	*Hyloscirtus staufferorum*	Ecuador: Napo: Parque Nacional Sumaco, Sumaco Lake, 2500 m	-0.5400	-77.6000
QCAZ 3704	*Hyloscirtus staufferorum*	Ecuador: Napo: 31 km SE Baeza, 2210 m	-0.7163	-77.9172
QCAZ 45962	*Hyloscirtus staufferorum*	Ecuador: Pastaza: ca. Santa Clara, 2250 m	-1.2792	-78.0779
QCAZ 17776	*Hyloscirtus tapichalaca*	Ecuador: Zamora Chinchipe: Reserva Tapichalaca, 2697 m	-4.4842	-79.1488
QCAZ 46887	*Hyloscirtus tapichalaca*	Ecuador: Zamora Chinchipe: Reserva Tapichalaca, 2637 m	-4.5500	-79.1291
QCAZ 40331	*Hyloscirtus tigrinus*	Ecuador: Sucumbíos: ca. Santa Bárbara, 2638 m	0.6437	-77.5322

Morphology. Specimens of the new species were compared to published descriptions and museum material. Ecuadorian localities of eleven species of the *Hyloscirtus larinopygion* group included in this study are given in Table 4. Morphological characters studied follow Duellman and Hillis (1990) and Kizirian *et al.* (2003), and

references therein. Sexual maturity of males was determined by dissection and by the presence of vocal slits, and/or nuptial glands on thumb. Sexual maturity of females was assessed by the presence of eggs or convoluted oviducts. Morphological measurements were recorded to the nearest 0.01 mm with electronic digital calipers (0–150 mm). Measurements taken were abbreviated as follows: SVL (snout–vent length), TIBL (tibia length), FEL (femur length), FOL (foot length), RDUL (radio-ulna length), HANDL (hand length — distance from the proximal edge of the inner palmar tubercle to the tip of Finger IV), THBL (thumb length from the distal margin of the thenar tubercule to tip of thumb), HLSQ (head length from the posterior margin of the squamosal to tip of snout), HDW (head width —measured at level of posterior mandibles), ITN (internarial distance), EYD (eye diameter), EYNO (eye-nostril distance —measured from anterior margin of eye to posterior margin of nostril), TYD (tympanum diameter), DFW (width of the disc of Finger III), DTW (width of the disc of Toe IV), and SW (sacrum width—measured between the distal margins of sacral diapophyses).

Fingers are numbered from I–IV. Webbing formulae are described following Savage and Heyer (1967) with modifications by Myers and Duellman (1982). We note that sometimes it is difficult to distinguish when the web ends and a lateral fringe begins. Therefore, the webbing formulae are not exact and some caution in defining and using this character is recommended.

Osteological descriptions are based on a series of thirteen specimens of eight species belonging to the *Hyloscirtus larinopygion* group (*H. criptico*, *H. lindae, H. pacha, H. pantostictus, H. princecharlesi, H. psarolaimus, H. ptychodactylus, H. staufferorum*). Cleared and double-stained (C&S) (with Alcian Blue and Alizarin Red) specimens were prepared following Dingerkus and Uhler (1977), with minor modifications. Additionally, osteological data for new species (*H. criptico* and *H. princecharlesi*) were obtained from X-ray images acquired with a Thermo Kevex X-ray machine, Model PXS5-925EA-LV with the following settings: max volt: 80 Kv, max power: 8 Watts, and max current: 0.18 mA. Osteological nomenclature follows Duellman and Trueb (1986), Trueb (1993), and Fabrezi and Alberch (1996). Figures were drawn from specimens or from scanned images. Illustrations were made with the aid of a stereo dissecting microscope equipped with a camera lucida.

Tadpoles and ontogeny. Developmental stages of tadpoles were determined following the methodology proposed by Gosner (1960). Oral disc characters and measurements follow Altig and McDiarmid (1999). The template for tadpole description mostly follows Castillo-Trenn (2004). Series of tadpoles for five species (*Hyloscirtus larinopygion, H. pantostictus, H. psarolaimus, H. princecharlesi,* and *H. tigrinus*) were collected and raised in the laboratory to document their ontogenetic variation until the subadult stage, at which point the specific identity was confirmed. Individuals in Stage 25 with complete mouth parts were chosen for a detailed description, except for *H. lindae, H. princecharlesi* and *H. tigrinus,* for which preserved specimens with complete mouth parts were not available (i.e., denticles and pigmentation in oral apparatus were not present). Since some specimens in the dataset were not complete (e.g., terminus of tail or some mouth structures were missing) or suffered dehydration due to poor preservation, some measurements were not recorded. Accordingly, in some cases the sample size of particular measurements differed from the total number of specimens available for each species. Body and tail measurements were taken using a micrometer on dissecting microscopes. Internarial distance was measured between the centers of narial apertures and interorbital distance was measured between the centers of the pupils. Digital images are displayed within species accounts in the electronic encyclopaedia at AnfibiosWebEcuador (www.anfibioswebecuador.ec/anfibioswebecuador.aspx)

Tadpoles were kept in the lab in stable physical and chemical conditions at a mean temperature of 21°C and pH 6.8. Groups of two and three individuals were placed in glass tanks 50 cm long x 30 cm wide x 30 cm deep with a capacity of 40 liters of water. We used only half the capacity of the tanks (20 liters of water) since the tanks were opened under a water inlet and outlet, which ensured a daily renewal of 30–40% of water of each tank. The water entering the container was filtered to prevent the entry of components or substances like chlorine, arsenic, bacteria, and other harmful agents that may threaten the life of tadpoles. In addition, each container was fitted with a powerhead water pump (200 gallons per hour) to keep the water circulating.

Tadpoles were fed daily with SAR Type I (Super Alimento de Renacuajos), a specific food for herbivorous tadpoles with protein (25.16%), fiber (13.08%), and carbohydrates (49.08%). SAR was supplied in two ways: (1) as powder that was placed directly on the water surface, and (2) as a paste in a stone that was located at the bottom of the aquarium. The paste was smeared on the upper and lateral surfaces of a stone with a diameter of about 10 cm. These stones with the paste were dried at 30 °C for 12 hours before being used, and the two forms of food supply were used alternately during development.

Juveniles and subadults were kept in individual terraria (Penn Plax SW 03) using an open water system with spraying four times a day for five minutes each time. Terraria were assembled with a false floor with water at the bottom and plants and shelter for frogs above, following Barnet *et al.* (2001). Temperature in the terraria varied from 19–22 °C, and relative humidity ranged between 85–95%. Frogs were fed crickets (3–5 mm; *Gryllus* sp. complex *assimilis*) and wax moths (*Galleria mellonella*). Juvenile and subadults were fed three times a week. Insects were dusted with vitamin supplements rich in calcium and vitamin D3 (Repashy Super Foods) once a week before being placed in the terraria, to help prevent nutritional problems arising from a poor diet.

Calls. Recordings of advertisement calls were obtained from seven species: *Hyloscirtus criptico*, *H. lindae*, *H. pacha*, *H. pantostictus*, *H. psarolaimus*, *H. staufferorum*, and *H. tapichalaca*. Air temperature was recorded in all cases, except for *H. staufferorum*. Recordings were made with an Olympus LS-10 Linear PCM Field Recorder and a Sennheiser K6–ME 66 unidirectional microphone with a sample size of 16 bits at a sampling rate of 44,100 Hz. Calls were analyzed in the Sound Analysis Software RAVEN 1.2.1 (Charif *et al.* 2004). Eight variables were examined, including both spectral and temporal characters: (1) pulses per call, (2) call length, (3) call repetition rate (number of calls/min), (4) interval between calls, (5) rise time, (6) call shape (rise time/note length), (7) fundamental frequency, and (8) dominant frequency. Call structure (pulsed/unpulsed) was defined following Littlejohn (2001). The spectrogram analyses were generated with fast fourier transform (FFT) used settings of window size 899 samples and filter bandwidth 70.6 Hz. Voucher specimens and sound archives are deposited at CJ, QCAZ, and FonoZoo.

Conservation status. We categorized the conservation status of the two new species and *Hyloscirtus tigrinus* by applying IUCN categories, criteria, and guidelines (IUCN 2001). We measured the area of extent of occurrence for the species as the area contained by a minimum convex polygon (the smallest polygon in which no internal angle exceeds 180 degrees and which contains all the sites of occurrence).

Results

Phylogenetic relationships. The dataset of 2256 pb includes 926 variable and 712 parsimony-informative characters. The MP majority-rule consensus, ML, and Bayesian majority-rule consensus trees resulted in the same ingroup topology, except for placement of *Hyloscirtus larinopygion* (Fig. 2). The MP analysis resulted in four most parsimonious trees of 2157 steps with a consistency index of 0.6115 and a retention index of 0.779. The four most parsimonious trees differed in the unresolved placement of *H. palmeri* within the *H. bogotensis* group. Regarding outgroup relationships, there are differences in the topology obtained in MP, ML, and Bayesian analyses. The placement of the *H. armatus* group as sister taxa to *H. larinopygion* group is supported (Bootstrap value = 90.0%) under the MP analysis, whereas it is not supported (Bayesian Posterior Probabilities = 0.51) in the Bayesian analyses. In the ML analysis, the *H. armatus* group is placed as the sister taxa of the *H. bogotensis* group without support (Bootstrap value = 57.0%).

TABLE 5. Datasets and partitions used in this study. Number of nucleotides (nt), selected model under the Bayesian information criterion (BIC), Akaike information criterion (AIC), and likelihood-ratio tests (LRTs). BIC difference between BIC and AIC/ and between BIC and LRTs selected models (Δ BIC).

Dataset	nt	Selected model			Δ BIC
		BIC	AIC	LRTs	(AIC/LRTs)
12S rRNA + valine-tRNA	853	TIM2+I+G	GTR+I+G	GTR+I+G	4.6/4.6
16S rRNA	1403	TIM2+I+G	TIM2+I+G	GTR+I+G	–/14.3

The evolution model selected under the BIC criterion was TIM2 + I + Γ (for both partitions 12S+tval and 16S) and for the complete dataset. Differences between models selected under different criteria are summarized in Table 5. The analysis of ML resulted in a tree with -ln L = 12730.95 (Fig. 2). The ML topology was similar to the majority-rule consensus tree obtained under Bayesian analyses, in which *Hyloscirtus tapichalaca* is placed as sister taxon to a clade that includes the rest of the species of the *H. larinopygion* group (Figs. 2, 3). Within this group there are two evident clades, which we call A and B. Clade A consists of ((*H. ptychodaylus*, *H. princecharlesi*), (*H.*

tigrinus (*H. psarolaimus* (*H. criptico* (*H. pacha*, *H. staufferorum*))))), whereas Clade B consists of (*H. larinopygion* (*H. pantostictus*, *H. lindae*)). Placement of *H. larinopygion* differs in the MP analyses, where it was placed in Clade A (instead of B), but this difference is not supported (Bootstrap value = 56.2%). The monophyly of the *H. larinopygion* group and placement of *H. tapichalaca* inside this group had strong support in the MP analyses (Bootstrap value = 77.9%), but it was weakly supported in the Bayesian (Bayesian Posterior Probabilities = 0.76) and ML analyses (Bootstrap value = 59.3%).

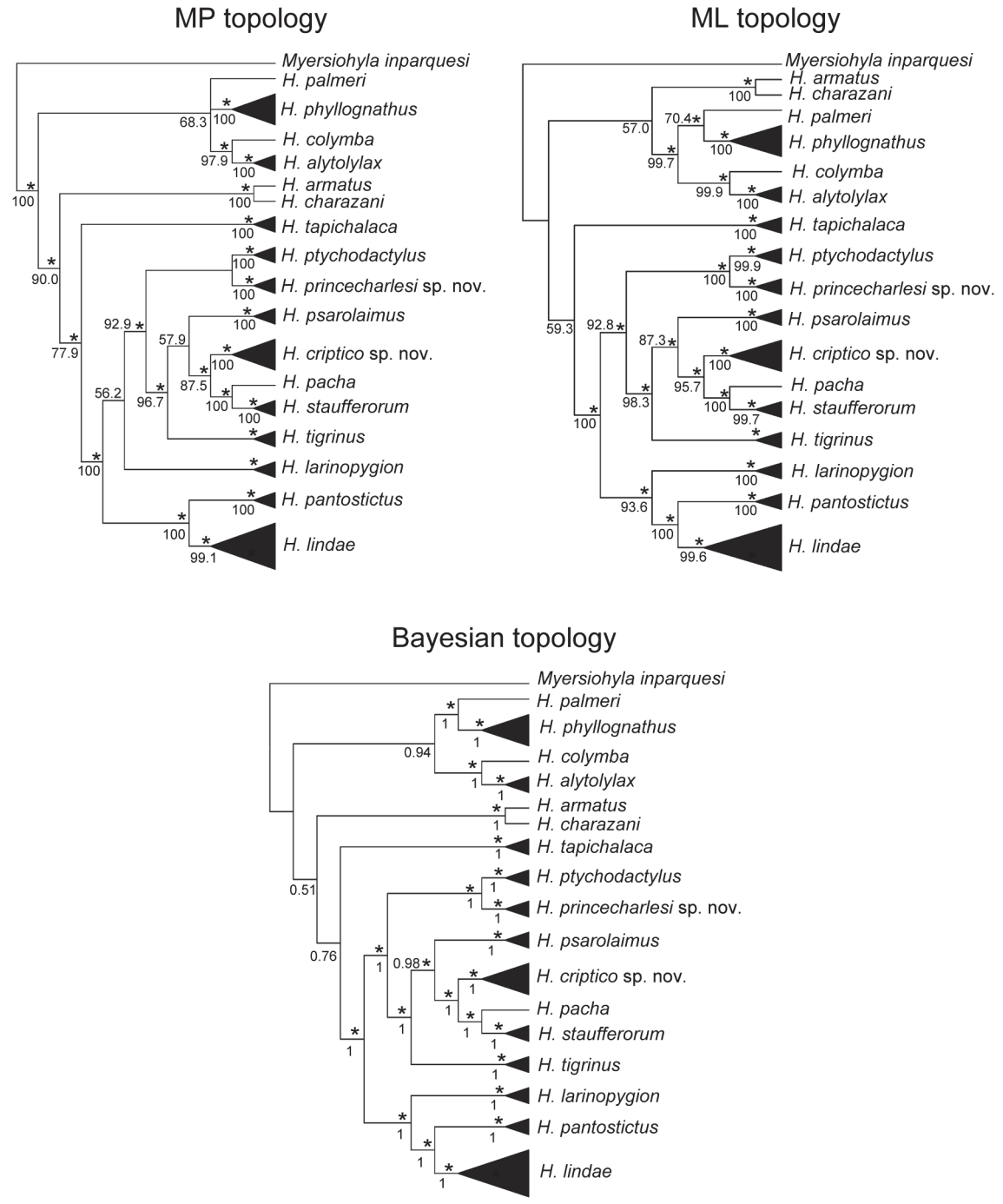

FIGURE 2.— Topologies from maximum parsimony, maximum likelihood, and Bayesian analyses. Bootstrap support > 50% and Bayesian posterior probalilities > 0.5 are indicated. * = significant support (Posterior probability > 0.95 in Bayesian tree; bootstrap support >70% in maximum parsimony and maximum likelihood trees).

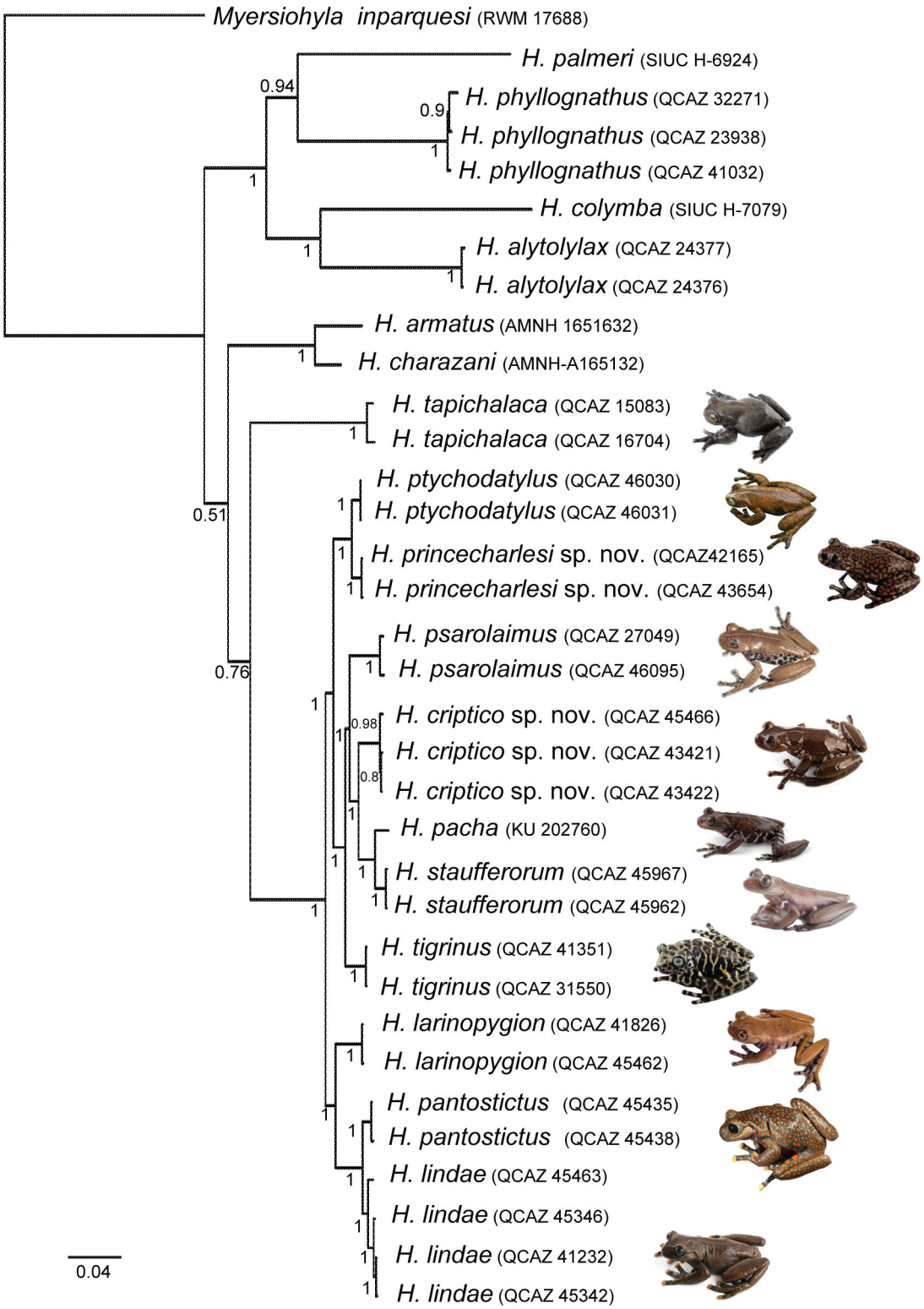

FIGURE 3.—Majority-rule consensus tree from Bayesian analysis depicting the phylogeny of the *Hyloscirtus larinopygion* group. Museum numbers and Bayesian posterior probalilities > 0.5 are indicated.

Sequence divergence between species of the *Hyloscirtus larinopygion* group and the *H. armatus* group ranged from 18.0% (*H. lindae* and *H. charazani*) to 22.6% (*H. tapichalaca* and *H. armatus*), and between species of the *H. larinopygion* group and *H. bogotensis* group ranged from 29.0% (*H. tigrinus* and *H. alytolylax*) to 44.5% (*H. staufferorum* and *H. palmeri*). Interspecific sequence divergence within the *H. larinopygion* group ranged from 1.3% (*H. ptychodactylus* and *H. princecharlesi*) to 22.3 % (*H. criptico* and *H. tapichalaca*). Sequence divergence among sympatric sister species (*H. lindae* and *H. pantostictus*) was 1.5%. Within species that were represented by samples from multiple populations, sequence divergence were variable: 0.2% in *H. criptico,* to 0.4% in *H. psarolaimus,* 0.7% in *H. phyllognathus,* and 0.9% in *H. lindae*. ML corrected distances values among species are shown in Table 6.

TABLE 6. Maximum likelihood-corrected pair-wise distances (mean and range are given in %) between species of *Hyloscirtus.*

	H. larinopygion (1)	*H. lindae* (2)	*H. pacha* (3)	*H. pantostictus* (4)	*H. psarolaimus* (5)	*H. ptychodactylus* (6)
2	4.83 (4.69–4.95)					
3	6.68 (6.65–6.71)	6.96 (6.81–7.04)				
4	4.78 (4.69–4.87)	1.46 (1.32–1.57)	6.43 (6.36–6.49)			
5	5.94 (5.84–6.03)	6.75 (6.54–6.85)	5.27 (5.26–5.27)	6.65 (6.57–6.73)		
6	4.73 (4.70–4.75)	5.81 (5.74–5.85)	5.30	5.64 (5.57–5.70)	5.57 (5.53–5.61)	
7	6.82 (6.73–6.89)	7.21 (6.97–7.38)	1.78 (1.77–1.78)	6.71 (6.57–6.82)	5.11 (5.04–5.18)	5.13 (5.06–5.19)
8	6.54 (6.43–6.63)	6.78 (6.60–6.95)	3.80 (3.74–3.85)	6.46 (6.35–6.57)	4.31 (4.24–4.41)	5.12 (5.05–5.18)
9	18.58 (18.54–18.62)	17.64 (17.54–17.72)	20.59	18.08 (17.97–18.20)	21.19 (21.89–21.49)	18.55
10	5.21 (5.18–5.24)	5.98 (5.86–6.04)	4.01	5.93 (5.86–6.00)	4.24 (4.19–4.29)	4.04
11	4.86 (4.80–4.92)	5.96 (5.88–6.02)	6.10 (6.06–6.14)	5.88 (5.77–5.98)	5.45 (5.37–5.53)	1.31 (1.28–1.33)
12	19.93 (19.89–19.97)	18.19 (17.95–18.34)	21.58	18.78 (18.66–18.89)	19.37 (19.29–19.44)	20.50
13	18.61 (18.57–18.65)	17.98 (17.64–18.15)	20.70	18.24 (18.13–18.36)	18.44 (18.33–18.55)	18.61
14	31.35 (31.19–31.52)	31.70 (30.26–32.30)	31.56 (31.47–31.65)	30.45 (30.17–30.72)	33.19 (32.84–33.54)	29.84 (29.75–29.93)
15	39.94 (39.87–40.02)	39.21 (38.76–39.47)	43.82	39.45 (39.37–39.54)	43.06 (42.63–43.06)	39.38
16	38.27 (38.21–38.34)	36.06 (35.90–36.27)	41.54	36.99 (36.77–37.20)	38.72 (39.29–38.15)	37.38
17	32.69 (32.58–32.82)	30.53 (29.75–30.95)	32.61 (32.49–32.84)	29.86 (29.64–30.02)	32.07 (31.56–32.55)	30.96 (30.87–31.11)

TABLE 6. Continued.

	H. staufferorum (7)	*H. criptico* (8)	*H. tapichalaca* (9)	*H. tigrinus* (10)	*H. princecharlesi* (11)	*H. armatus* (12)
8	3.74 (3.64–3.85)					
9	21.44 (21.22–0.2167)	22.30 (22.02–0.2255)				
10	4.07 (4.02–4.12)	3.66 (3.60–3.72)	19.59			
11	5.78 (5.68–5.89)	5.35 (5.24–5.45)	19.89 (19.80–19.98)	4.22 (4.19–4.25)		
12	21.23 (20.99–21.46)	19.87 (19.74–19.97)	22.61	18.96	20.57 (20.48–20.66)	
13	19.83 (19.61–20.06)	20.63 (20.49–20.73)	22.27	18.36	19.89 (19.81–19.98)	5.73
14	31.22 (30.36–31.85)	30.84 (30.45–31.17)	33.99 (33.89–34.09)	29.03 (28.94–29.12)	29.49 (29.28–29.70)	31.84 (31.80–31.87)
15	43.07 (42.87–43.26)	40.89 (40.42–41.30)	40.23	40.21	39.69 (39.52–39.86)	40.29
16	44.51 (44.09–44.93)	40.68 (40.54–40.92)	34.48	38.06	38.74 (38.57–38.91)	34.21
17	33.73 (33.25–34.23)	31.11 (30.70–31.60)	35.70 (35.55–35.80)	31.27 (31.07–31.54)	30.01 (29.88–30.36)	30.76 (30.32–31.20)

TABLE 6. Continued.

	H. charazani (13)	*H. alytolylax* (14)	*H. colymba* (15)	*H. palmeri*(16)
14	30.10 (30.01–30.18)			
15	39.68	27.27 (26.97–27.56)		
16	34.64	36.76 (36.68–36.84)	41.09	
17	27.73 (27.36–28.14)	28.08 (27.84–28.47)	35.42 (34.91–35.70)	29.74 (29.63–29.95)

Divergence-time estimates. Minimal age estimates of clades based on the hylid fossils and paleobiogeographic calibration were lower than the estimates obtained with *Pseudacris* substitution rate, especially for the most ancient clades (*Hyloscirtus* and *H. armatus* + *H. larinopygion* groups). However, divergence times for all nodes estimated with the fossil and paleogeographic calibrations fall within the 95% confidence intervals obtained with *Pseudacris* substitution estimation (Fig. 4). The former, minimal age estimates, divergence times within the *Hyloscirtus* clade range from 2.6–51.2 MYA (Figs. 4, 5). The oldest split corresponds to the separation between the *H. bogotensis* group and the *H. armatus* + *H. larinopygion* groups. The divergence time for the *H. larinopygion* group from the *H. armatus* group is estimated at 40.9 MYA. Within the *H. larinopygion* group, the times of divergence range from 2.6–31.9 MYA; the oldest node of this clade, corresponds to the split between *H. tapichalaca* and rest of the clade (Clade A + B). The split between Clade A and Clade B is estimated at 14.2 MYA. The split between *H. princecharlesi* and *H. ptychodactylus* is estimated at 3.2 MYA and between *H. criptico* and *H. pacha* + *H. staufferorum* is estimated at 5.6 MYA. The most recent split correspond to the speciation event between *H. staufferorum* and *H. pacha* (2.6 MYA).

A

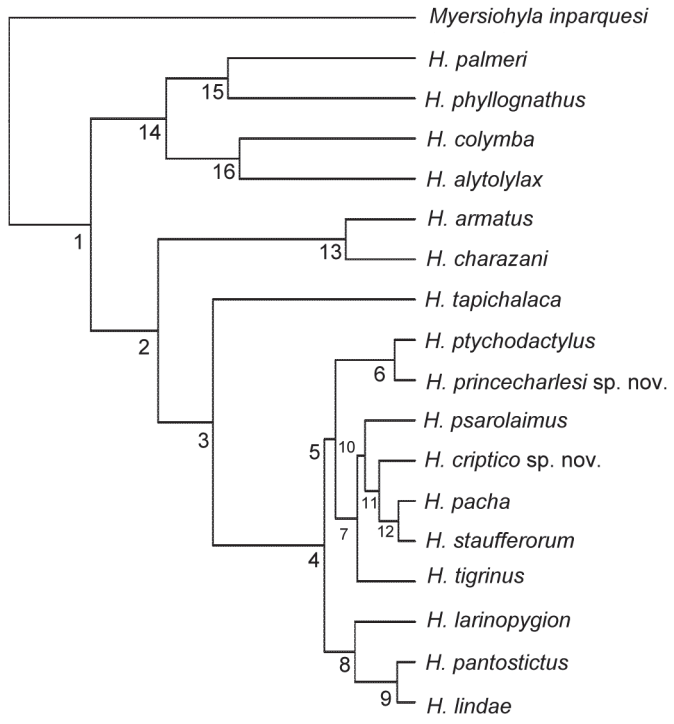

B

	Pseudacris substitution rate (0.00277)	Hylid Fossil calibrations + GAARlandia
Node 1	61.0 47.7–75.7	51.2 32.1–71.26
Node 2	48.6 34.1–62.6	40.9 24.7–59.8
Node 3	38.9 26.1–52.6	31.9 18.4–48.6
Node 4	15.3 11.2–19.9	14.2 8.6–21.0
Node 5	12.8 9.2–16.8	12.6 7.4–18.6
Node 6	3.2 1.3–5.6	3.2 0.6–6.7
Node 7	9.8 6.9–13	9.1 5.1–13.6
Node 8	11.2 6.9–15.7	9.4 4.4–15.3
Node 9	3.1 1.4–5.1	2.8 0.7–5.4
Node 10	8.7 6–11.6	7.9 4.1–11.9
Node 11	6.6 4.3–9	5.6 2.7–9.1
Node 12	3.1 1.6–4.8	2.6 0.9–4.7
Node 13	12.1 5.7–19.1	10.9 2.9–21.3
Node 14	49.1 35.7–62.5	39.2 22.5–55.7
Node 15	40.7 25.6–57.1	29.7 13.71–46.3
Node 16	35.1 22.4–48.1	27.7 13.3–43.5

FIGURE 4.—(A) Cladogram showing numbered clades of *Hyloscirtus* for which divergence times were estimated, (B) Divergence times estimated in MYA and 95% confidence intervals for each clade with hylid fossil and paleobiogeographic calibration methods.

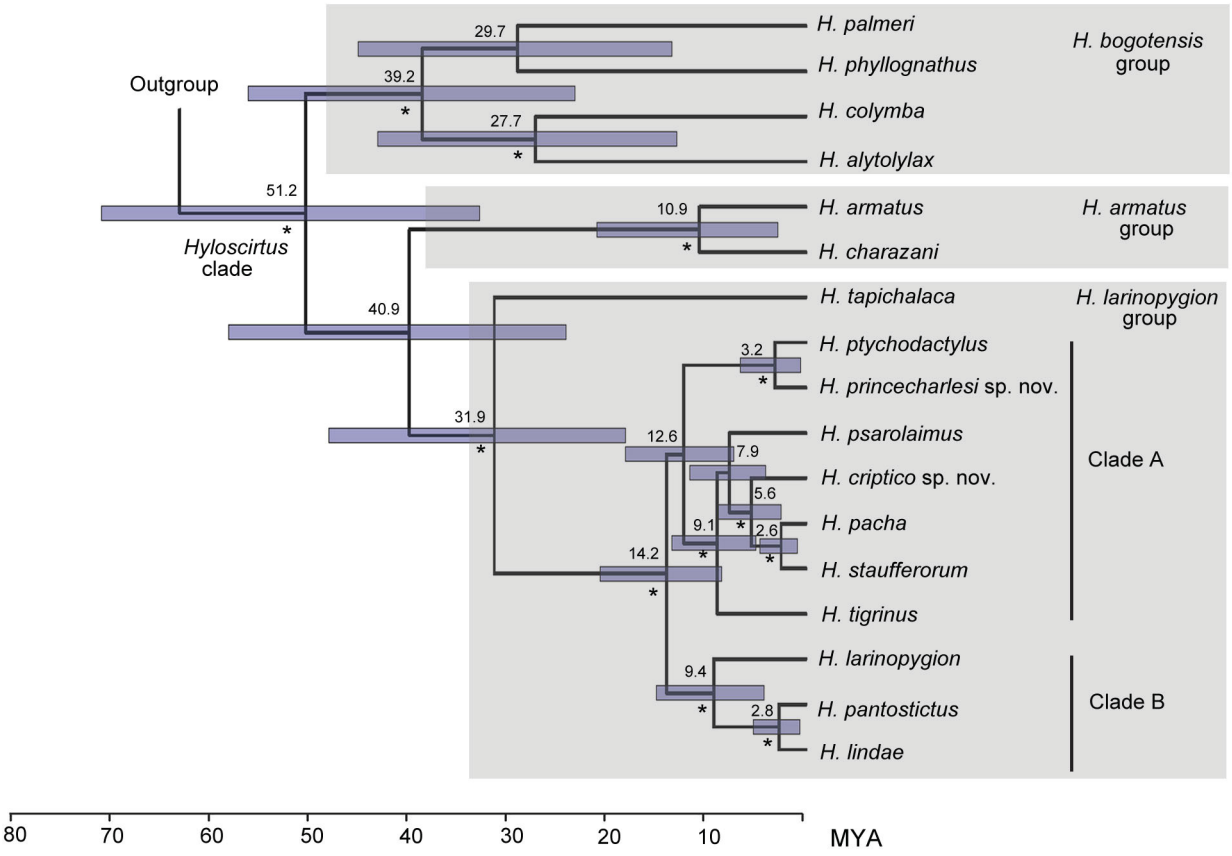

FIGURE 5.—Minimum divergence time estimates of *Hyloscirtus* clades obtained in BEAST using hylid fossil and paleobiogeographic calibrations. Bars indicate 95% confidence range and * Bayesian posterior probabilities > 95.

New species

***Hyloscirtus criptico* sp. nov.**
Figs. 1A, 6A, 7A–C

Holotype. CJ 311, an adult female from a cascading stream on the borderline between Reserva Cotacachi-Cayapas and private land owned by Manuel Quinchiguango, at Recinto San Antonio, Cuellaje, Provincia Imbabura, Ecuador (0º 28' 23.772" N, 78º 34' 12.756" W; 2794 m); obtained on 22 July 2011 by Elicio E. Tapia, Carl R. Hutter, Carlos Quinchiguango, and William Quinchiguango.

Paratypes. CJ 312–313, adult males with same collection data as holotype; CJ 309–310, adult females from Reserva Las Gralarias, Provincia Pichincha, Ecuador (0º 1' 30.66" S, 78º 42' 10.98" W; 2175 m); obtained on 9 and 11 June 2009 respectively, by Carl R. Hutter, Henry Imba, and Timothy Kell; QCAZ 43516–18, 43528, four adult females from the headwaters of a stream at borderline between Reserva Cotacachi-Cayapas and a private land owned by Manuel Quinchiguango, at Recinto San Antonio, Cuellaje, Provincia Imbabura, Ecuador (0º 28' 20.8194" N, 78º 33' 57.6" W; 2760–2885 m); obtained on 24 June 2009 by Luis A. Coloma, Manuel A. Morales-Mite, and Elicio E. Tapia.

Diagnosis. A member of the *Hyloscirtus larinopygion* group as diagnosed by Faivovich *et al.* (2005). *Hyloscirtus criptico* differs from other members of the group by having a unique combination of color patterns and external morphological features (see comparisons below), and a genetic distance from other species of at least 3.7 % in fragments ~ 2.3 kb of aligned mitochondrial DNA sequences. The most similar color patterns are seen in *H. larinopygion* (Fig. 1B), *H. pacha* (Fig. 1D), *H. psarolaimus* (Fig. 1G), *H. ptychodactylus* (Fig. 1H), and *H. staufferorum* (Fig. 1I), all of which have brown dorsums and black and white bars on the flanks and concealed surfaces of the limbs. The new species differs from *H. larinopygion* by having small orange flecks and stippling on the dorsum and venter (absent in *H. larinopygion*), and a dark brown dorsum (pale brown in *H. larinopygion*). Additionally, these are not sister species (Fig. 3). *Hyloscirtus criptico* differs from *H. ptychodactylus,* a species from the slopes of western Ecuador, by having well defined black and white bars on the limbs (white bars absent in *H. ptychodactylus*), and by having a dark gray iris color (sky-blue in *H. ptychodactylus*). *Hyloscirtus criptico* differs from *H. pacha* from the slopes of southeastern Ecuador by having a small calcar on the heel (larger in *H. pacha*) and by lacking tubercles along the ventrolateral edge of the arm (prominent in *H. pacha*). *Hyloscirtus criptico* differs from *H. psarolaimus* from the slopes of eastern Ecuador by having black and white bars on flanks (spots and irregular marks in *H. psarolaimus*) and by lacking a mid-dorsum cream line (present in *H. psarolaimus*). Finally, the new species differs from *H. staufferorum* from the slopes of eastern Ecuador by having a boldly, mottled black and cream ventral pattern (venter uniform gray or nearly uniform in *H. staufferorum*).

Description of holotype. SVL 71.4 mm. Body and limbs robust. Snout nearly truncate in dorsal and lateral view. Head about as broad as long. Head widest at posterior level of mandible (22.7 mm), representing 31.8% of SVL. Canthus rostralis rounded. Loreal region slightly concave. Lips rounded, not flared. Dorsal surface of internarial region nearly flat. Nostrils barely protuberant, directed anterolaterally, slightly posterior to anterior margin of lower jaw. Top of head slightly concave. Tympanum vertically ovoid, tympanic annulus distinct. Supratympanic fold thick, curved, not covering posterodorsal edge of tympanum, extending from eye to posterior end of mandible and to shoulder.

Forearms robust compared to upper arms. Axillary membrane absent. Ulnar tubercles absent. Fingers broad. Disks round, expanded, wider than finger. Relative lengths of fingers 1<2<4<3. Lateral fringes absent. Palmar surface (Fig. 7B) with deep folds and low raised, oval, supernumerary tubercles. Subarticular tubercles single, large, thick, rounded, or oval. Thenar tubercle thick, elliptical. Palmar tubercle round. Prepollex absent. Fingers webbed basally, manus webbing formula: I 3–3 II 2–3 III 2 1/2–2 1/2 IV. Hind limbs robust. Tibia length 47.6% of SVL. Small conical heel tubercle present. Inner tarsal fold absent. Foot length 47.3% of SVL. Inner metatarsal tubercle large, oval (Fig. 7C). Outer metatarsal tubercle absent. Subarticular tubercles round or oval. Supernumerary tubercles absent. Toe discs wider than fingers. Relative lengths of toes I<2<3<5<4. Foot webbing formula: I 2–3 II 2–2 1/2 III 2–2 1/2 IV 2–1 1/2 V.

Skin on throat, chest and belly smooth, the latter bearing a transversal fold at gular level. Pelvic patch areolate. Transverse supracloacal flap long. Margins of vent with numerous small folds and two large lateral swollen glandular areas at proximal posterior thighs. Cloacal opening directed posteriorly. Dentigerous processes of vomers

long, transverse, separated medially, behind level of large, ovoid choana, bearing 28 teeth evident in the buccal mucosa. Tongue broad, cordiform, shallowly notched posteriorly, fully attached to mouth floor.

Color in preservative (~70% ethanol). Dorsum of head, body, forearms, shanks, and outer margin of feet grayish-brown densely stippled with minute, cream flecks. Anterior and posterior surfaces of thighs barred with four or five white and brown bars crossed by a transverse dark brown stripe. Ventral surfaces of upper arms with dark brown marks on a cream background and shanks barred with cream and brown. Dorsal surfaces of Fingers I–II and toes I–III bearing white and dark brown marks, fingers III–IV and toes IV–V mostly dark brown. Glandular area lateral to vent having brown with cream stippling. Flanks bearing white and bold brown markings. Throat, chest, abdomen with boldly, mottled dark brown and cream, larger cream marks toward the distal longitudinal axis. Pelvic patch brown. Palmar and plantar surfaces gray. Tympanum brown with cream stippling similar to adjacent areas.

FIGURE 6.—Holotypes of (A) *Hyloscirtus criptico* (CJ 311), and (B) *H. princecharlesi* (CJ 308). Photos by Luis A. Coloma.

Color in life. (Fig. 6A). Same as above except in that dorsum marks and blotches are bright orange varying to pale orange and yellow-cream. Blotches on hidden surfaces of thighs are creamy-white. Ventral surfaces are black with yellow-cream marbling. Tips of dorsal surfaces of fingers and toes are pale creamy-orange. Ventral pads of digital discs on fingers and toes are gray. Iris is dark gray.

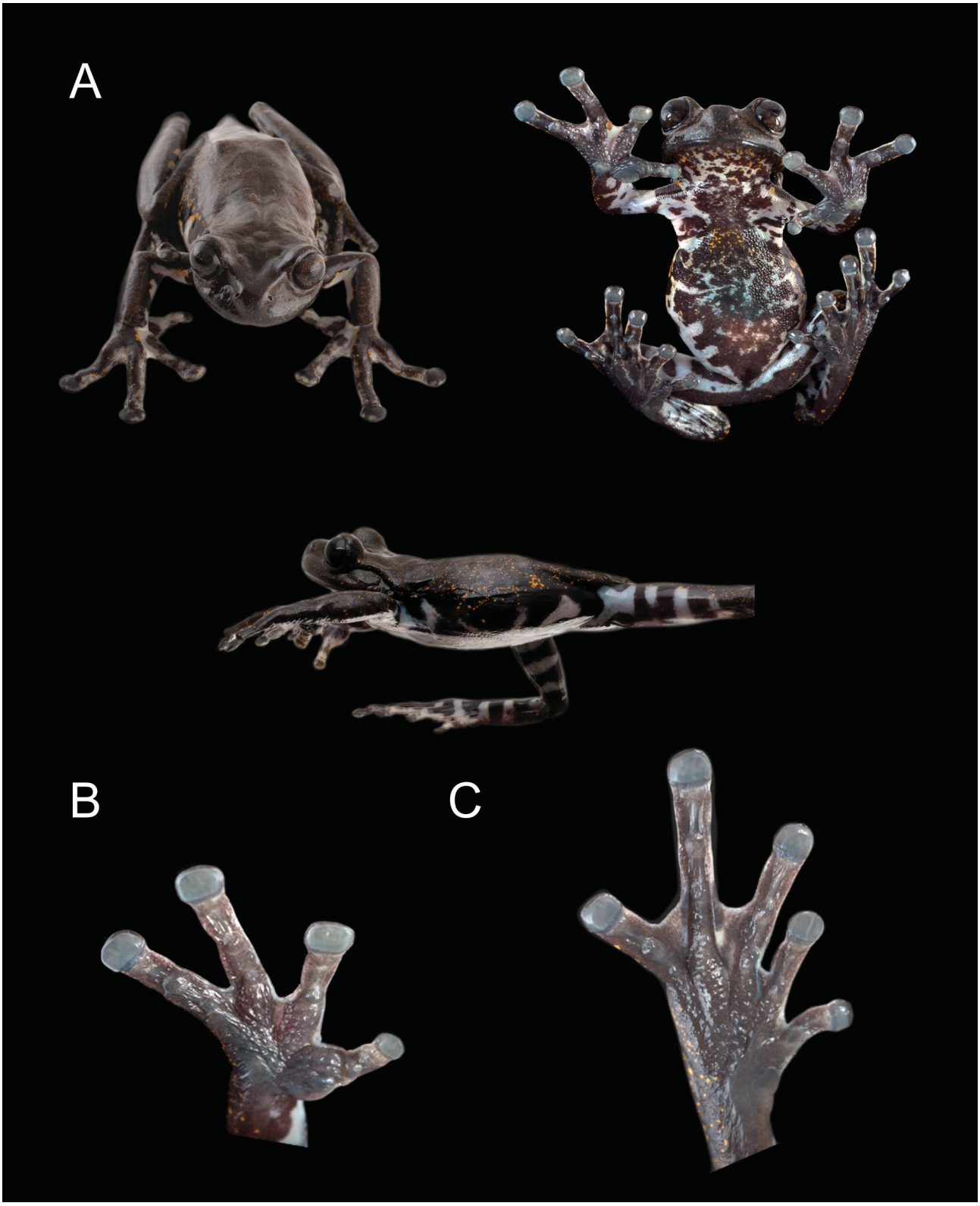

FIGURE 7.—Holotype of *Hyloscirtus criptico*, adult female (CJ 311), SVL = 71.4 mm: (A) dorsal, ventral and lateral views, (B) ventral view of right hand, enlarged 2X of A, and (C) ventral view of right foot, enlarged 2.6X of A. Photos by Luis A. Coloma.

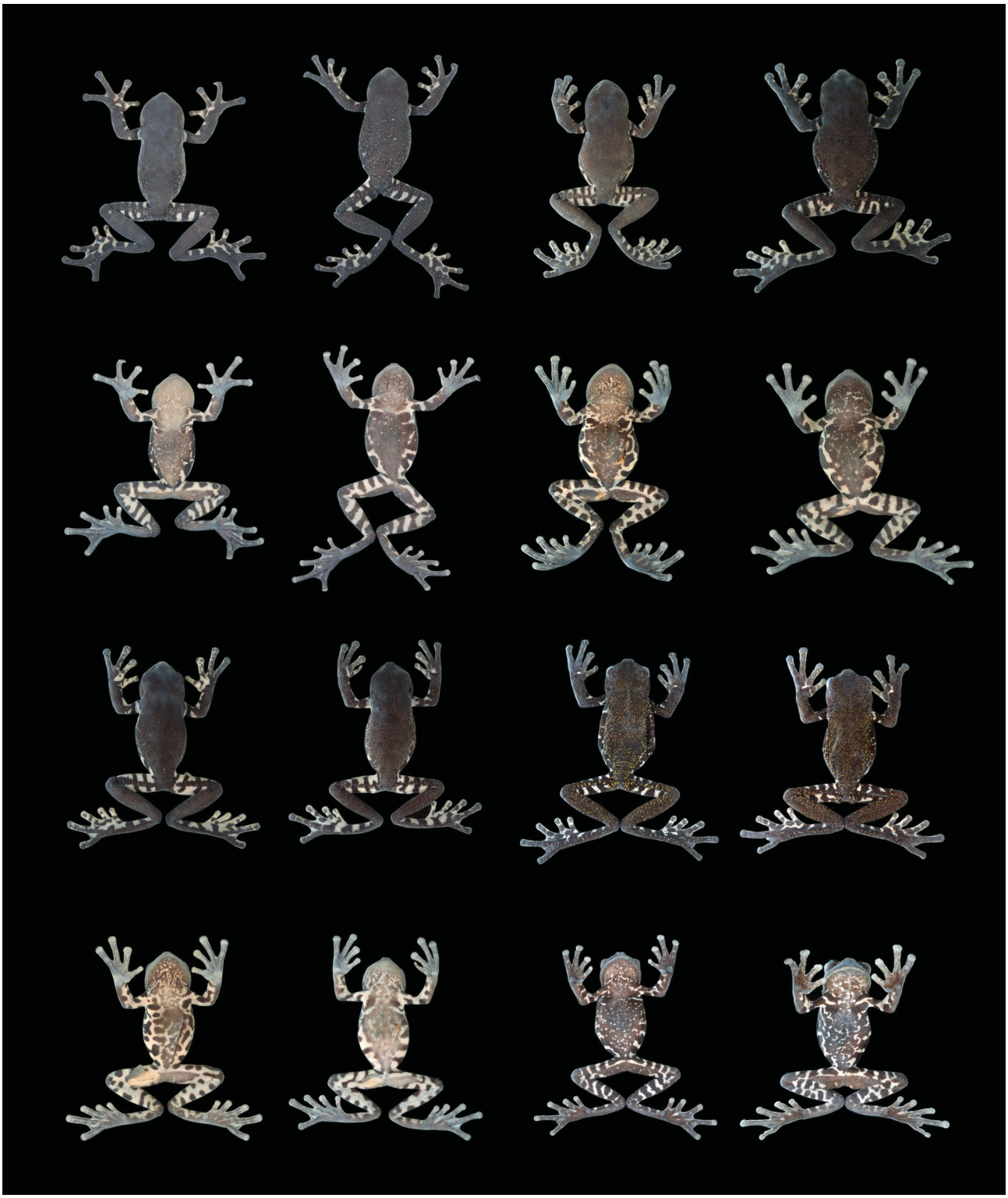

FIGURE 8.—Adults of *Hyloscirtus criptico* showing variation in dorsal and ventral color pattern (from left to right): CJ 312, CJ 313, QCAZ 43516, QCAZ 43517, QCAZ 43518, QCAZ 43528, CJ 309, CJ 310. Not to scale. Photos by Luis A. Coloma.

Measurements of holotype (mm). SVL 71.4, TIBL 34, FEL 30.3, FOL 33.8, RDUL 20.1, HANDL 24.5, THBL 15.9, HLSQ 23, HDW 22.7, ITN 4.5, EYNO 3.9, TYD 3.4, DFW 4.6, DTW 4, SW 13.7.

Variation. Dorsum and ventral color pattern variation of paratypes is depicted on Figure 8. Morphometric variation is indicated in Table 7. Dentigerous processes of vomers are abutted medially, and vomerine teeth number varies from 16 to 30 as follows: 26 teeth (CJ 309), 26 (CJ 310), 16 (CJ 313), 22 (CJ 312), 25 (QCAZ 43516), 19

(QCAZ 43517), 20 (QCAZ 43518), 30 (QCAZ 43528). Dorsum color varies from nearly uniform dark brown in CJ 365 to heavily stippling on a dark brown background in CJ 250 and 251. Dorsal bars on thighs and ventral bars on shanks vary between 4 or 5. Sexual dimorphism is apparent in males having a venter more uniform (dark brown or gray) than females, which have more cream marks. Besides, males have vocal slits.

Tadpoles. Tadpoles of this species are unknown.

Distribution, natural history, and conservation status. *Hyloscirtus criptico* is known from three localities at elevations of 2175–2794 m, in cascading streams in Montane Cloud Forest (Valencia *et al.* 1999) on the western versant of Cordillera Occidental de los Andes from Carchi, Imbabura, and Pichincha provinces (Fig. 9). The area of distribution is approximately 1570 km^2. At the known localities annual mean precipitation is 1516, 1597, and 1653 mm, and the annual mean temperatures are 14.3, 16.0, and 13.4 ºC (estimated from the WorldClim data set; Hijmans *et al.* 2005). Distribution at "Hercules Creek" at Reserva Las Gralarias is indicated in Figure 10. Average daily rainfall from 17 January 2011 to 1 July 2011 at Las Gralarias is given in Hutter and Guayasamin (2012).

Toral *et al.* (2002) provide a detailed description of the type locality and a record of three males of this species (cited as *Hyla larinopygion*). Quiguango (1997) provided a map, a description of biotic and abiotic features at San Venancio, El Rosario (ca. Cuellaje), Cordillera de Toisán, and abundance data of *Hylocirtus criptico* (cited as *Hyla larinopygion*). At the mentioned locality, *H. criptico* is an uncommon species, and was only found in the rainy season in January 1994.

At San Antonio (ca. Cuellaje) (type locality) (Fig. 11B–D), *Hyloscirtus criptico* was found at the upper part of a cascade that is about 10 m wide and 8 m high. The headwater springs are about 20 m higher than the collecting site and about 80 m from the nearest divide. Mosses and epiphytes were abundant on the vegetation along the stream. Adults were collected during night at the stream, except a female (QCAZ 43528) that was collected on the ground in a primary forest of the mountain crest. CJ 311 (holotype) and CJ 312–313 (paratypes) were collected among branches of a fallen tree and shrubs, which were decomposing over the streambed, which had small water ponds. QCAZ 43516–17 were collected on branchs 1.5–4 m above ground over the streambed; there was no rain, but clouds were inside the forest. QCAZ 43518 was on a stone in the streambed. At this locality, *H. criptico* was found in microsympatry with *H. princecharlesi*, and in one case within 10 m of each other.

The habitat at Reserva Las Gralarias is undisturbed. A trail to the stream was recently established, but no pastures or agricultural activity occurs upstream. The stream is 2–4 m across. Water temperatures were: 14.1, 13.9–14.3 ºC (n = 4) and pH values were 7.6, 7.5–7.7 (n = 4). Specimens were found during the night within 20 m of each other at an air temperature of 13 ºC. There was a light rain, no moonlight, and no clouds. CJ 309 was found at 3:49 am, perched on a large aroid leaf, 4 m directly above the stream, and about 0.5 meters above ground. CJ 310 was found at 2:35 am, perched on a horizontal branch, facing the stream, 2.5 m vertically above stream and 1 m horizontally away from water, on a sloping bank, and 0.5 m above the ground. At this locality, *Hyloscirtus criptico* occurs microsympatrically with five stream breeding glassfrogs (*Centrolene ballux* Duellman and Burrowes 1989*, C. heloderma* [Duellman 1981]*, Nymphargus grandisonae* [Cochran and Goin 1970]*, N. griffithsi* [Goin 1961], and *N. lasgralarias* Hutter and Guayasamin 2012).

Hyloscirtus criptico is considered as Endangered (A3ce IUCN criteria) due to a suspected population size reduction of ≥ 50% suspected to be met within the next 10 years, where the reduction or its causes may not have ceased. The area of extent of ocurrence (1570 km^2) is relatively small, and the localities of its small known areas of occupancy are being modified by human activities and is being severely affected by growing habitat destruction. Threats are logging, burning, unregulated use of land for agriculture, cattle raising, pesticide use, and invasive trout in the regional streams. Besides, it is likely that climate change and emerging pathogens are affecting its populations as has been documented for numerous other Andean frogs (Pounds *et al.* 2010). Rapid and integrative conservation measures are urgently needed, among which the protection and restoration of its habitat are a priority, as well as the establishment of an *ex-situ* assurance colony.

Etymology. The specific name *criptico* is used as a noun in apposition. Criptico is a Spanish word that means hidden and it is used in reference to specimens of this species, which were initially confused with a sympatric species *Hyloscirtus larinopygion*. Its name calls attention to cryptic species, which are being revealed frequently in the recent taxonomic literature, especially with the advent of molecular analyses and integrative taxonomy (e.g., Elmer and Cannatella 2008, Páez-Vacas *et al.* 2010, Funk *et al.* 2011, Hutter and Guayasamin 2012).

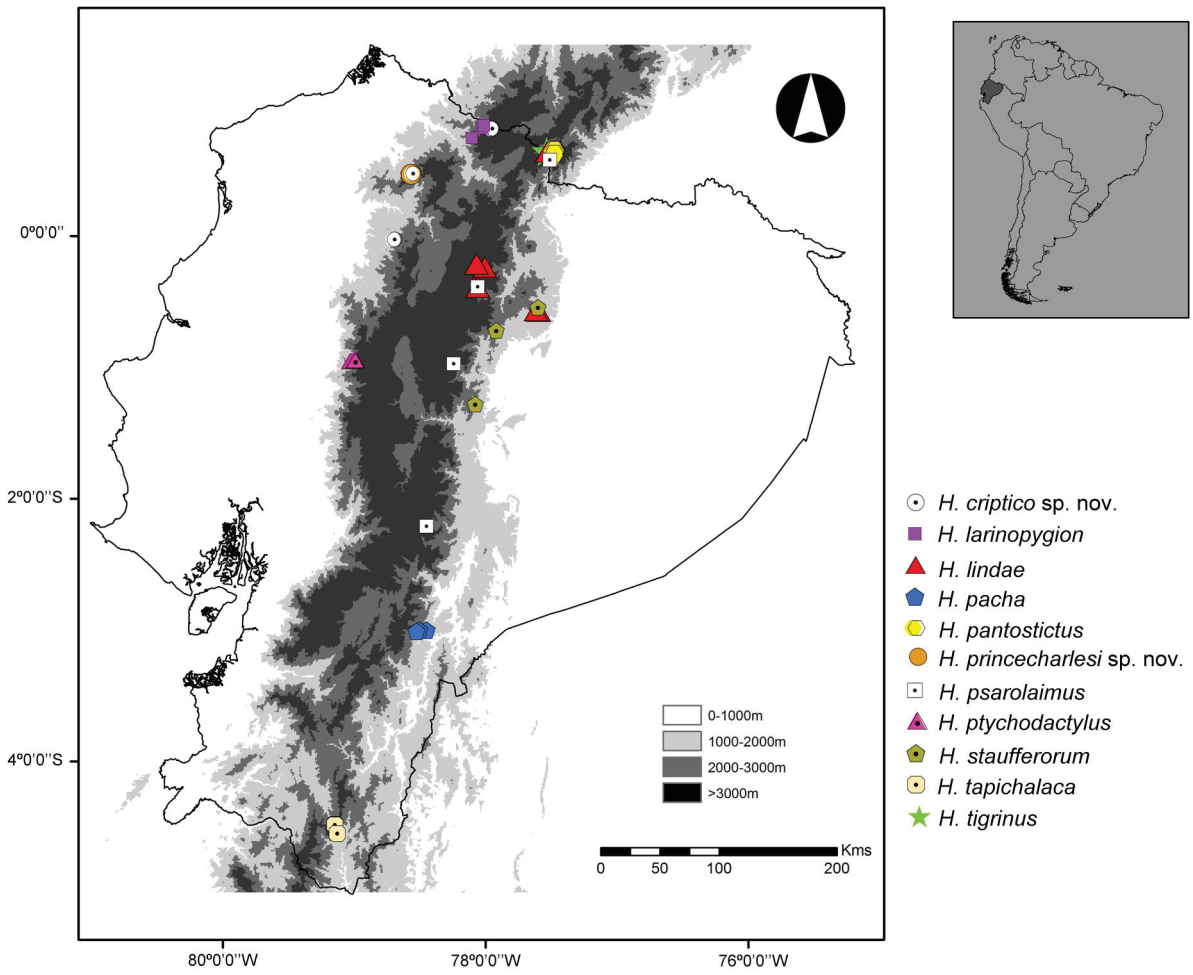

FIGURE 9.—Ecuadorian localities of eleven species of the *Hyloscirtus larinopygion* group included in this study. See Table 4 for detailed locality data. Some nearby localities are represented by a single symbol.

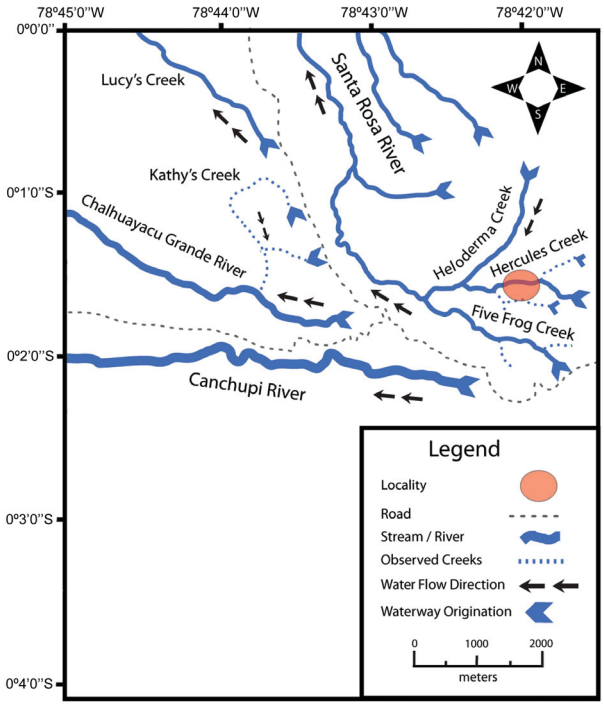

FIGURE 10.—Map showing the collection site of *Hysloscirtus criptico* at Las Gralarias Reserve, Provincia Pichincha, Ecuador. Illustration by Carl R. Hutter.

Comments. Most previous records of *Hyloscirtus larinopygion* from Ecuador in the provinces of Carchi and Imbabura are erroneous, and belong to *H. criptico* as described herein. Duellman and Coloma (1993) assigned the name *Hyla larinopygion* to five adult males (QCAZ 4167–71) and eight tadpoles (QCAZ 4172) from 22 Km E of Maldonado, Provincia Carchi. Their assignment was done on the basis of size and overall phenetic similarity of adults when compared to specimens from Municipio Sonsón in Departamento Antioquia, Colombia. Nonetheless, they noted differences in dorsal coloration. All these adult males (QCAZ 4167–71) are herein referred to *Hyloscirtus criptico.* A series of tadpoles (QCAZ 4172) may be either *H. criptico* or *H. larinopygion,* which co-occur at nearby sites. Quiguango (1997) and Toral (2002) also assigned the name *Hyla larinopygion* to specimens from San Venancio, Cuellaje, Provincia de Imbabura; these specimens also represent *H. criptico.* Additional records of *H. larinopygion* from Provincia Imbabura provided by Bolívar *et al.* (2004) are unconfirmed because no voucher specimens were provided.

Yánez-Muñoz and Meza-Ramos (2006) published a color photo of *Hysloscirtus larinopygion* from Morán, Provincia de Carchi, Ecuador. Herein we provide records (based on voucher specimens) of adults of *H. larinopygion* that were collected in Provincia de Carchi. They are: QCAZ 29211–12 from 24 Km E of Maldonado (0º 49' 23.376" N, 78º 1' 31.4" W; 2664 m; on the Tulcán-Maldonado road), Provincia Carchi collected on 4–5 June 2004 by Néstor Acosta-Buenaño, Ítalo G. Tapia, and Catherine Graham; QCAZ 41826 from Comunidad de Morán (0º 44' 48.1194" N, 78º 6' 14.004" W; 2452m), Provincia Carchi, collected on 23 September 2008 by Ítalo G. Tapia, Juan F. Dueñas, and Carlos Castro; QCAZ 38418 (a series of tadpoles) from Cerro Centella, cascada Centella, 2709 m, on the road Tulcán-Maldonado), Provincia Carchi, collected on 17 September 2008 by Juan F. Dueñas and Ítalo G. Tapia. Tadpoles were raised under lab conditions and their identification as *H. larinopygion* was confirmed (see description provided under Tadpoles and ontogeny).

***Hyloscirtus princecharlesi* sp. nov.**
Figs. 1F, 11A, 12A–C

Holotype. CJ 308 an adult male from a cascading stream on the border between Reserva Cotacachi-Cayapas and a private land owned by Manuel Quinchiguango, at Recinto San Antonio (ca. Cuellaje), Provincia Imbabura, Ecuador (0º 28' 23.772" N, 78º 34' 12.756" W; 2794 m); obtained on 22 July 2011 by Elicio E. Tapia, Carl R. Hutter, and Carlos Quinchiguango.

Paratypes. QCAZ 43654, 44893 adult males with same locality as holotype (0º 28' 20.8194" N, 78º 33' 57.6" W; 2720–2794 m); the former obtained on 23 June 2009 by Elicio E. Tapia and William Quinchiguango, and the latter on 24 June 2009 by Luis A. Coloma, Manuel A. Morales-Mite, and Elicio E. Tapia.

Diagnosis. A member of the *Hyloscirtus larinopygion* group as diagnosed by Faivovich *et al.* (2005). The new species differs from other members of that group by having a unique pattern of dorsal coloration (series of well defined orange blotches or spots densely and uniformly distributed on a black background), a genetic distance from other members of the group of at least 1.31% (for fragments of ~ 2.3 kb of aligned mitochondrial DNA sequences), poorly expanded digital discs, and a glandular nuptial pad on thumb. The most similar dorsal coloration is seen in *H. pantostictus* (Fig. 1E) and *H. ptychodactylus* (Fig. 1H), both of which have orange spots or blotches. *Hyloscirtus princecharlesi* differs from *H. pantostictus* from the slopes of northeastern Ecuador by having gray digital discs (yellow in *H. pantostictus*); also, the two species are not sister taxa (Fig. 3). The new species is distinguished from its sister species, *H. ptychodactylus* from the slopes of western Ecuador at Cotopaxi province by having well defined spots or blotches on dorsum (scattered, diffuse, spots or blotches and dense stipling among blotches in *H. ptychodactylus*), and by having a gray iris color (sky-blue in *H. ptychodactylus*).

Description of holotype. SVL 70.5 mm. Body and limbs robust. Snout nearly truncate in dorsal and lateral view. Head about as broad as long. Head width at level of eyes (21.8 mm), 30.9% of SVL. Canthus rostralis rounded. Loreal region slightly concave. Lips rounded, not flared. Dorsal surface of internarial region nearly flat. Nostrils barely protuberant, directed anterolaterally, slightly posterior to anterior margin of lower jaw. Top of head nearly flat. Tympanum vertically ovoid, tympanic annulus distinct. Supratympanic fold thick, curved, covering dorsal edge of tympanum, extending from eye to posterior end of mandible and to shoulder.

Forearms robust compared to upper arms. Axillary membrane absent. Ulnar tubercles absent. Fingers broad. Disks round, barely expanded or Finger I about same width as finger. Relative lengths of fingers 1<2<4<3. Lateral

fringes absent. Palmar surface (Fig. 12B) with deep folds and low raised, round, supernumerary tubercles. Subarticular tubercles single, large, thick, rounded, or oval. Thenar tubercle thick, elliptical. Palmar tubercle barely noticeably. Prepollex absent. Glandular nuptial pad covering the outer margin of Finger I (Fig. 13A). Fingers webbed basally, manus webbing basal (Fig. 12B). Hind limb robust. Tibia length 46.5% of SVL. Heel tubercles absent. Inner tarsal fold absent. Foot length 44.7% of SVL. Inner metatarsal tubercle large, oval (Fig. 12C). Outer metatarsal tubercle absent. Subarticular tubercles round. Supernumerary, low raised tubercles present. Toe discs not expanded. Relative lengths of toes I<2<3<5<4. Foot webbing basal (Fig. 12C).

Skin on throat and anterior portion of chest bearing irregular scattered folds on a weakly areolate skin that extends to abdomen. Pelvic patch areolate. Transverse supracloacal flap long. Margins of vent with numerous small folds and two large lateral swollen glandular areas at proximal posterior thighs. Cloacal opening directed posteriorly. Vocal slits present at posterior lingual margins of mandibles. Dentigerous processes of vomers long, transverse, abutting medially, behind level of large, ovoid choana, bearing 24 teeth evident in the buccal mucosa. Tongue broad, cordiform, shallowly notched posteriorly, fully attached to mouth floor, rugose on its anterior portion. Vocal sac single, median, subgular.

Color in preservative (~70% ethanol). Dorsum with a pattern of dense, brown-orange, round-oval marks, and blotches on a black background, forming a reticulated pattern at mid-dorsum and more isolated blotches towards the flanks. Dorsum of limbs with larger marks and blotches than body. Anterior and posterior surfaces of thighs nearly black with two large faint gray blotches. Dorsum of inner fingers and toes gray with faint creamy-gray blotches that become brighter toward Fingers IV and Toes IV–V. Glandular area lateral to vent brown-orange. Throat, chest, abdomen with diffuse black-gray marbling. Inner margin of lower lip cream. Anterior flanks with three large round marks, posterior flanks barred. Tympanum mostly black.

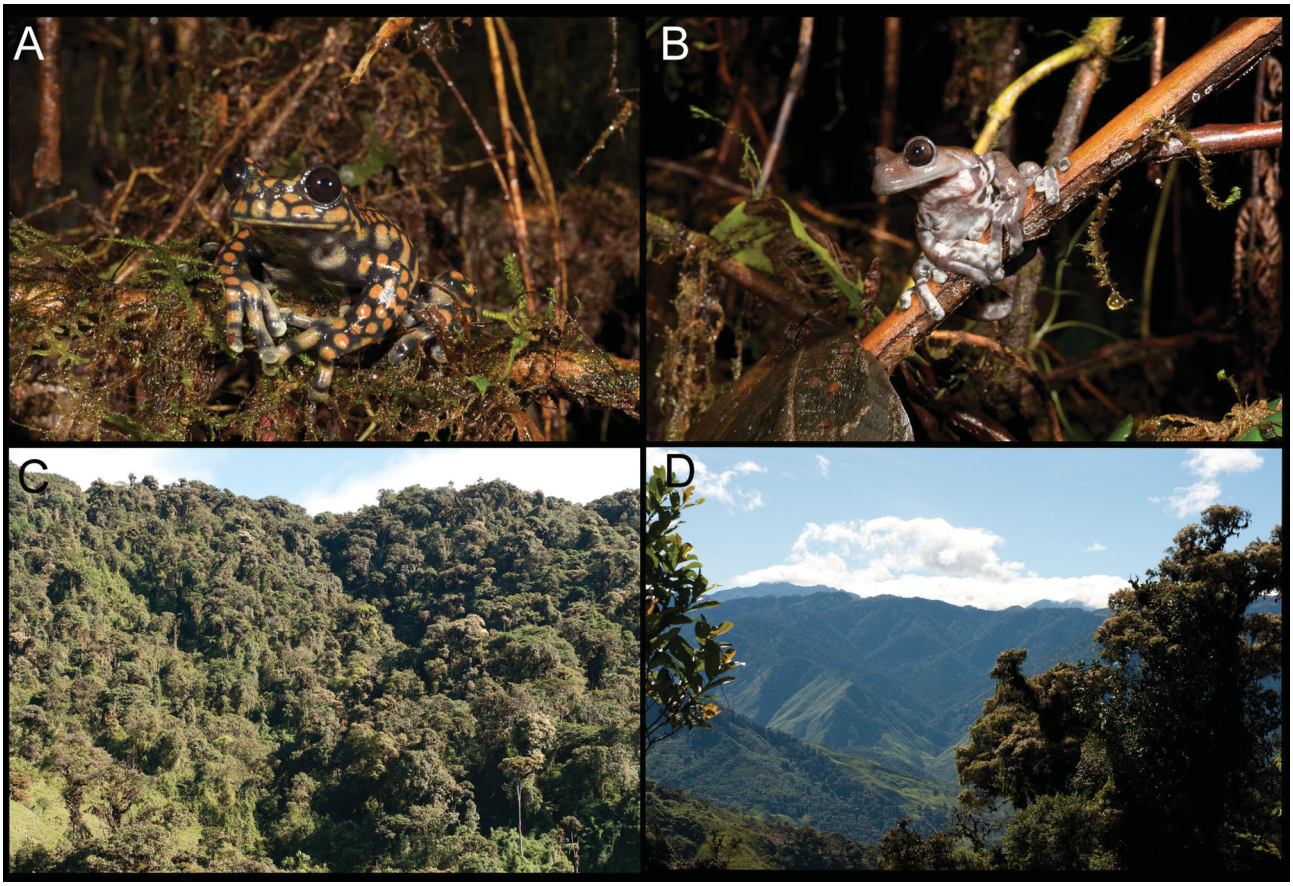

FIGURE 11.—(A) *Hyloscirtus princecharlesi in situ,* (B) *H. criptico in situ,* (C) cloud forest at the type locality, San Antonio, of *H. criptico* and *H. princecharlesi*, and (D) type locality in the Cordillera de Toisán, Provincia Imbabura. Photos by Luis A. Coloma.

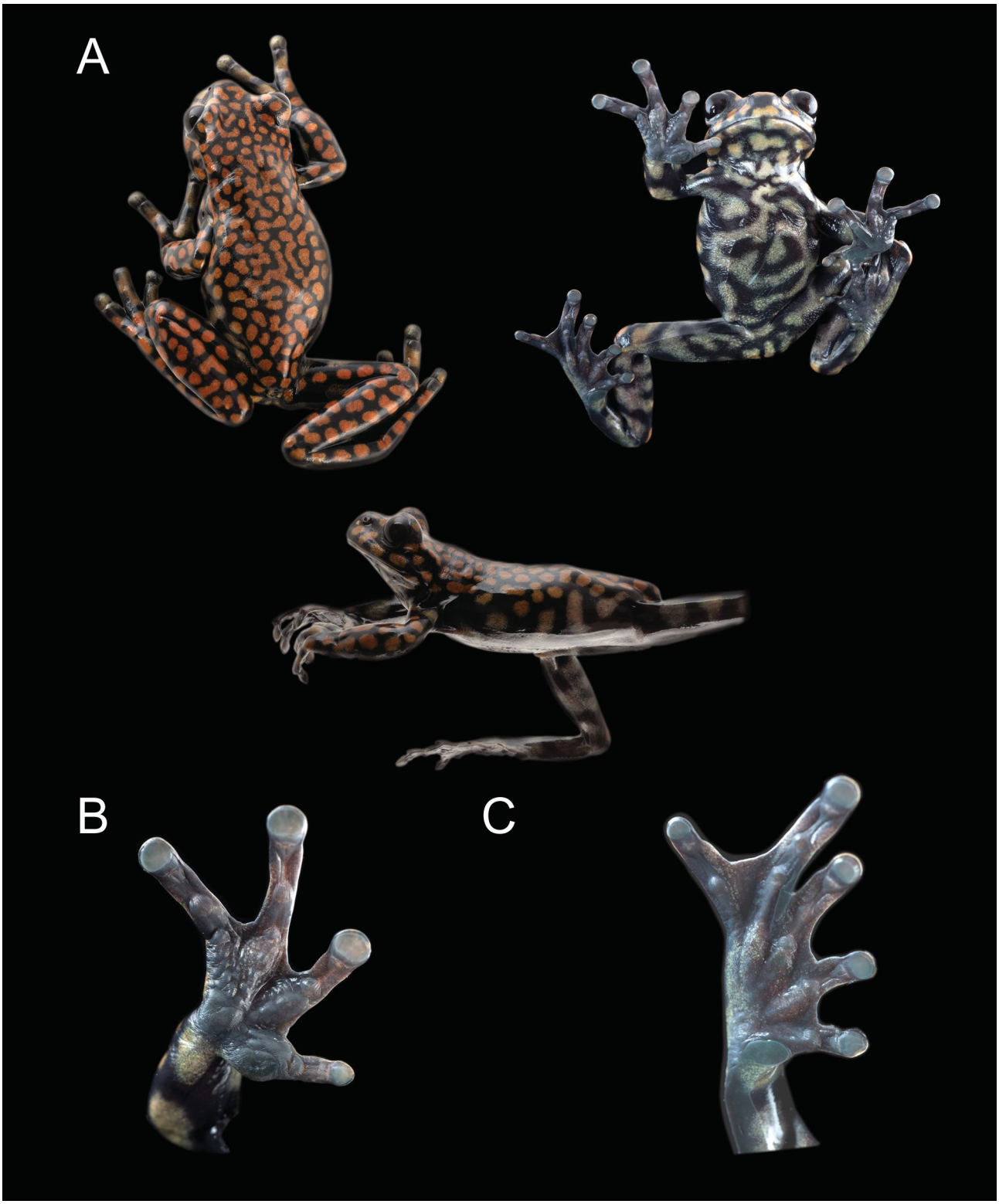

FIGURE 12.—Holotype of *Hyloscirtus princecharlesi*., adult male (CJ 308), SVL = 70.5 mm: (A) dorsal, ventral and lateral views, (B) ventral view of right hand, enlarged 2.6X of A, and (C) ventral view of right foot, enlarged 2.6X of A. Photos by Luis A. Coloma.

Color in life (Fig. 6B). Same as above except in that dorsal marks and blotches are orange, varying to pale orange. Blotches on hidden surfaces of thighs are creamy white. Ventral surfaces are black with yellow-cream marbling, more yellow at gular region. Tips of dorsal surfaces of fingers and toes are pale creamy-orange with gray. Palmar and plantar surfaces are gray to black. Ventral pads of digital discs on fingers and toes are gray. Iris is dark gray.

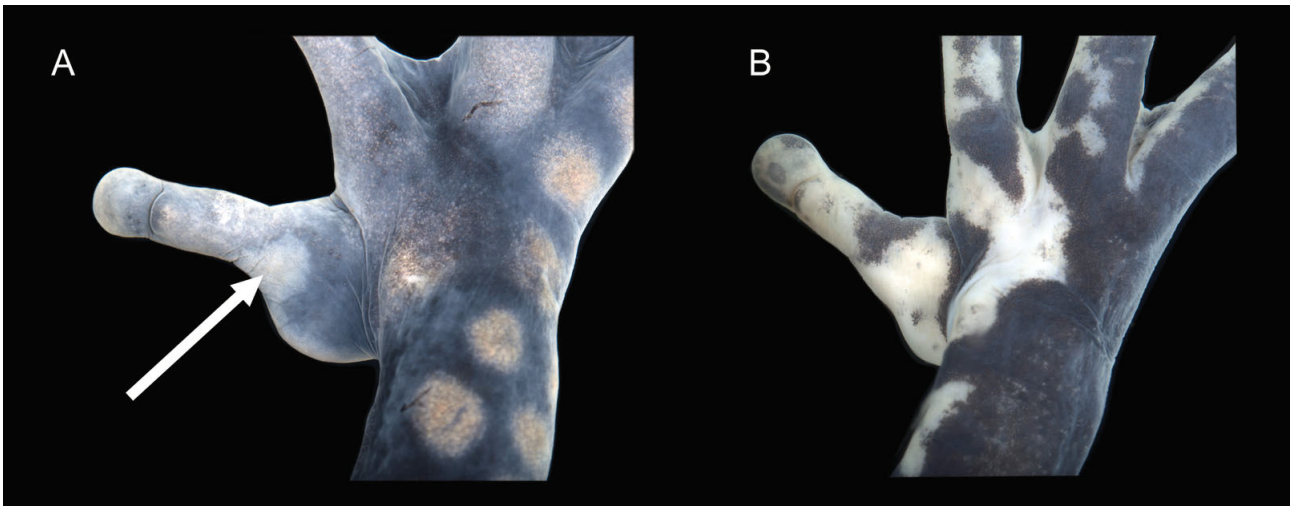

FIGURE 13.—Dorsal view of right hand of males of (A) *Hyloscirtus princecharlesi* (QCAZ 43654), and (B) *H. criptico* (QCAZ 43517). The arrow indicates a glandular nuptial pad covering the outer margin of Finger I, absent in *H. criptico.* Photos by Luis A. Coloma.

Measurements of holotype (mm). SVL 70.5, TIBL 32.8, FEL 31.5, FOL 31.5, RDUL 17.9, HANDL 24.7, THBL 16.7, HLSQ 23.9, HDW 23.4, ITN 6.0, EYD 7.2, EYNO 4.7, TYD 3.6, DFW 3.9, DTW 3.1.

Variation. Measurements variation of two paratypes (QCAZ 44893, 43654) and the holotype (CJ 308) are indicated in Table 7. The adult male paratypes overall are very similar to the holotype except for differences in color strength and patterns (Fig. 14), by bearing 29 vomerine teeth in QCAZ 44893 and 23 in QCAZ 43654, and by having slightly smaller finger discs in QCAZ 44893.

Tadpoles. See under Tadpoles and ontogeny section.

Distribution, natural history, and conservation status. *Hyloscirtus princecharlesi* is known only from its type locality (San Antonio, ca. border of Reserva Ecológica Cotacachi-Cayapas), a cascading stream in Montane Cloud Forest (Fig. 11C, D) (according to the classification proposed by Valencia *et al.* 1999). The locality is in northwestern Ecuador in the Cordillera de Toisán, a mountain range that is part of the Cordillera Occidental of the Ecuadorian Andes, in Provincia de Imbabura, at an elevation of 2720–2794 m (Fig. 9). At the type locality, the annual mean precipitation is 1671 mm and the annual mean temperature is 14.1 ºC (based on the WorldClim database; Hijmans *et al.* 2005). Toral *et al.* (2002) provide a detailed description of the type locality and a record of a female of this species (under the name *Hyla* sp 1.).

The holotype CJ 308 was active during the night (21:50h) 2 m above the ground, on bushy vegetation, containing decomposing leaves mixed with mosses, and epiphytes, and surrounded by dense natural vegetation. It was located at the upper part of a cascade that was about 10 m wide and 8 m high. The headwater springs are about 20 m higher than the collecting site and about 80 m from the nearest divide.

Paratypes QCAZ 44893 and 43654 were found active at 19:50h and 21:30h, respectively, at about the same site as the holotype. QCAZ 44893 was 1 m above ground on a leaf (approximately 30 x 40 cm) of an *Anthurium* sp., at the margin of a stream with natural vegetation. QCAZ 43654 was climbing on a branch 2 m above ground, close to a natural wall of stones, with abundant earth and epiphytic vegetation. There was no rain, the forest was cloudy. QCAZ 43654 was found at about 10 m from an individual of *Hyloscirtus criptico.*

Hyloscirtus princecharlesi herein is considered as Endangered (A3ce IUCN criteria) due to a suspected population size reduction of ≥ 50% suspected to be met within the next 10 years, where the reduction or its causes may not have ceased. The single locality currently known for this species is being modified by human activities and is being severely affected by growing habitat destruction. Threats are logging, burning, unregulated use of land for agriculture, cattle raising, pesticide use, and invasive trout in the regional streams. Besides, it is likely that climate change and emerging pathogens are affecting its populations as has been documented for numerous other Andean frogs (Pounds *et al.* 2010). Rapid and integrative conservation measures are urgently needed, among which the protection and restoration of its habitat are a priority, as well as the establishment of an *ex-situ* assurance colony.

FIGURE 14. —Adults of *Hyloscirtus princecharlesi* showing variation in dorsal and ventral color pattern (from left to right to): QCAZ 43654, SVL = 69.8 mm; QCAZ 44893, SVL = 68.1 mm. Photos by Luis A. Coloma.

TABLE 7. Measurements (in mm) of adults of *Hyloscirtus princecharlesi* and *H. criptico.* Mean ± one SD, and range are given. Abbreviations are: SVL (snout-vent length), TIBL (tibia length), FEL (femur length), FOL (foot length), RDUL (radio-ulna length), HANDL (hand length), THBL (thumb length), HLSQ (head length), HDW (head width), ITN (internarial distance), TYD (tympanum diameter), DFW (width disc of Finger III), DTW (width disc of Toe IV).

	Hyloscirtus princecharlesi	*Hyloscirtus criptico*	
	♂ (n = 3)	♀ (n = 7)	♂ (n = 2)
SVL	69.5 ± 1.2 68.1–70.5	67.1 ± 4.3 60.8–72	63.1 ± 1.4 62.1–64.1
TIBL	32.6 ± 0.3 32.3–32.8	33.3 ± 2.4 30.1–36.6	31.4 ± 0.5 31.0–31.7
FEMUR	31.4 ± 1.1 30.3–32.4	30.7 ± 2.8 26.5–34.7	28.4 ± 0.7 27.9–28.9
FOOT	33.2 ± 1.5 31.5–34.2	32.4 ± 2.6 28.4–34.9	30.4 ± 0.8 29.8–31
HLSQ	23.9 ± 0.1 23.8–24	23.0 ± 1.3 21.0–24.7	21.7 ± 0.4 21.4–21.9
HDWD	23.8 ± 0.4 23.4–24.2	22.8 ± 1 21.3–24.1	21.1 ± 0.1 21.0–21.2
ITNR	6.2 ± 0.4 6.0–6.7	5.1 ± 0.4 4.5–5.7	4.8 ± 0.1 4.7–4.8
HAND	25.9 ± 1.1 24.7–26.9	23.0 ± 1.5 20.3–24.7	21.9 ± 0.8 21.3–22.5
THBL	17.0 ± 0.4 16.7–17.4	15.7 ± 1.1 13.7–16.6	14.4 ± 0.1 14.3–14.4
RDUL	17.4 ± 0.6 16.8–17.9	17.8 ± 1.8 14.7–20.1	16.6 ± 0.1 16.5–16.6
TYM	3.8 ± 0.5 3.4–4.4	3.5 ± 0.4 3.0–4.1	3.1 ± 0.1 3.0–3.2
DISC III (hand)	3.9 ± 0.2 3.6–4.1	4.1 ± 0.2 3.9–4.6	4.0 ± 0.4 3.7–4.2
DISC IV (foot)	3.3 ± 0.2 3.1–3.5	3.7 ± 0.3 3.3–4.0	3.5 ± 0.1 3.4–3.6

Etymology. The specific name *princecharlesi* is a patronym that honors His Royal Highness Charles, Prince of Wales (Charles, Philip, Arthur, George, Windsor). In his call to halt tropical deforestation, Prince Charles uses frogs as symbols, and his Rainforests SOS Campaign includes a video with a frog as a rainforest ambassador. For this reason he is affectionately known by the media as the 'frog prince'. Prince Charles is contributing significantly to the growth of awareness in the battle against tropical deforestation, climate change, and the catastrophic extinction of rainforest amphibians. His work is leading to increased awareness of these issues, and this increased awareness benefits biodiversity conservation, sustainability, alleviation of poverty, and ensures ecosystem services for present and future generations.

New country record for Ecuador: *Hyloscirtus trigrinus*

Hyloscirtus tigrinus was named and described from Nudo de los Pastos Departamento Nariño, Colombia, at Municipio de Pasto, Corregimiento El Encano, Reserva Natural Privada Castelví (ca. 01° 10'55.18" N, 77° 09'44.45 W; 3060 m) (Mueses-Cisneros and Anganoy-Criollo, 2008). The description was based on three adult males and one adult female. Additionally, Montezuma and Mueses-Cisneros (2009) provided a record of an adult female from Puracé Natural National Park, Departamento Cauca, Colombia. Later, Mueses-Cisneros and Perdomo-Castillo (2011) provided data on geographic distribution in four additional localities, adding departamentos Putumayo and Huila, Colombia, to the previously known distributional range. In Colombia the distribution of *H.*

tigrinus incorporates 1154.35 km^2 and encompassing an elevational range of 2720–3467 m. Mueses-Cisneros and Perdomo-Castillo (2011) also searched for specimens in northern Ecuador (with no success). They provided data on natural history and conservation of populations in Colombia.

Herein, we report *Hyloscirtus tigrinus* from Ecuador based on tadpoles collected near the Colombian border. Some of these tadpoles were raised to the juvenile stage, and preserved when the identity of juveniles was confirmed (see description under Tadpoles). A comparison of these juveniles (Fig. 27) to the original description of *H. tigrinus* does not reveal any major differences. However, there are subtle differences in coloration, which might be the result of geographic variation or effects of laboratory conditions. Tadpoles were collected at Santa Bárbara, Provincia de Sucumbíos, Ecuador, for the first time on 17 May 1995 by Luis A. Coloma and Felipe Campos-Yánez (QCAZ 10770). Tadpoles have been found in stream pools with slow running water in patches of forest in secondary montane vegetation. The Ecuadorian locality extends the geographic range of *H. tigrinus* 62.4 km (airline) southwest of its type locality, which was the southernmost locality previously known.

Distribution, ecology, and conservation status. *Hyloscirtus tigrinus* is known from paramo and subparamo habitats at elevations of 2620–3467 m on the Cordillera Central in Departamentos del Cauca and Huila to the high massif of the Nudo de Pasto, as defined by Duellman (1979), in southern Colombia to the Cordillera Oriental in Provincia Carchi in northern Ecuador. The area of its extent of occurrence is of about 1782 km^2. In Ecuador, it occurs in Montane Cloud Forest (according to the classification proposed by Valencia *et al.* 1999). At the Ecuadorian locality annual mean rainfall is 1192 mm and the annual mean temperature is 13.5 °C (Hijmans *et al.* 2005). At Santa Bárbara, *H. tigrinus* occurs in microsympatry (tadpoles in the same ponds) with *H. pantostictus* and in macrosympatry with *H. psarolaimus* and *H. lindae* (Fig. 9).

Hyloscirtus tigrinus was considered by Mueses-Cisneros and Perdomo-Castillo (2011) to be Endangered (B1ab [iii,v], IUCN Red List categories and criteria). The population in Ecuador suffers threats similar to those that affect Colombian populations. However, we recommend that the species to be considered Critically Endangered because of the relatively small area of the extent of occurrence (1782 km^2), in which habitat destruction is intense. Threats at the Santa Bárbara region are logging, burning, unregulated use of land for agriculture (especially for tree tomatoes and potatoes), cattle raising, pesticide use, and invasive trout in the regional streams. Additionally, urban development is altering the streams and severe fragmentation is occurring. The presence of the amphibian chytrid fungus was reported for *H. psarolaimus* from the site (Merino-Viteri 2001). In spite of 16 searching efforts in herpetological field trips to Santa Bárbara (since June 1989 to December 2009), we have only found a few tadpoles and no frogs. This seems to indicate that this species is rare. Rapid and integrative conservation measures are urgently needed, among which the protection and restoration of its habitat are a priority, as well as the establishment of an *ex-situ* assurance colony.

Tadpoles

All tadpoles described below belong to the suctorial ecomorphological guild as defined by Altig and Johnston (1989). They have one simple triangular fleshy projection on the inner margin of naris, and the anterior jaw sheath in the mouth is narrow and has small serrations (Fig. 15A–F) as described by Sánchez (2010). They have a bag over the vent tube as described by Lötters *et al.* (2005) and Sánchez (2010).

Hyloscirtus larinopygion

Description. The oral disc of an individual of series QCAZ 38418 is depicted in Figure 15A. The following description is based on another individual in Stage 25 from the same tadpole series (QCAZ 38418) obtained from a margined pool (with algae) in a stream at Cerro Centella, Cascada Centella (on Tulcán–Maldonado road), 2709 m, Provincia de Carchi, Ecuador, by Juan F. Dueñas and Ítalo G. Tapia on 17 September 2008. All values are in millimeters. Total length 46.7; body length 17.8 (38.0% of total length). Body ovoid and depressed; width at the level of spiracle 8.8, and height at same position 7.5; head width at level of eyes 8.5; anterior margin of snout uniformly rounded in dorsal view and sloping at level of nares in lateral view; lateral-line system evident displaying supraorbital, infraorbital, longitudinal oral, mandibular, angular, posterior infraorbital, middle body, dorsal body, and ventral body lines; the arrangement of the lateral-line system is symmetrical, except for ventral

lines. The nostrils are small, rounded and directed anterolaterally; aperture situated 3.6 from tip of snout; internarial distance 4. Eyes positioned and directed dorsolaterally; eye length 1.9, eye width 1.2; interorbital distance 6.8. Spiracle sinistral, located at mid-body level, inner wall free from body; tube length 1.7, tube transverse width 1.4; spiracular opening directed posterodorsally, diameter 0.7. Vent tube free, opening directed dextrally; tube length 3.0, tube transverse width 4.6. Tail length 28.8; caudal musculature robust, narrowing gradually until tail terminus; at tail/body junction, tail muscle width 4.7; tail muscle height 5.4; maximun height of tail 10.3.

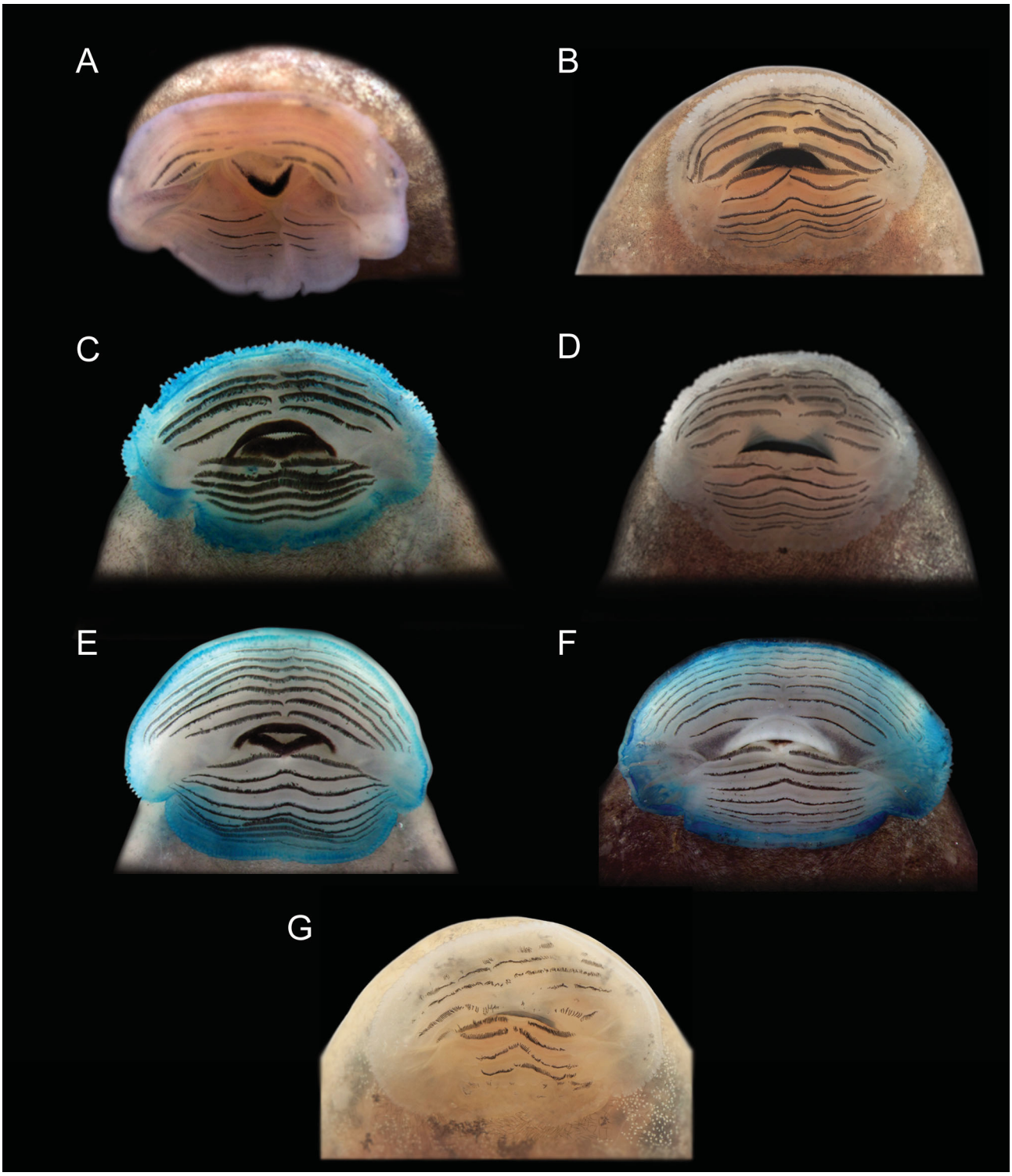

FIGURE 15.—Oral discs in Gosner Stage 25 of (A) *Hyloscirtus larinopygion*, QCAZ 38418, (B) *H. lindae,* QCAZ (sc 31031), (C) *H. pantostictus*, QCAZ 45440, (D) *H. princecharlesi,* CJ 382, (E) *H. psarolaimus,* QCAZ 46098, (F) *H. ptychodactylus*, QCAZ 46023, and (G). *H. tigrinus*, QCAZ 41351. A–C are from preserved specimens with Alcian blue staining to highlight mouth papillae. D–G are from living tadpoles. Not to scale.

Oral disc located anteroventrally, emarginated twice ventrally; transverse width 6.3; completely bordered by two rows of small rounded papillae; submarginal papillae present; upper jaw sheath forming an arch, no pigmentation present; transverse width including lateral processes 2.1 (33.3% of transverse width of oral disc); lower jaw sheath V-shaped; finely serrate edges present in both sheaths.

Labial tooth row formula 5(4–5)/7(1). Only A-3 and A-4 have natural gaps, other gaps were caused by labial tooth losses. Tooth row A-1, 4.01 in length; A-2 length is 5.0; A-3 length 4.9; A-4 length is 4.5 with medial gap included; A-5 3.8 with medial gap included; P-1 length 3.1 including medial gap; P-2 length 3.5; P-3 length 3.8; P-4 length 3.8; P-5 length 4.1; P-6 length 2.8; P-7 length 2.8.

Color in preservative. In dorsal view, body brown. Tail muscles cream, flanked by two brownish tan parallel stripes. Snout brown to translucent. In lateral view, flanks brown at spiracle level, becoming progressively gray towards the venter. Fins translucent. Tail muscles uniformly cream. Dorsal stripes are bold and continuous in the proximal two-thirds of the tail, becoming progressively thinner and irregular up to the tip of the tail muscles. Spiracle translucent. Base of spiracle gray. In ventral view, venter translucent (gut visible through skin); oral apparatus cream.

Color in life. In dorsal view, body olive brown. Tail having a golden mid-dorsal stripe flanked by a pair of tan brown stripes. Snout brown, gradually becoming pale brown anteriorly. In lateral view, flanks olive brown covered by mottled cream suffusion. Fins translucent; predominantly cream blotches scatter irregularly over dorsal fins and ventral fins. Caudal muscles reddish brown at tail/body junction to beige near the terminus. Spiracle unpigmented. Venter translucent, pigmented by widely scattered cream melanophores. Oral apparatus cream. Iris bluish gray.

Variation. Meristic variation of tadpoles in Stages 25–35 (QCAZ 38418, 45462, and 4172) from Provincia de Carchi, Ecuador, is shown in Table 8. QCAZ 45462 was collected in an artificial reservoir of a stream in Quebrada Centella, 2806 m, by Juan F. Dueñas on 26 September 2008, and QCAZ 4172 was collected in an artificial reservoir of a stream at 22 km E of Maldonado, 2560 m, (on Tulcán-Maldonado road), by Felipe Campos-Yánez and Luis A. Coloma on 17 July 1993. Nine tadpoles in Stages 25–35 greatly varied in total length, ranging from 46.7–82.8 mm; body length 14.8–27.4 mm; tail length ranged from 28.8–58.0 mm.

LTRF varied from 5(4–5)/7(1) to 5(4–5)/6(1) in two specimens that were in Stage 25 (Fig. 15D); 77.8% of tadpoles showed incomplete oral apparatus, partially or entirely depleted of denticles, showing variable number of labial papillae and abraded tooth rows. Absence of keratinized teeth may be due to chytrid infection. Lateral-line system was evident in all individuals examined; however, a slight difference in the placement and start of lines is observed among individuals.

During ontogenetic development considerable changes in coloration occurred (Fig. 16). Between Stages 40–42, posterior limbs developed and acquired cream coloration, the dorsum and flanks of the body also acquired black mottling and the anterior area of the tail developed numerous aggregated cream blotches (Fig. 16). By Stage 42, the dorsum and flanks have became grayish brown with black mottling (except near the ventral lateral areas of the flanks, which became cream), and the limbs developed a contrasting black mottling pattern over a cream and gray combined background. At Stage 44, the dorsum and head became uniformly brown, the flanks and limbs became mottled, and the fingers and toes became cream and started to show a black coloration on the dorsal surfaces of the discs. Finally as a metamorphosed juvenile (Fig. 16), the dorsum, head, and limbs became yellow brown with the some black spots on the dorsum and head, and black vertical bars on limbs. The ventral lateral surface became white with black vertical bars.

Hyloscirtus lindae

Description. The oral disc of an individual of series QCAZ (sc 31031) is depicted in Figure 15B. It was collected in a stream of Quebrada Negra at 11–12 km E of Papallacta (2600 m, Provincia Napo, Ecuador) by Juan F. Dueñas and Diego Almeida-Reinoso on 20 February 2010. The following description is based on a single specimen in Stage 36 (series QCAZ 23087), from 11 km SE of Papallacta, Provincia de Napo, Ecuador, collected on 1 August 1999 by Luis A. Coloma and Santiago R. Ron. Total length 65.5; body length 20.4 (31.1% of total length). Body ovoid and depressed; body width at spiracle level 10.3, body height 8.0; head width at the eyes level 9.8; anterior margin of snout uniformly rounded in dorsal view and sloping at level of nares in lateral view. Lateral-line system evident, showing supraorbital, infraorbital, posterior supraorbital, posterior infraorbital, longitudinal oral, anterior

oral, angular, middle body, dorsal body, and ventral body lines; Longitudinal oral line rises at tip of snout, at middle level of oral disc. Supra ocular and infra ocular lines start at the tip of the head and merge behind the eye. Dorsal body and middle body lines run perpendicularly on the second half of the body, but distance between both lines narrows at the first half of the body, where finally merges above spiracle insertion point. Angular line starts at distal part of the eye level, near post supra orbital line, and runs down perpendicularly to infra ocular and longitudinal

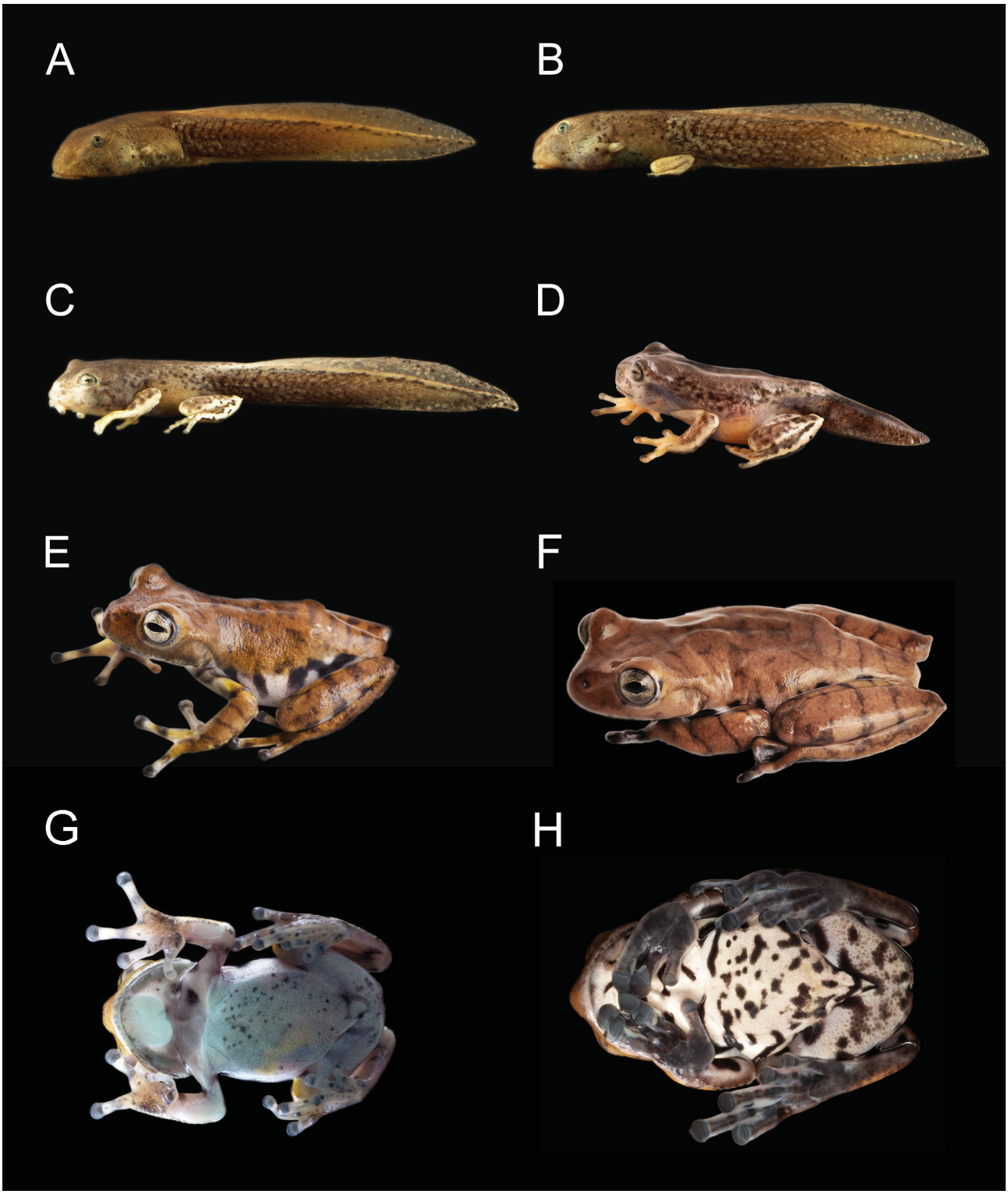

FIGURE 16.—Ontogenetic changes in *Hyloscirtus larinopygion* (QCAZ 38418) from Cerro Centella, Provincia de Carchi, Ecuador. Gosner stages: (A) Stage 25, (B) Stage 40, (C) Stage 42, (D) Stage 44, and (E–H) juveniles. Not to scale. Photos by Luis A. Coloma.

oral lines. The nostrils are small, ovoid, not protruding and directed anterolaterally; opening 3.6 from tip of snout; internarial distance (measured between the center of nares) 4.2. Eyes positioned and directed dorsolaterally, eye length 2.8, eye width 1.8; interorbital distance (measured between center of pupils) 7.5. Spiracle sinistral located at midbody level and oriented postero-dorsally; inner wall attached to the body, except for distal half, which is free and rounded in shape; spiracle length 2.5, spiracle width at its base 1.8. Vent tube with apical opening directed posteriorly. Vent tube length 5.7, vent tube width 4.8.

Tail length 42.8, caudal musculature robust, tapering gradually until tail terminus, which includes caudal fins; caudal fins low, rising near tail-body junction; Tail musculature height 6.0, tail musculature width 4.6 (both measured at tail-body junction), maximum tail height 11.1.

Oral disc emarginated and located anteroventrally; width of the oral disc 5.9, completely bordered of small rounded papillae. Labial tooth row formula 5(3–5)/7(1), oral apparatus well preserved, showing complete teeth rows.

Color in life. In dorsal view, body brown, with scattered gold flecks, showing lighter areas around the tip of snout and distal part of the trunk; the lateral line system is evident, in form of creamy white stitches. The tip of spiracle and oral apparatus are cream and translucent. Caudal fins translucent, with an opaque brown shade, and goldish flecks in some specimens. In lateral view, flanks are dark brown to translucent, covered by a suffusion of lighter mottling, from cream to gold hues. Tail musculature is dark brown in two proximal thirds of its extension, the distal third been creamy white; a dark brown, discontinuous stripe is evident in dorsal part of tail musculature, alternating with lighter (cream) areas. A black longitudinal stripe is evident in the first half of the myomeres insertion point. Vent tube translucent, iris dark brown with an extensive gold reticulation.

FIGURE 17.—Variation of living tadpoles in Gosner Stage 25 of *Hyloscirtus lindae* from Provincia de Napo, Ecuador. (A) QCAZ 41306 from Pacto Sumaco, (B) QCAZ (sc 31031) from Quebrada Negra, Papallacta, and (C) QCAZ 45194 from 11 km SE of Papallacta. Differences in color intensity may be an artifact of amount of lighting. Scale = 5 mm. Photos by Luis A. Coloma.

Variation. Variation of twenty three meristic characters of tadpoles in Stages 25–36 are shown in Table 8. Twenty tadpoles in Stages 25–36 greatly varied in total length that ranged from 33.6 to 74.0 mm; seventeen tadpoles (85.0%) in Stage 25 ranged between 33.6 and 67.1 in body length; body length ranged from 11.6–22.6; tail length ranged from 21.6–51.0.

TABLE 8. Measurements (in mm) of characters of tadpoles of *Hyloscirtus larinopygion*, *H. lindae*, *H. pantostictus, H. psarolaimus,* and *H. tigrinus*. Values are ranges and sample sizes in parentheses. Abbreviations are: TL (total length), BL (body length), TAL (tail length), TAL/TL (ratio of tail length related to total length), MHT (Maximum Height of Tail, including dorsal and ventral fins), WOD (transverse width of oral disc), WUJ (transverse width of upper jaw sheath, including lateral processes), WUJ/WOD (ratio of width of upper jaw sheath related to width of oral disc).

	H. larinopygion		*H. lindae*		*H. pantostictus*
Character	Stage 25	Stages 27–35	Stage 25	Stages 27–36	Stage 25
TL	46.7–60.2 (4)	71.0–82.8 (5)	33.6–67.1 (17)	57.3–74.0 (3)	37.7–74.6 (11)
BL	14.8–19.6 (4)	23.9–27.4 (5)	10.8–22.4 (17)	16.8–22.6 (3)	12.0–24.0 (11)
TAL	28.8–41.7 (4)	46.2–58.0 (5)	21.6–44.2 (17)	42.3–51.0 (3)	25.7–50.7 (11)
TAL/TL	0.6–0.7 (4)	0.6–0.7 (5)	0.6–0.7 (17)	0.6–0.7 (3)	0.6–0.7 (11)
MHT	7.8–11.0 (4)	12.6–14.3 (5)	5.5–11.7 (17)	7.6–11.6 (3)	5.0–10.8 (11)
WOD	5.0–6.5 (4)	7.1–9.2 (5)	1.2–10.0 (15)	1.5–5.9 (2)	3.5–6.0 (11)
WUJ	2.0–2.1 (2)	–	0.8–3.1 (7)	1.2–3.0 (3)	1.3–2.3 (11)
WOD/WUJ	2.5–3.0 (2)	–	1.5–3.2 (7)	1.2– 2.2 (2)	1.9–4.1 (11)
TUW	1.0–1.6 (4)	1.7–2.4 (5)	0.5–2.8 (14)	0.9–1.8 (2)	1.0–2.6 (11)
TUL	1.1–2.4 (4)	2.8–4.2 (5)	1.0–2.8 (14)	2.5 (1)	1.4–2.9 (11)

TABLE 8. Continued.

	H. pantostictus		*H. psarolaimus*	*H. tigrinus*	
Character	Stages 26–39	Lab-Reared Stages 40–41	Stage 25	Stage 25	Stages 26–39
TL	57.6–80.5 (10)	67.5–83.8 (5)	32.3–42.1 (5)	48.0–67.6 (2)	61.2–96.7 (2)
BL	18.6–25.8 (10)	22.4–25.4 (5)	10.2–14.2 (5)	14.1–23.9 (6)	20.9–36.5 (3)
TAL	39.2–53.8 (10)	46.5–59.1 (5)	21.7–28.8 (5)	34.4–6.0 (2)	40.4–66.4 (2)
TAL/TL	0.7 (10)	0.7 (5)	0.7 (5)	0.7 (2)	0.7 (2)
MHT	7.5–15.0 (10)	7.8–14.0 (5)	5.4–6.4 (5)	8.0–13.7 (6)	10.7–10.6 (3)
WOD	5.2–8.1 (10)	4.5–6.8 (5)	4.3–6.5 (5)	4.3–7.0 (6)	6.7–11.1 (3)
WUJ	1.9–2.6 (10)	2.0–2.7 (4)	1.1–2.3 (4)	2.0–3.2 (5)	3.2–4.8 (3)
WOD/WUJ	2.3–3.1 (10)	2.3–2.6 (4)	2.6–3.9 (4)	1.8–2.5 (5)	1.9–2.5 (3)
TUW	1.2–2.9 (10)	1.4–2.5 (4)	0.8–1.2 (5)	1.2–2.7 (6)	2.2–5.2 (3)
TUL	2.0–3.3 (10)	1.4–2.5 (4)	1.0–1.8 (5)	1.4–5.3 (6)	2.3–5.7 (3)

Variation in LTRF cannot be correctly described, 50.0% of tadpoles (in Stages 25, 35) showed deformed oral apparatus, completely or partially depleted of denticles, with variable number of labial papillae. From the tadpoles that had relatively distinct tooth rows (in Stages 25, 36), oral tooth row formulae varied from 4(3–4)/5(1) to 5(4–5)/7(1) in Stage 25 and 5(3–5)/7(1) in Stage 36. Absence of keratinized teeth may be due to chytrid infection. Lateral-line system was evident in all individuals examined; however, a difference in the placement and start of lines is observed among individuals. Arrangement of ventral bodyline may be symmetrical or asymmetrical on the left flank of body where spiracle is located.

Overall color patterns as well as arrangement and coloration of blotches in fins varied among individuals in Fig. 17. Individuals of about the same size and Gosner stage show variation in dorsal and lateral color patterns from light brown (Fig. 17A) to dark brown (Fig. 17C). Pattern of blotches on dorsal and ventral fins varies from dense stippling (Fig. 17A) to scattered brown and reddish brown blotches (Fig 17B) to more numerous blotches (Fig. 17C). Bold dark brown stripes at the upper tail musculature run parallel to dorsal fin and are nearly straight at the first half of tail and sinuous at the distal portion.

Considerable ontogenetic change occurs in coloration of individuals of *Hyloscirtus lindae* from tadpoles to adults as illustrated in Figure 18. Approximately at Stage 40, when posterior limbs are fully developed, an overall soles and concealed parts of the limbs are yellow tan. By Stage 45, the entire dorsum is chocolate brown with a fine creamy reticulation, and an orange coloration start to be evident at the upper part of the discs, although some specimens in Stage 46 still have lighter (yellow) coloration at the top of the discs and are finely stippled in yellow. creamy white coloration is especially notorious in dorsum and dorsal part of legs. Approximately at Stage 42, the

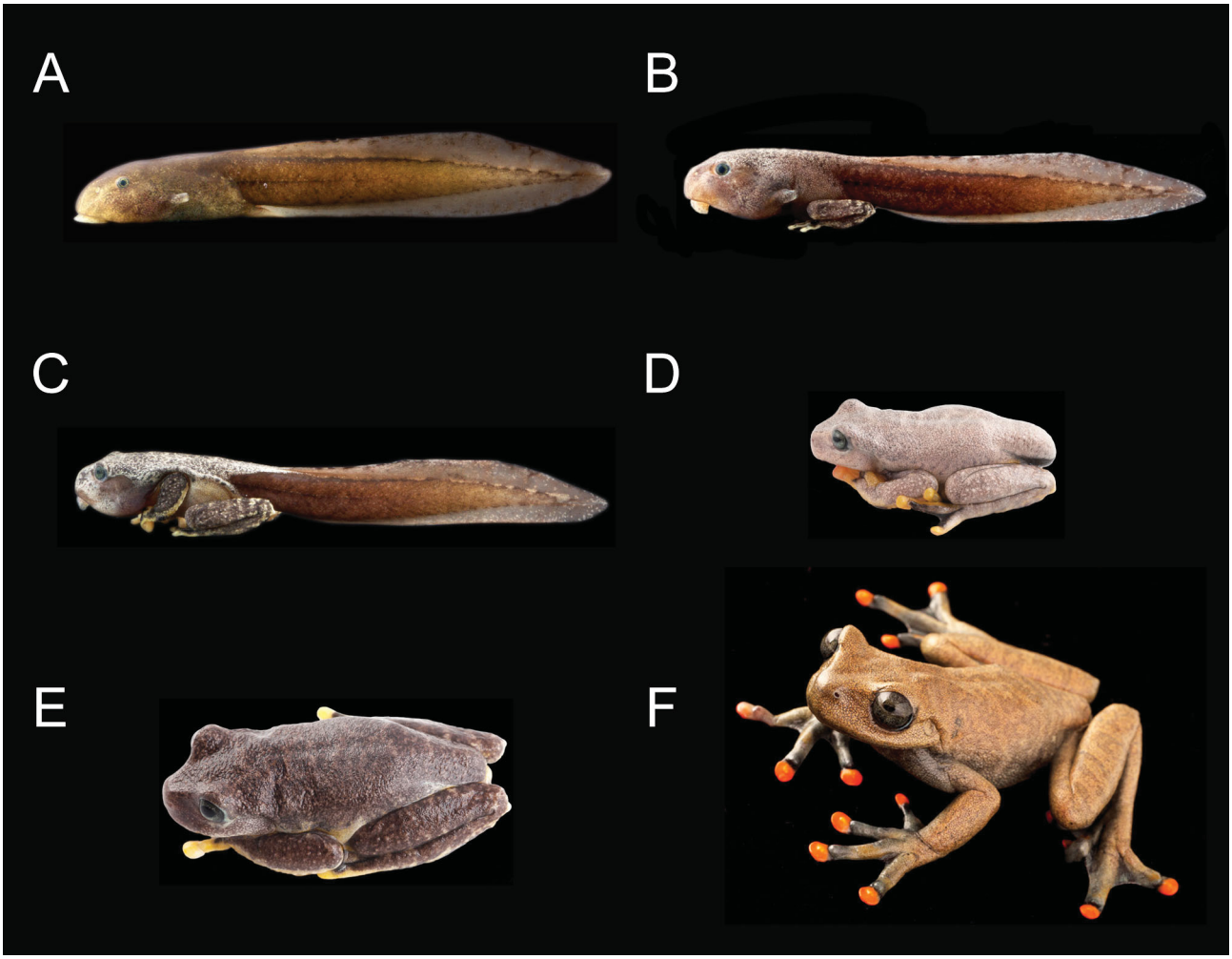

FIGURE 18.—Ontogenetic changes in *Hyloscirtus lindae* (QCAZ sc 31031) from Quebrada Negra, Papallacta, Provincia de Napo, Ecuador. Gosner stages: (A) Stage 29, (B) Stage 40, (C) Stage 42, (D) Stage 46, (E) juvenile, and (F) adult (MZUTI 707) from Oyacachi-El Chaco, Provincia de Napo. Not to scale. Photos by Luis A. Coloma.

overall dorsal coloration is cream with dark brown reticulation; a dorsolateral fold is evident in distal part of the body, oral disc is still present; pupil coloration changes from brown with gold reticulations to dark grey. At Stage 46, characteristic color pattern of the adult includes light brown ground coloration, with some irregular darker marking, especially notorious at the shanks level, in form of several transverse bars; the tip of the digits and interdigital membranes are black and the discs are bright orange; the iris is grey with a fine darker reticulation.

Hyloscirtus pantostictus

Description. The oral disc of an individual of series QCAZ 45440 is depicted in Figure 15C. The following description is based on another individual in Stage 25 from the same tadpole series (QCAZ 45440). The specimen was obtained in a slow moving pool along the margins of the stream margins at Creek 2 (00° 38' 37" N, 77° 31' 56" W; 2586 m), Santa Bárbara, Provincia de Sucumbíos, Ecuador, by Juan F. Dueñas and Ítalo G. Tapia on 29 September 2008. Tadpoles were gregarious and took shelter under the sand at bottom of pool when disturbed. All values are in millimeters. Total length 48.4; body length 13.6 (28.2% of total length). Body ovoid and depressed; width at the level of spiracle 7.0, and height at same position 5.5; head width at level of the eyes 6.5; anterior margin of snout uniformly rounded in dorsal view and sloping at level of nares in lateral view; lateral-line system evident displaying supraorbital, infraorbital, longitudinal oral, mandibular, angular, posterior infraorbital, middle body, dorsal body, and ventral body lines. The arrangement of the lateral-line system is symmetrical, except for ventral lines; mandibular line originates at anterior end of venter and runs laterally forming an arch around each side of oral apparatus; ventral lines originate anterior to vent tube, run diagonally over trunk until they make a sharp turn down and return to the venter; angular line continuous with infraorbital line and extends perpendicular to infraorbital, longitudinal oral, and mandibular lines. The longitudinal oral line originates at midlevel of angular line and runs parallel to longitudinal axis until reaching the arch of mandibular line. Supra and infra orbital lines originate at snout and run posteriorly until they merge around the eyes. The nostrils are small, bean-shaped and directed anterolaterally; opening 2.6 from tip of snout; internarial distance 3.3. Eyes positioned and directed dorsolaterally; eye length 1.5, eye width 1.1; interorbital distance 5.0. Spiracle sinistral, located at midbody level, inner wall free from body; tube length 1.4, tube transverse width 1.1; spiracular opening directed posterodorsally, diameter 0.4; distance from tip of snout to spiracular opening 9.7. Vent tube free, opening directed dextrally; tube length 2.9, tube transverse width 1.8. Tail length 34.1; caudal musculature robust, narrowing gradually until tail terminus; at tail-body junction, tail muscle width 3.2; tail muscle height 4.1; maximum height of tail 7.3.

Oral disc located anteroventrally, emarginated twice ventrally; transverse width 4.9; completely bordered by two rows of small and rounded papillae; submarginal papillae absent; upper jaw sheath forming an arch, no pigmentation present; transverse width including lateral processes 2.1 (42.9% of transverse width of oral disc); lower jaw sheath V-shaped; finely serrate edges present in both sheaths. Labial tooth row formula 4(3–4)/6(1). Only A-3 and A-4 have natural gaps, other discontinuities were caused by labial tooth losses. Tooth row A-1, 2.8 in length, having one region with missing teeth; A-2 length 3.7; A-3 length 3.6 including medial gap; A-4 length 3.1 with medial gap included. P-1 length 2.5 including medial gap; P-2 length 2.8; P-3 length 2.8; P-4 length 2.8; P-5 length 2.4; P-6 length 1.8.

Color in preservative. In dorsal view, body tan gray with dark T-shaped fleck between eyes. Tail having a cream streak, flanked by two black parallel stripes, starting slightly anterior to tail/body junction. Snout gray. In lateral view, flanks tan gray at level of spiracle, becoming progressively lighter towards the venter. Fins translucent; black stippling and gray filiform melanophores scattered irregularly over tail muscles, and dorsal and ventral fins. Tail muscles are uniformly gray. Dorsal stripes bold and continuous in the proximal two-thirds of tail, becoming progressively thinner and irregular towards posterior end of tail. Distal half of spiracle translucent, only pigmented by few widely scattered stipples and filiform melanophores. Base of spiracle gray as body flanks. Iris black. Venter translucent (gut visible through skin); oral apparatus cream covered with dark gray blotches.

Color in life. In dorsal view, body brown and covered with thin sandy-gold suffusion that extends over the proximal third of tail muscles. Black transverse bar between eyes. Tail with white streak flanked by two segmented black stripes. Snout brown, gradually clearing as approaching tip. In lateral view, flanks reddish brown to translucent, covered by mottled golden suffusion; dorsal fins with predominantly cream and few scattered black blotches. Ventral fins exhibit only white blotches. Caudal muscles reddish brown at tail-body junction to beige near

FIGURE 19.—Variation of living tadpoles in Gosner Stage 25 of *Hyloscirtus pantostictus* from Santa Bárbara, Provincia de Sucumbíos, Ecuador. (A) QCAZ 45440, (B) QCAZ 41417, and (C) QCAZ 45446. Differences in color intensity may be an artifact of amount of lighting. Scale = 5 mm. Photos by Luis A. Coloma.

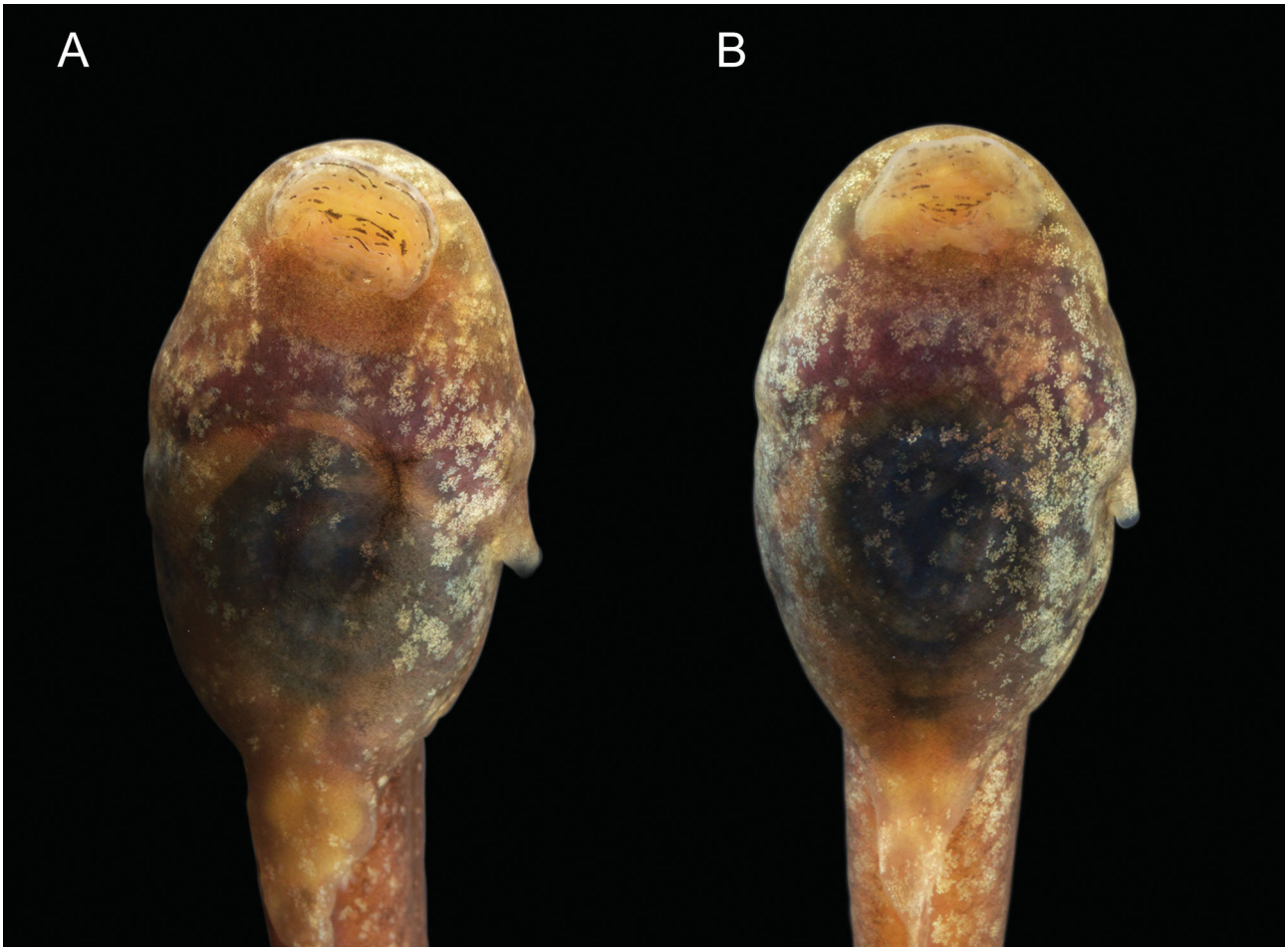

FIGURE 20.—Living tadpoles in Gosner Stage 25 of *Hyloscirtus pantostictus* from Santa Bárbara, Provincia de Sucumbíos, Ecuador. (A) QCAZ 41417, (B) QCAZ 41414, showing ventral variation in amount of pigmentation patterns. Lack of keratinized teeth is possibly due to chytrid infection. Photos by Luis A. Coloma.

terminus. Spiracle unpigmented, however a silver gold iridescence can be depicted in certain light conditions. Venter translucent, pigmented by widely scattered golden melanophores. Oral apparatus cream. Iris black, with a single irregular green concentric reticulation.

Variation. There is variation in ventral pigmentation patterns (Fig. 20). Meristic variation of tadpoles in Stages 25–41 (QCAZ 45440) are shown in Table 8. Eleven tadpoles in Stages 25–39 greatly varied in total length, ranging from 37.7–80.5; body length ranged from 12–25.8; tail length ranged from 25.7–53.8. Five lab-reared tadpoles in Stages 40–41 also varied in total length measuring 67.5–83.8; body length was 22.4–25.4, and tail length ranged from 46.5–59.1.

LTRF greatly varied from 4(4)/5(1) to 6(4–6)/7(1) (Fig. 15B); 53.6% of tadpoles showed incomplete oral apparatus (Stages 25–27, 36–39), partially or entirely depleted of denticles, showing variable number of labial papillae and abraded tooth rows. Absence of keratinized teeth may be due to chytrid infection. The lateral-line system was evident in all individuals examined; however, a slight difference in the placement and origin of lines is observed among individuals. Arrangement of ventral bodyline may be symmetrical or asymmetrical on the left flank of body where spiracle is located.

Overall color patterns as well as arrangement and coloration of blotches in fins greatly varied among individuals and through ontogenetic development (Fig. 19). Individuals of about the same size and Gosner stage show variation in dorsal and lateral color patterns from opaque brown (Fig. 19A) to light brown (Fig. 19C) passing through an intermediate state where both tones produce a contrasting pattern in overall body coloration (19B). The same applies for the blotches on dorsal and ventral fins, where the pattern ranges from small randomly scattered cream blotches to small, more numerous blotches. An alternative state is shown in one individual (Fig. 19B), in which dark blotches are also present.

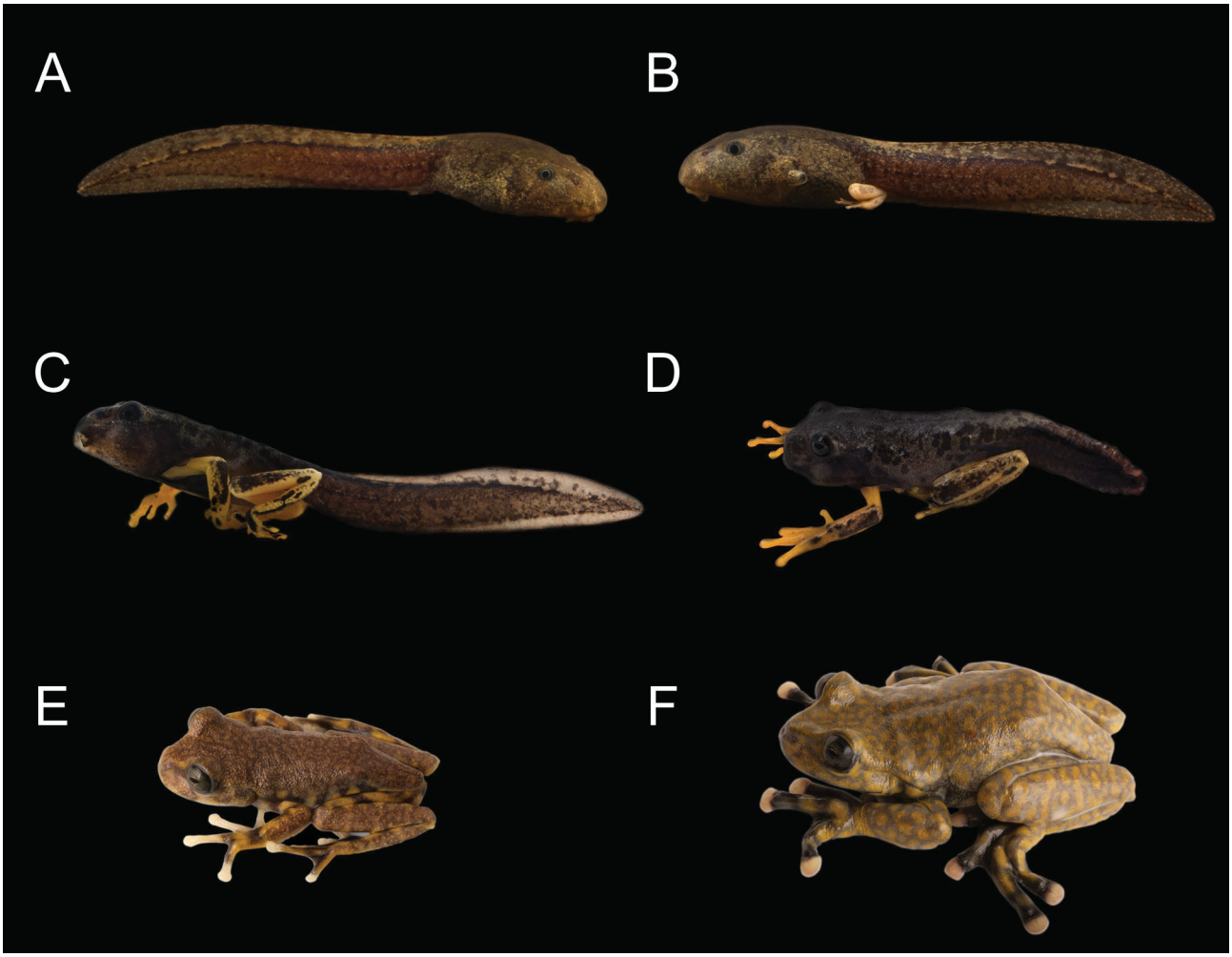

FIGURE 21.—Ontogenetic changes in *Hyloscirtus pantostictus* (QCAZ series sc 24305) from Santa Bárbara, Provincia de Sucumbíos, Ecuador. Gosner stages: (A) Stage 25, (B) Stage 40, (C) Stage 42, (D) Stage 44, (E) juvenile, QCAZ (series sc 31051), and (F) subadult, QCAZ 45435. Not to scale. Photos by Luis A. Coloma.

Considerable change in coloration occurred during ontogenetic development of lab-reared *Hyloscirtus pantostictus* (Fig. 21). Between Stages 39–41, the posterior limbs developed yellow coloration and the dorsum became opaque and gray but the flanks of the body still exhibited a golden brown suffusion. By Stage 42, the entire dorsum and flanks had become dark gray with black mottling all over, the snout was reduced, and the limbs developed a pattern of black mottling pattern over a bright yellow background. At Stage 45, the dorsum and head were uniformly tan-gray with lighter flanks. Black mottling was still present, especially on anterior and posterior limbs and over the posterior portion of the dorsum.

Juveniles showed great variation in coloration. Some exhibited a pale gray dorsal pattern (QCAZ 42350 from Santa Bárbara, 2709 m, Provincia de Sucumbíos, Ecuador, collected as tadpole by Juan F. Dueñas, Ítalo G. Tapia, Diego Páez-Moscoso, and Jennifer M. García on 18 September 2008; SVL 32.4 mm) whereas most exhibited a predominantly tan brown dorsum with black blotches. Cephalic flanks as well as anterior and posterior limbs showed a slightly lighter brown color with yellow dots and bars. The venter and digits were white. Finally, a subadult exhibited a pattern resembling that of adults but with slightly different colors; the dorsal surfaces of the head and dorsum were brown with yellow spots. The hidden surfaces of the hind limbs were black with yellow vertical bars and the exposed surfaces of all limbs had yellow spots both in anterior and posterior limbs.

Hyloscirtus princecharlesi

Description. The oral apparatus of an individual of series CJ 382 is depicted in Figure 15D. The following description is based on a single specimen in Stage 36 (CJ 385) collected in borderline between Reserva Cotacachi-Cayapas and private land owned by Manuel Quinchiguango, at Recinto San Antonio, Cuellaje, Provincia Imbabura, Ecuador (0º 28' 23.772" N, 78º 34' 12.756" W; 2794 m); obtained by Elicio E. Tapia, Carl R. Hutter, and Carlos Quinchiguango on 22 July 2011. Two tadpoles of the same series (CJ 381–382) are depicted in Figure 22. All values are given in millimeters. Total length 89.1; body length 28.4 (31.9% of total length). Body ovoid and depressed; body width at spiracle level 19.0, body height 13.2; head width at eye level 16.2; anterior margin of snout uniformly rounded in dorsal view and sloping at level of nares in lateral view; lateral-line system evident, showing supraorbital, infraorbital, posterior supraorbital, posterior infraorbital, longitudinal oral, anterior oral, angular, middle body, dorsal body, and ventral body lines. The arrangement is symmetrical. The longitudinal oral line arises at the lower end of the oral disc. The anterior oral line begins behind behind the oral disc, ventrally. Supraocular and infraocular lines start at the tip of the head and merge behind the eye. Dorsal body and middle body lines run perpendicularly on the posterior half of the body and merge dorsally at the spiracle insertion point. The angular line runs downward at level of the distal part of the eye, where it reaches the postsupraorbital line. The anterior oral line is continuous with the longitudinal oral and angular lines. The anterior oral line continues ventrally until it merges with the angular line, ventrolaterally. The ventral line surrounds the spiracle laterally and turns backward ventrally, running near the middle of the body on both sides. The nostrils are small, ovoid, not protruding and directed anterolaterally; opening 6.0 from tip of snout; internarial distance 6.7. Eyes positioned and directed dorsolaterally, eye length 3.0, eye width 2.9; interorbital distance 11.5. Spiracle sinistral, located at midbody level and oriented postero dorsally; inner wall attached to the body, except for distal half, which is free and rounded in shape; spiracle length 3.8, spiracle width at its base 2.6. Distance from tip of snout to spiracular opening 20.8. Vent tube medial, with opening directed posteriorly. Vent tube length 7.5, vent tube width 3.8. Tail length 62.4, caudal musculature robust, tapering gradually until tail terminus, which includes caudal fins; caudal fins low, rising near tail-body junction. Tail musculature height 10.6, tail musculature width 9.4 (both measured at tail-body junction). Dorsal fin height 5.2, ventral fin height 4.1, maximum tail height 10.6; fins height at midtail 15.7.

Oral disc located anteroventrally, emarginated twice ventrally; width of the oral disc 10.0, completely bordered by two rows of small rounded papillae, 271 in upper lip and 86 in lower lip; submarginal papillae absent, except for emargination zone where five submarginal papillae are present on each side. Upper jaw sheath forming an arch, transverse width, including lateral processes 3.6 (36.0% of width of oral disc), upper jaw sheath height 0.8; most of keratin cover was detached; lower jaw sheath V-shaped, and finely serrate at least at the middle level, keratin cover of both ends of the sheath detached, lower jaw sheath width 2.6, lower jaw sheath height 0.3.

Labial tooth row formula 8(8)/10, although some tooth rows were incomplete, particularly A1 which was poorly developed; A8 row interrupted medially by jaw sheaths, but several other unnatural breaks were observed, in all tooth rows, caused by labial tooth losses. Measures of labial tooth rows correspond to the straight line between the two ends of each row, which are bow-shaped. A1 tooth row 6.9 in length with 172 teeth; A2 tooth row 8.6 in length with 339 teeth; A3 tooth row 9.4 in length with 534 teeth; A4 tooth row 8.6 in length with 768 teeth; A5 tooth row 8.6 in length with 396 teeth; A6 tooth row 8.1 in length with 307 teeth; A7 tooth row 8.0 in length with 189 teeth; A8 right row 2.0 in length with 68 teeth; A8 left row 2.2 in length with 82 teeth; A8 gap 3.9 in length. P1 tooth row 5.8 in length with 159 teeth; P2 tooth row 6.4 in length with 250 teeth; P3 tooth row 6.6 in length with 249 teeth; P4 tooth row 6.7 in length with 248 teeth; P5 tooth row 6.9 in length with 317 teeth; P6 tooth row 6.4 in length with 155 teeth; P7 tooth row 6.9 in length with 384 teeth; P8 tooth row 6.4 in length with 275 teeth; P9 tooth row 6.5 in length with 249 teeth; P10 tooth row 5.7 in length with 48 teeth.

Color in preservative. In dorsal view, body grayish brown covered by minute dark brown flecks, with lighter areas in the temporal region and on the posterior half of the body. Tail light gray with cream areas distally, finely dotted in gray, myomeres insertion point demarcated by a dark line that runs backward to the middle of the body. In lateral view, flanks tan gray at spiracle level. The venter is lighter and translucent in the belly region, guts exposed. Fins translucent, with evident innervations and profusion of darker dotes, particularly notorious on the borders. Tail musculature dark gray, getting progressively lighter from mid body to tail terminus; a dorsal stripe is evident on dorsal border of tail musculature. Oral apparatus cream, covered with minute flecks on the border. Eyes are gray lavender.

Color in life. In dorsal view, body brown, spectacled with a suffusion of cream flecks, with tip of snout and distal part of the trunk lighter; the lateral line system is evident, in the form of a discontinuous line of cream dots. The spiracle and oral apparatus are cream and translucent. Dorsal fin cream. In lateral view, flanks are dark brown to translucent, covered by a suffusion of darker mottling. Caudal musculature is dark brown in the two proximal thirds of its extension, the distal third is creamy white, with several darker marks, of different sizes and shapes. Caudal fins are pale brown in coloration and translucent, with heavy innervations that are more evident near the tail-body junction. A dark brown longitudinal stripe is evident along the upper border of tail musculature, and a thinner one in the lower border of the distal portion of tail musculature. Anterior half of venter reddish brown, posterior half dark brown, both with profusion of cream dots and some dispersed melanophores; vent tube translucent; iris turquoise blue, with tiny white flecks and a green lavender annulus around pupil.

Considerable change in coloration occurred during ontogenetic development of lab reared *Hyloscirtus princecharlesi* (Fig. 23). Between Stages 40–42, the hindlimbs developed from cream to greenish-gray, the dorsum became gray, and the flanks exhibited a gray-brown suffusion. By Stage 44, the entire dorsum and flanks became plain yellow-green, and hidden surfaces of both anterior and posterior limbs developed a contrasting black mottling pattern over a bright yellow background. Early juveniles are plain yellow-green and mottling increases on the flanks. The tips of the digits are dark gray. The iris is also dark gray.

Hyloscirtus psarolaimus

Description. The oral disc of an individual of series QCAZ 46098 is depicted in Figure 15E. The following description is based on another individual in Stage 25 from the same tadpole series (QCAZ 46098), obtained in a streamside pond 2 km down the river near km 60 on the road between Salcedo and Tena (00° 58' 16" S, 78° 14' 29" W; 2748 m), Provincia de Napo, Ecuador, by Elicio E. Tapia and Fernando Núñez on 18 November 2009. The stream is located in mostly natural forest at about 80 m from the larger Río Mulatos; the stream bed was about 2 m width with an inclination of about 45 degrees. Tadpoles (QCAZ 46098; 46095, same locality and collection data) seem to mimic fallen, old *Chusquea* sp. leafs in the water, which have similar size and color patterns. Water temperature was 9 ºC at about 20:00h. All values are in millimeters. Total length 42.0; body length 13.7 (32.8% of total length). Body ovoid and depressed; width at level of spiracle 6.7, and height at same position 6.5; head width at level of eyes 6.0; anterior margin of snout uniformly rounded in dorsal view and sloping at level of nares in lateral view; lateral-line system barely conspicuous, and includes supraorbital, infraorbital, mandibular, posterior infraorbital, middle body, and ventral body lines. The arrangement is symmetrical, except for ventral lines.

FIGURE 22.—Living tadpoles in Gosner Stage 25 of *Hyloscirtus princecharlesi* from San Antonio, Cuellaje, Provincia de Imbabura, Ecuador. (A) CJ 381, (B) CJ 382. Differences in color intensity may be an artifact of amount of lighting. Scale = 5 mm. Photos by Luis A. Coloma.

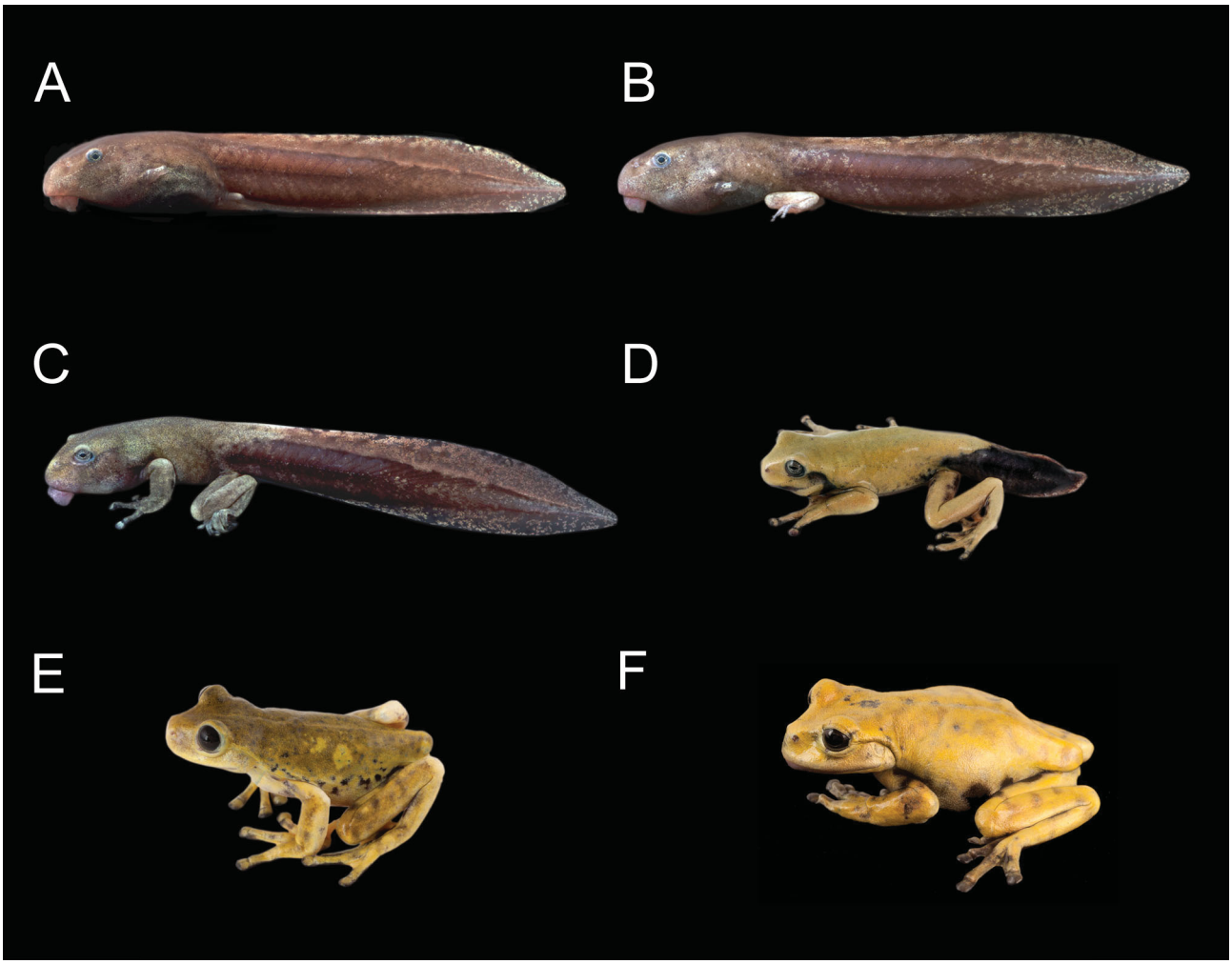

FIGURE 23.—Ontogenetic changes in *Hyloscirtus princecharlesi* from San Antonio, Cuellaje, Provincia de Imbabura, Ecuador. Gosner stages: (A) Stage 29, CJ 381, (B) Stage 40, CJ 383, (C) Stage 42, CJ 381, (D) Stage 44, CJ 381, (E) juvenile, CJ 384, and (E) juvenile, CJ 381. Not to scale. Photos by Luis A. Coloma.

Nostrils small, bean-like and directed anterolaterally; opening 2.0 from tip of snout; internarial distance 2.9. Eyes positioned and directed dorsolaterally; eye length 1.5, eye width 1.1; interorbital distance 4.7. Spiracle sinistral, located at mid-body level, inner wall free from body; tube length 1.8, tube transverse width 1.1; spiracular opening directed posterodorsally, diameter 0.4; distance from tip of snout to spiracular opening 9.6. Vent tube free, opening directed dextrally; tube length 2.0, tube transverse width 1.4. Tail length 28.3; caudal musculature robust, narrowing gradually to tail terminus; at tail-body junction, tail muscle width 2.9; tail muscle height 3.9; maximum height of tail 6.3.

Oral disc located anteroventrally, emarginated twice ventrally; transverse width 5.9; completely bordered by a single row of small rounded papillae; submarginal papillae absent; upper jaw sheath black, forming an arch; transverse width including lateral processes 2.3 (39% of transverse with of oral disc); lower jaw sheath V-shaped; finely serrate edges present in both sheaths. Labial tooth row formula 7(6–7)/9(1). Only A-6, A-7, and P-1 present natural gaps. Tooth row A-1, 3.4 in length; A-2 length 4.8; A-3 length 5.1; A-4 length 4.8; A-5 4.5; A-6 length 4.3 including medial gap; A-7 length 3.6 including medial gap. P-1 length 3.04 including medial gap; P-2 length 3.7; P-3 length 4; P-4 length 4.09; P-5 length 4.3; P-6 length 4.06; P-7 length 4.02; P-8 length 3.8; P-9 length 2.4.

Color in preservative. In dorsal view, body gray. Two rounded white marks located in between the eyes, slightly posterior to nares. Tail with white streak along top of caudal musculature edged by two tan-gray stripes. Snout translucent. In lateral view, flanks gray. Fins translucent; dorsal and ventral fins with predominantly gray blotches scattered irregularly over dorsal and ventral fins. Caudal muscles uniformly white, flecked with gray. Dorsal stripes on caudal musculature are well defined, becoming progressively thinner towards the posterior end of the tail. Iris black. Spiracle translucent. Venter translucent (gut visible through skin); oral apparatus and base of caudal musculature white.

Color in life. In dorsal view, body and caudal musculature brown with a heavy golden suffusion. Top of dorsal musculature with a golden streak edged by brown stripes. Snout golden yellow. In lateral view, flanks brown with heavy golden suffusion. Fins yellow; tail musculature cream flecked with brown over the proximal two-thirds. Spiracle translucent flecked with golden dots of cromatophores. Venter translucent, pigmented by widely scattered golden melanophores, pectoral area red. Oral apparatus translucent. Iris black, rounded by two concentric golden reticulations.

Variation. Variation of ten meristic characters of tadpoles in Stage 25 is shown in Table 8. Tadpoles varied in total length from 32.3– 42.1; body length ranged from 10.2–14.2; tail length ranged from 21.7– 28.8. LTRF varied from 7(6–7)/8(1) to 7(6–7)/9(1); 40.0% of tadpoles showed incomplete oral apparatus, partially or entirely depleted of denticles, having variable number of labial papillae, and abraded tooth rows. The individual depicted on Figure 15E show two rows of papillae (instead of only one) at the distal left side of the posterior margin of the oral disc. Absence of keratinized teeth may be due to chytrid infection. Lateral-line system was not conspicuous in all individuals examined. Arrangement of ventral bodyline may be symmetrical or asymmetrical on the left flank of body where the spiracle is located. Overall color patterns, as well as arrangement and coloration of marks in fins varied among individuals in Fig. 24. Individuals of about the same size and Gosner stage show variation in dorsal and lateral color patterns from light brown (Fig. 24A) to dark brown (Fig. 24B). Pattern of marks on dorsal and ventral fins and caudal musculature varies from stippling (Fig. 24A) to brown blotches (Fig. 24B). Color patterns varied through ontogenetic development (Fig. 25). The most noticeable features are the appearance of numerous spots on body, caudal fins and musculature, and a progressively pronounced brown suffusion. At Stage 41 (Fig. 25B), an overall brown-gray coloration appears at dorsum and flanks of body with numerous black spots irregularly distributed at flanks. Anterior and posterior limbs are light brown. By Stage 42 (Fig. 25C) a cream calcar is visible in the hind limbs. At Stage 45, flanks have more numerous black spots. Juveniles at latter stages show a brown dorsum with minute stippling mixed with black dots. Iris is cream in juveniles. One individual showed a middorsal cream stripe (Fig. 25F).

Hyloscirtus tigrinus

Description. The oral disc of an individual of series QCAZ 41351 is depicted in Figure 15G. It was collected in Quebrada Corazón, 2638 m, Santa Bárbara, Provincia de Sucumbíos, Ecuador, in a slow moving pool under a cascade of 2.5 m high in a stream by Luis A. Coloma and Juan F. Dueñas on 3 March 2009. The following description is based on a single specimen in Stage 34 (QCAZ 31550), from Quebrada Corazón (ca. 01° 38' 42" N,

77° 31' 48" W; 2620 m), Santa Bárbara, Provincia de Sucumbíos, Ecuador, collected in a slow moving pool in a stream by Fernando P. Ayala, Wesley Chun, and Rosario Castañeda on 23 February 2006. All values are in millimeters. Total length 98.5, body length 36.5 (37.1% of total length). Body ovoid and depressed; width at level of spiracle 22.9, and height at same position 19.2; head width at level of eyes 19.2; anterior margin of snout uniformly rounded in dorsal view and sloping at level of nares in lateral view; lateral-line system evident and symmetrical, having supraorbital, infraorbital, longitudinal oral, mandibular, angular, posterior infraorbital, middle body, dorsal body, and ventral body lines. The middle bodyline originates dorsally approximately 1.0 behind the posterior end of eyes, and runs dorsolaterally at the level of the trunk, becoming completely lateral at level of tail. Dorsal lines run parallel to dorsal fin. Mandibular line originates at anterior end of venter and runs laterally forming an arch around each side of the oral apparatus. Ventral lines start anterior to vent tube, run diagonally over trunk until they make a sharp turn down and return to the venter. Angular line is continuous with infraorbital line and extends perpendicular to infraorbital, longitudinal oral, and mandibular lines. Longitudinal oral line originates at midlevel of angular line and runs parallel to the longitudinal axis until it reaches the arch of the mandibular line. Supra- and infraorbital lines begin at the snout and run posteriorly until they merge around the eyes.

Nostrils small, oval, and directed anterolaterally; opening 8.0 from tip of snout; internarial distance 7.3. Eyes positioned and directed dorsolaterally; eye length 3.0, eye width 2.9; interorbital distance 12.0. Spiracle sinistral, located at midbody level, inner wall free from body; tube length 5.7, tube transverse width 5.2; spiracular opening directed posterodorsally, diameter 1.9; distance from tip of snout to spiracular opening 24.5. Vent tube free, opening directed dextrally; tube length 6.9, tube transverse width 0.4. Developing hind-limb bud 4.5 in length, with indentation between second and third, third and fourth, and fourth and fifth toes. Tail length 63.4; caudal musculature robust, narrowing gradually up to the tail terminus; at tail-body junction, tail muscle width 11.7; tail muscle height 13.1; maximum height of tail 20.6.

Oral disc located anteroventrally, emarginated twice ventrally; transverse width 11.1; border of disc irregular, ventral papillae absent (see variation); 66 papillae located laterally (49 on left side and 17 on right side); submarginal papillae absent; upper jaw sheath forming an arch, no pigmentation present; transverse width including lateral processes 4.4 (39.6% of transverse width of oral disc); serrate edges absent in both sheaths. Labial tooth row formula 5(3–5)/7(1), not clearly conformed. Dental crests show many losses and no gap is clearly demarcated; in all rows teeth are missing.

Color in preservative. In dorsal view, body and caudal musculature are dark brown. In lateral view, flanks lighter brown, fins brown; dorsal and ventral fins with dark blotches scattered irregularly on tail muscles. Tail muscles cream flecked with brown. Spiracle unpigmented. In ventral view, venter grayish blue; oral apparatus cream and covered with dark gray blotches. Iris tan gray. Closer examination of skin shows that overall pigmentation is composed by filiform cromatophores, except for the blotches at muscles and fins, composed of melanophores in dots.

Color in life. In dorsal view, body and caudal musculature dark brown to olive green. Tail about same coloration as body. Snout light brown. In lateral view, flanks lighter brown with blue iridescences at spiracle level. Fins translucent to brown; dark blotches and creamy white dots scattered irregularly on tail muscles and dorsal and ventral fins. Caudal muscles cream flecked with brown, becoming clearer towards tail terminus. Spiracle unpigmented, however a blue iridescence can be seen in certain light conditions. Venter metallic blue. Oral apparatus cream. Iris metallic green with fine black reticulations.

Variation. Variation of ten meristic characters of tadpoles in Stages 25–39 are shown in Table 8; nine tadpoles in Stages 25–39 greatly varied in total length that ranged from 48.0– 96.7; body length ranged from 14.1–36.5; tail length ranged from 34.4–66.4. Variation in LTRF cannot be correctly described because 66.6% of tadpoles (Stages 25, 27, 34) showed deformed oral apparatus, completely or partially depleted of denticles, with variable assymetric numbers of labial papillae, absence and presence of papillae in the posterior labium of oral disc. Absence of keratinized teeth may be due to chytrid infection. Assymetry in the number of papillae on each side of the labium and absence of papillae in the posterior labium is intriguing since there are no hylid tadpoles without ventral papillae. We interpret the assymetry and absence of papillae as abnormal development or damaged oral discs. From the tadpoles that had relatively distinct tooth rows, variation in number of this structure was from 5(4–5)/7(1) (Stage 25) to 7(7)/7(1) (Stage 31). The later tadpole seems abnormal and has labial tooth row ridges with no teeth. Nonetheless, the same number of upper and lower tooth rows is interesting.

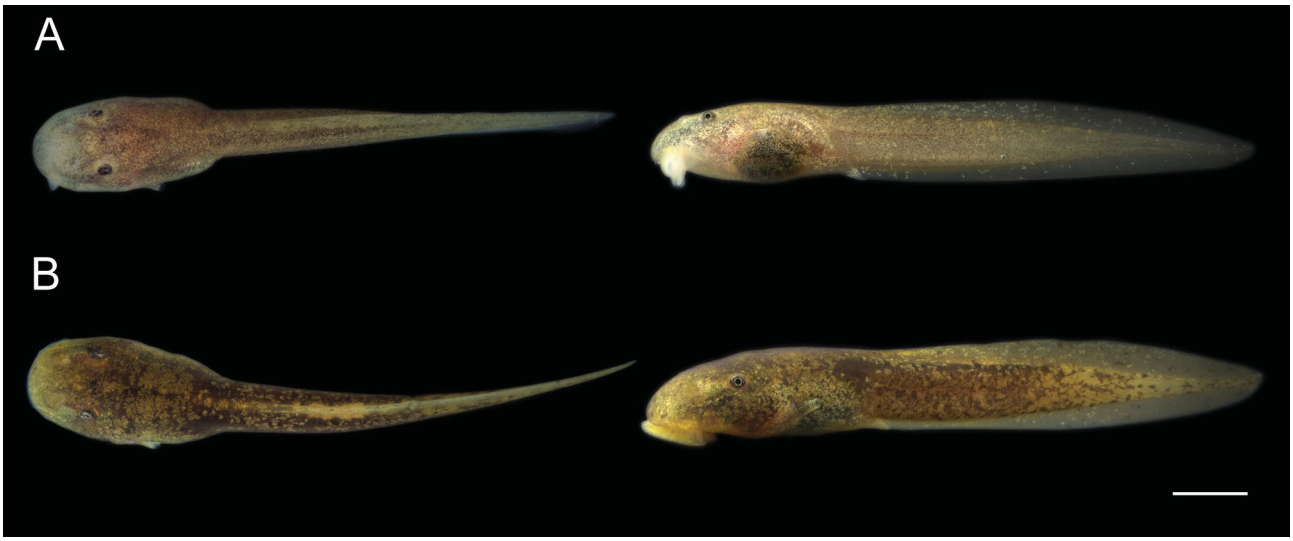

FIGURE 24.—Variation of living tadpoles in Gosner Stage 25 of *Hyloscirtus psarolaimus* from km 60 km on the Salcedo-Tena road, Provincia de Napo, Ecuador. (A) QCAZ 50423 and (B) QCAZ 50373. Differences in color intensity may be an artifact of amount of lighting. Scale = 5 mm. Photos by Luis A. Coloma.

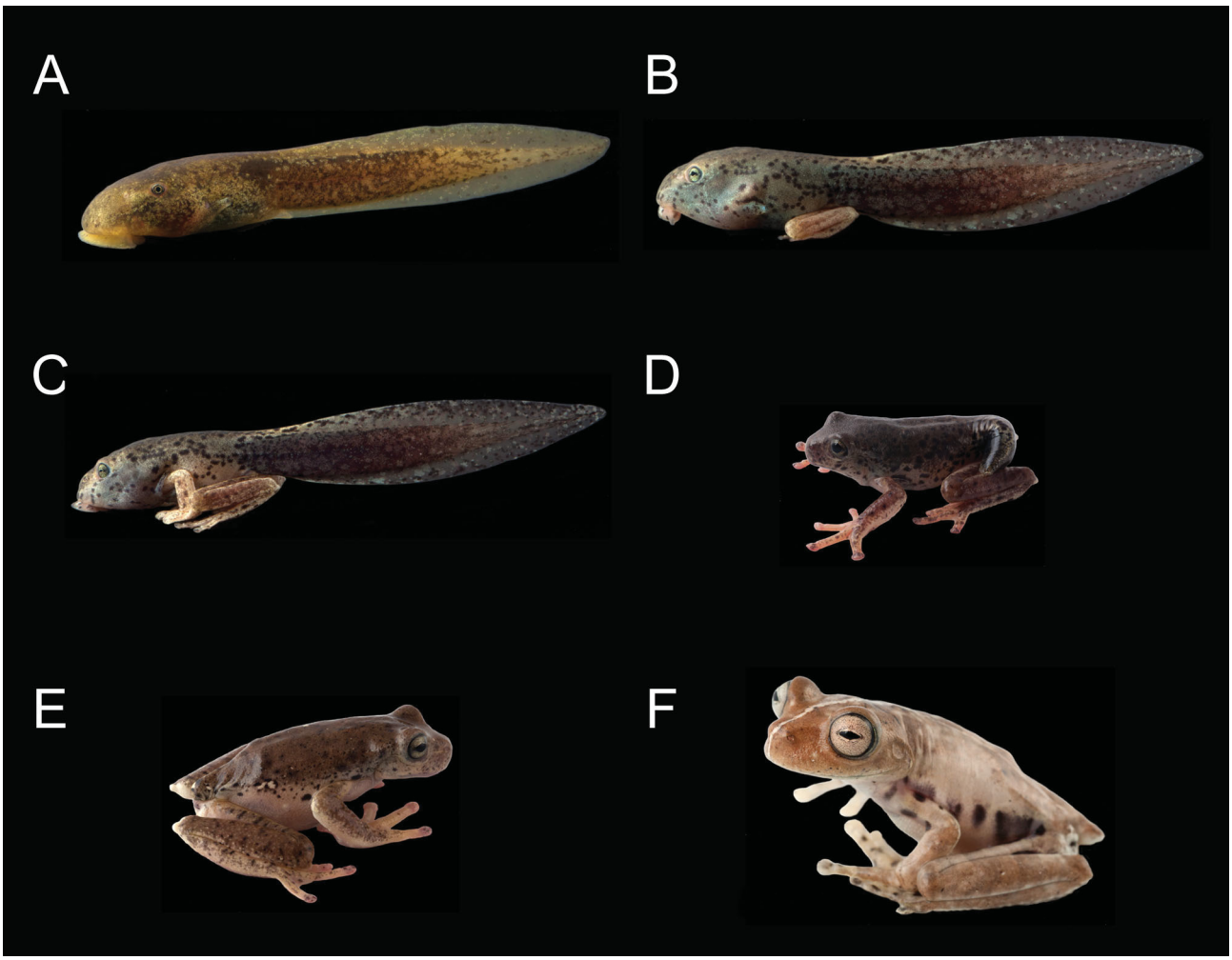

FIGURE 25.—Ontogenetic changes in *Hyloscirtus psarolaimus* from km 60 on road Salcedo-Tena, Provincia de Napo, Ecuador, Gosner stages: (A) Stage 25, QCAZ 50373, (B) Stage 41, QCAZ 50373, (C) Stage 42, QCAZ 50373, (D) Stage 45, QCAZ 50373, (E) juvenile, QCAZ 50423, and (F) subadult, QCAZ 45957. Not to scale. Photos by Luis A. Coloma.

The lateral-line system was evident in all individuals examined; however, variation in the placement and origin of lines is observed among individuals. Arrangement of ventral bodyline may be symmetrical or asymmetrical on the left flank of body, where the spiracle is located.

Color patterns and arrangement of blotches in fins as well as tail muscles varied through ontogenetic development (Figs. 26, 27). In the smallest individuals at Stage 25, numerous creamy white cromatophores can be seen against a black background both in dorsal and ventral fins. As ontogenetic development advances, creamy white dots are replaced by dark blotches, which in turn become numerous in older stages giving the overall tail coloration a darker appearance. Closer examination reveals that blotches are made up of cromatophores in dots that merge progressively as individuals grow. Individuals at Stage 25 have cream tail muscles, whereas some of the largest individuals at advanced pre-metamorphic stages show a reddish brown coloration in the muscles of the proximal half of the tail (Fig. 27).

FIGURE 26.—Variation in size of three living tadpoles at Gosner stages 37 (A) and 25 (B, C) of *Hyloscirtus tigrinus* (series of tadpoles QCAZ 38419) from Santa Bárbara, Provincia de Sucumbíos, Ecuador. Scale = 5 mm. Photos by Luis A. Coloma.

Considerable ontogenetic change occurs in coloration of individuals of *Hyloscirtus tigrinus* from tadpoles to adults (Fig. 27). Approximately at Stage 42, when the limbs are developed, an overall light green coloration appears on the dorsum and flanks. The limbs go from yellow to light green. At Stage 42 when the first pattern of black dots pattern appear, contrasting against the green background. By Stage 45, the entire dorsum is green with black dots in the peripheral areas of the flanks, vent, and head; the snout changes from brown to yellowish green. The toes and venter acquire a bright yellow coloration. At Stage 46, small black dots are extensive on the dorsum,

where a tan-yellowish green background begins to appear. A black mottled pattern and elongated bars appear against a yellowish green background at the level of the thighs, flanks, and upper maxillae. Snout–vent length of an individual fixed at this stage measured 36.0 mm (QCAZ 40331 from Santa Bárbara, 2638 m, Provincia de Sucumbíos, Ecuador, collected as tadpole by Juan F. Dueñas and Ítalo G. Tapia on 17 September 2008). Finally, juveniles at latter stages show a reticulated pattern of black mottling on the limbs, as well as the dorsum, thighs and feet, giving the individual a jaguar-like appearance. The sides of the head have a silvery-white coloration. Well-defined black bars extend on the flanks of body. Bright yellow mottling is evident in the hidden surfaces of thighs of posterior limbs.

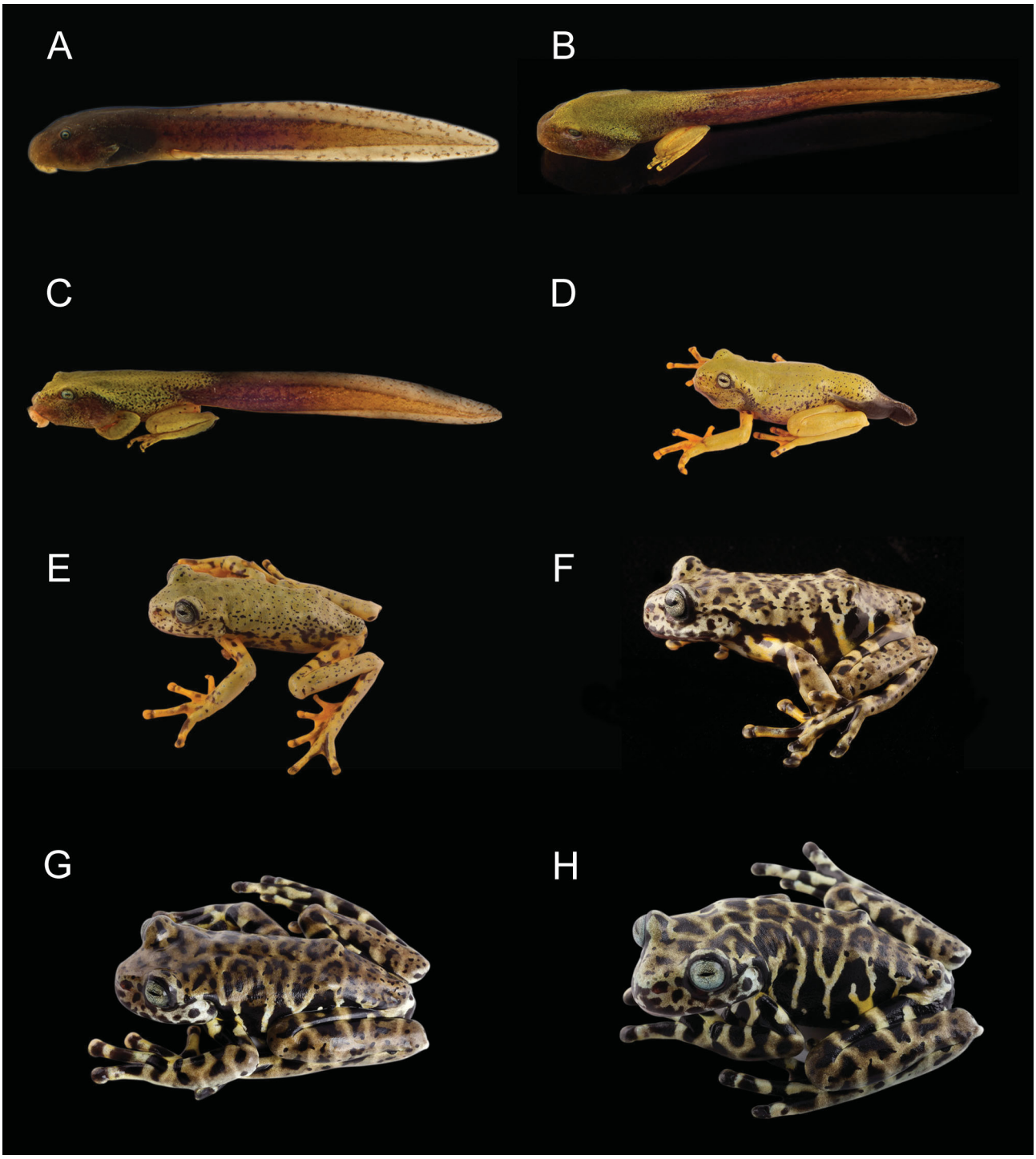

FIGURE 27.—Ontogenetic changes in *Hyloscirtus tigrinus* (QCAZ 40331) from Santa Bárbara, Provincia de Sucumbíos, Ecuador. Gosner stages: (A) Stage 25, QCAZ (sc 38419), (B) Stage 41, (C) Stage 42, (D) Stage 45, (E) Stage 46, and (F–H) subadults. Not to scale. Photos by Luis A. Coloma.

Osteology

The following description applies to all adults (double C&S) of *Hyloscirtus criptico*, *H. lindae, H. pacha, H. pantostictus, H. princecharlesi, H. psarolaimus, H. ptychodactylus,* and *H. staufferorum,* unless otherwise indicated. Museum numbers, sex, locality, and measurements of osteological features are given in Table 9. We mention only noticeable features for a male of *H. princecharlesi* (for which only an x-ray image was available, QCAZ 43654, SVL = 69.8, from Cuellaje, Provincia Imbabura, Fig. 28B). Characters depicted on the x-ray image of a female of *H. criptico* (QCAZ 43516, SVL = 60.8 mm, from Cuellaje, Provincia de Imbabura, Fig. 28A) are mentioned only when exhibiting noticeable differences from other species. General osteological features of *H. criptico* (QCAZ 10486, 43516), *H. lindae* (QCAZ 10484), *H. pacha* (KU 217573), *H. pantostictus* (QCAZ 10488), *H. princecharlesi* (QCAZ 43654), *H. psarolaimus* (KU 202727), *H. ptychodactylus* (QCAZ 2275), and *H. staufferorum* (QCAZ 11146) are depicted in Figures 28–42.

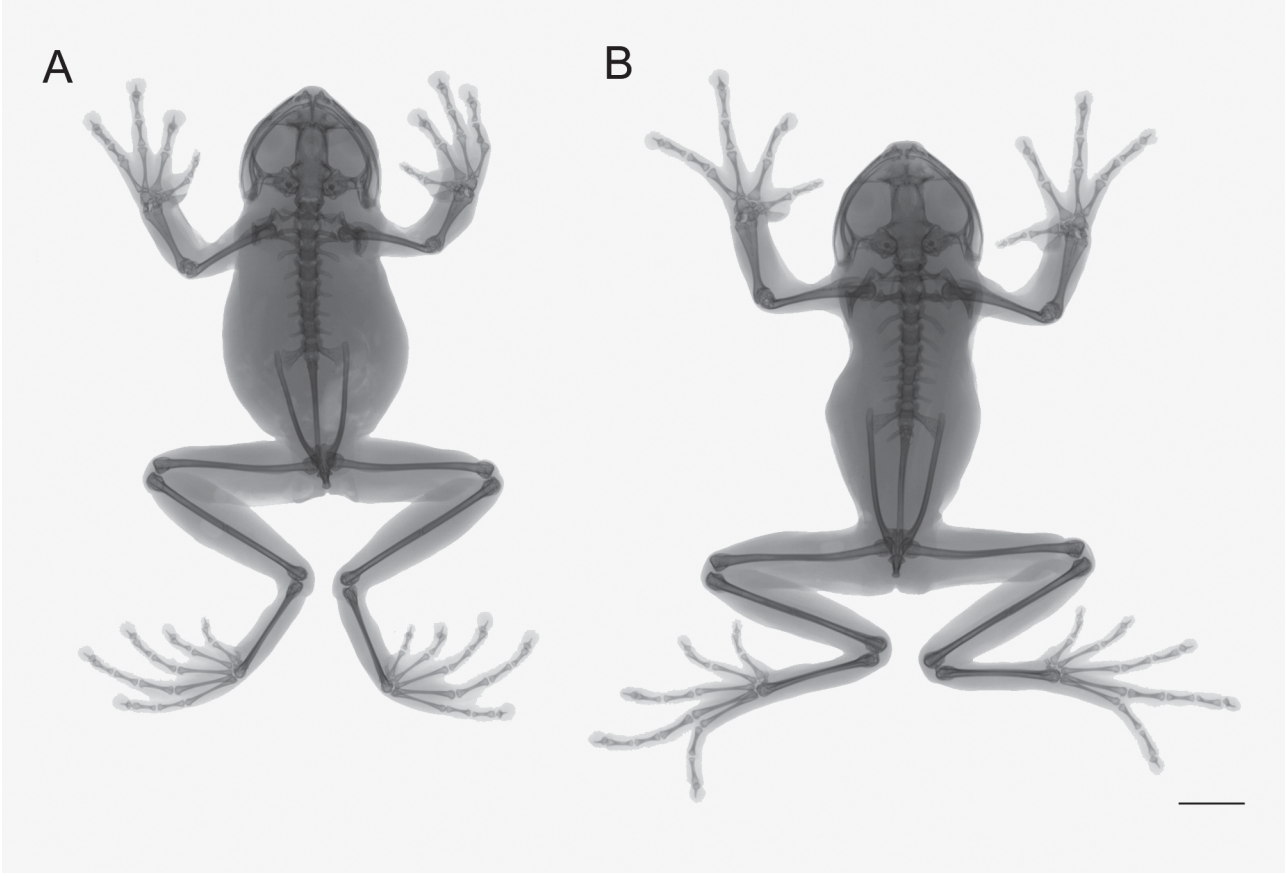

FIGURE 28.—X-rays showing skeletons of adult male paratypes of: (A) *Hyloscirtus criptico,* QCAZ 43516, SVL = 60.8 mm, and (B) *Hyloscirttus princecharlesi,* QCAZ 43654, SVL = 69.8 mm. Scale = 1 cm.

Skull. (Figs. 29, 31, 33, 35, 37, 39, 41). The skull presents the following general features, which are described in more detail under descriptions of each of the bones. It is broad, depressed, and gymnokrotaphic; it is characterized by having an opened temporal region; a large orbit, with its posterior margin formed by the anterior edge of the prootic and the posterolateral edge of the frontoparietal. The single sphenethmoid is endochondral. Prootics and exoccipitals are co-ossified; crista parotica is completely ossified. Stapes are well ossified, and a cartilaginous tympanic ring is present. Frontoparietals are paired, fused or not at midline level; when fused, there are no evident sutures and they do not contact the squamosal or the nasals; the frontoparietal fontanelle is small and exposed. The frontoparietals have interfrontal exostosis. Vomers are paired, denticulate, and not in contact medially. Prechoanal rami are triangular and prominent; postchoanal rami are not prominent. The neopalatine is present, it does not have sawed edges, and it is in contact with the sphenethmoid. The pars facialis of the maxilla lacks preorbital processes. The pars palatina is present. Maxillary and premaxillary teeth are present; they are present, short, and monocuspid. The pterygoid has an anterior ramus and a medial ramus. The medial ramus

contacts the otic capsule. The zygomatic ramus of the squamosal is elongate and its anterior end is cartilaginous. In most of the species the otic ramus of the squamosal is reduced and does not contact the prootic, except in *Hyloscirtus pantostictus* and *H. staufferorum*. Jaw articulation is located posterior to level of the fenestra ovalis. The mentomeckelian bones are present.

TABLE 9. Specimens of *Hyloscirtus* examined in the osteological analysis. Locality data, sex, and measurements (in mm) are given. Abbreviations are: SVL (snout-vent length), TIBL (tibia length), FOL (foot length), HLSQ (head length), HDW (head width), SL (sternum length), StW (sternum width), HYL (Hyobranchium corpus length), HYW (Hyobranchium corpus width), SW (sacrum width).

Museum number	Species	Locality	Sex	SVL	TIBL	FOL
QCAZ 10486	*Hyloscirtus criptico*	Ecuador: Imbabura: Cuellaje	M	61.2	31.7	47.2
QCAZ 10490	*Hyloscirtus criptico*	Ecuador: Imbabura: Cuellaje	M	62.1	32.0	49.1
QCAZ 10483	*Hyloscirtus lindae*	Ecuador: Napo: Oyacahi	H	64.8	34.7	52.4
QCAZ 10484	*Hyloscirtus lindae*	Ecuador: Napo: Oyacachi	M	61.0	32.5	46.9
KU 217573	*Hyloscirtus pacha*	Ecuador: Morona Santiago: 25.6 km E of borderline between Azuay and Morona Santiago on road Gualaceo-Limón	M	61.9	30.9	40.2
QCAZ 10489	*Hyloscirtus pacha*	Ecuador: Morona Santiago: 25.6 km E of borderline between Azuay and Morona Santiago on road Gualaceo-Limón	M	60.1	29.9	44.9
QCAZ 4506	*Hyloscirtus pantostictus*	Ecuador: Sucumbíos: Santa Bárbara	H	67.5	32.4	28.4
QCAZ 10488	*Hyloscirtus pantostictus*	Ecuador: Sucumbíos: Santa Bárbara	M	62.7	32.1	47.3
KU 202727	*Hyloscirtus psarolaimus*	Ecuador: Morona Santiago: 26.2 km WSW Plan de Milagro	M	58.8	29.4	43.3
QCAZ 2275	*Hyloscirtus ptychodactylus*	Ecuador: Cotopaxi: Pilaló	H	67.8	36.2	53.1
QCAZ 11146	*Hyloscirtus staufferorum*	Ecuador: Napo: Cordillera de los Guacamayos	M	60.5	30.4	40.1

TABLE 9. Continued.

Museum number	HLSQ	HDW	SL	StW	HYL	HYW	SW
QCAZ 10486	18.1	19.9	5.9	3.8	1.8	4.4	10.0
QCAZ 10490	21.7	20.9	6.2	5.0	1.6	4.0	10.2
QCAZ 10483	22.0	23.9	7.0	4.4	2.1	4.3	10.8
QCAZ 10484	19.2	21.9	5.4	4.3	1.0	2.5	10.2
KU 217573	18.1	19.7	5.0	4.0	0.8	3.0	10.4
QCAZ 10489	19.6	19.7	–	–	–	–	10.1
QCAZ 4506	20.2	22.3	6.9	4.5	1.9	3.9	11.5
QCAZ 10488	19.0	20.4	7.1	5.0	1.7	4.1	10.7
KU 202727	15.2	18.3	5.8	4.0	1.5	3.4	9.1
QCAZ 2275	22.2	23.8	8.5	6.5	1.8	3.8	14.6
QCAZ 11146	16.5	19.2	6.6	3.6	1.3	3.1	10.1

The neurocranium is composed of nasal capsule cartilages (tectum, solum, and septum nasi) and the following bones: septomaxilla, sphenethmoid, prootics, and exoccipitals. The septum nasi is medial and cartilaginous, the paired tectum nasi and oblique cartilages form part of the olfactory capsule ceiling; dorsally, they appear as a thin

and continuous band in the anterior end of the sphenethmoid and the anterolateral edge of the nasal. The solum and septum nasi are synostotically fused to the sphenetmoid; the septum and tectum nasi vary in their shape and degree of mineralization among species, from ossified in one individual of *Hyloscirtus pacha* (QCAZ 10489) to cartilaginous in the other six species. Septum nasi contributes to the snout medial anterodorsal configuration. Between the tectum nasi and premaxilla are the alar cartilages, which are dorsal components of the nasal capsule. The septomaxilla is a short and compact ∩-shaped bone, with medial and lateral rami. The lateral ramus is poorly developed; in *H. pacha* this branch is thinner than in all the other species; the medial ramus is prominent and presents processes at its posterior end.

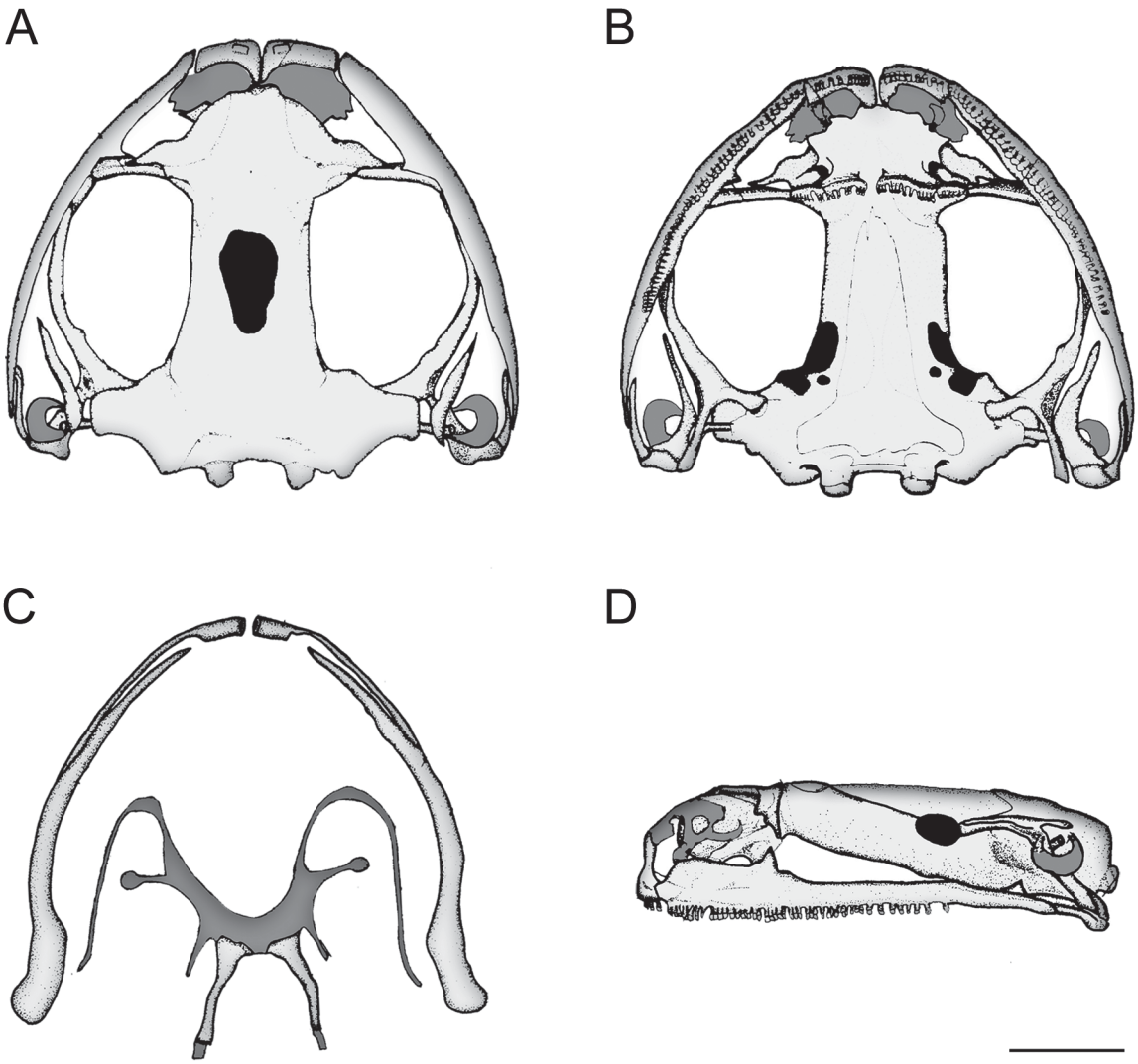

FIGURE 29.—Skull and hyobranchium of adult male *Hyloscirtus criptico* from Cuellaje, Provincia de Imbabura (QCAZ 10486, SVL = 61.2 mm). (A) dorsal view, (B) ventral view, (C) ventral view of mandible and hyobranchium, and (D) lateral view. Cartilage is shown in dark gray. Scale = 0.5 cm. Drawings by Arturo Paredes-Recalde.

The sphenethmoid is fused to septum nasi, tectum nasi, and planum antorbitale; posteriorly, it ends at the level of the anterior portion of the orbit. The sphenethmoid and neopalatine form the anterior edge of the optic foramen. The ventral surfaces of the sphenethmoid are strongly sculptured in *Hyloscirtus criptico, H. lindae, H. pacha, H. princecharlesi, H. ptychodactylus,* and *H. staufferorum,* and moderately so in *H. pantostictus* and *H. psarolaimus*. The posterior region of the sphenethmoid is ossified and overlaps the anterior margin of the parasphenoid cultriform process, which is completely ossified in all examined skeletons.

Paired prootics are synostotically united ventromedially and a suture line is visible. Dorsally, they contact the posterolateral margins of the frontoparietals; *Hyloscirtus lindae, H. pantostictus, H. ptychodactylus,* and *H.*

staufferorum have joint sutures, while *H. critpico*, *H. psarolaimus,* and *H. pacha* do not present sutures. The prootic shows little interspecific variation. The crista parotica is dorsally oriented and it is perpendicular to the midline in *H. criptico, H. psarolaimus, H. pacha,* and *H. staufferorum*; in one specimen of *H. lindae, H. pantostictus,* and *H. ptychodactylus,* the dorsal orientation remains, also has a slight anterior orientation. In all species examined, the anterior margin of the prootic forms the posterior edge of the optic foramen; oculomotor and prootic foramens are located in the anteroventral portion of the prootic. The posteroventral margin of the prootic forms the anteroventral margins of the postotic foramen.

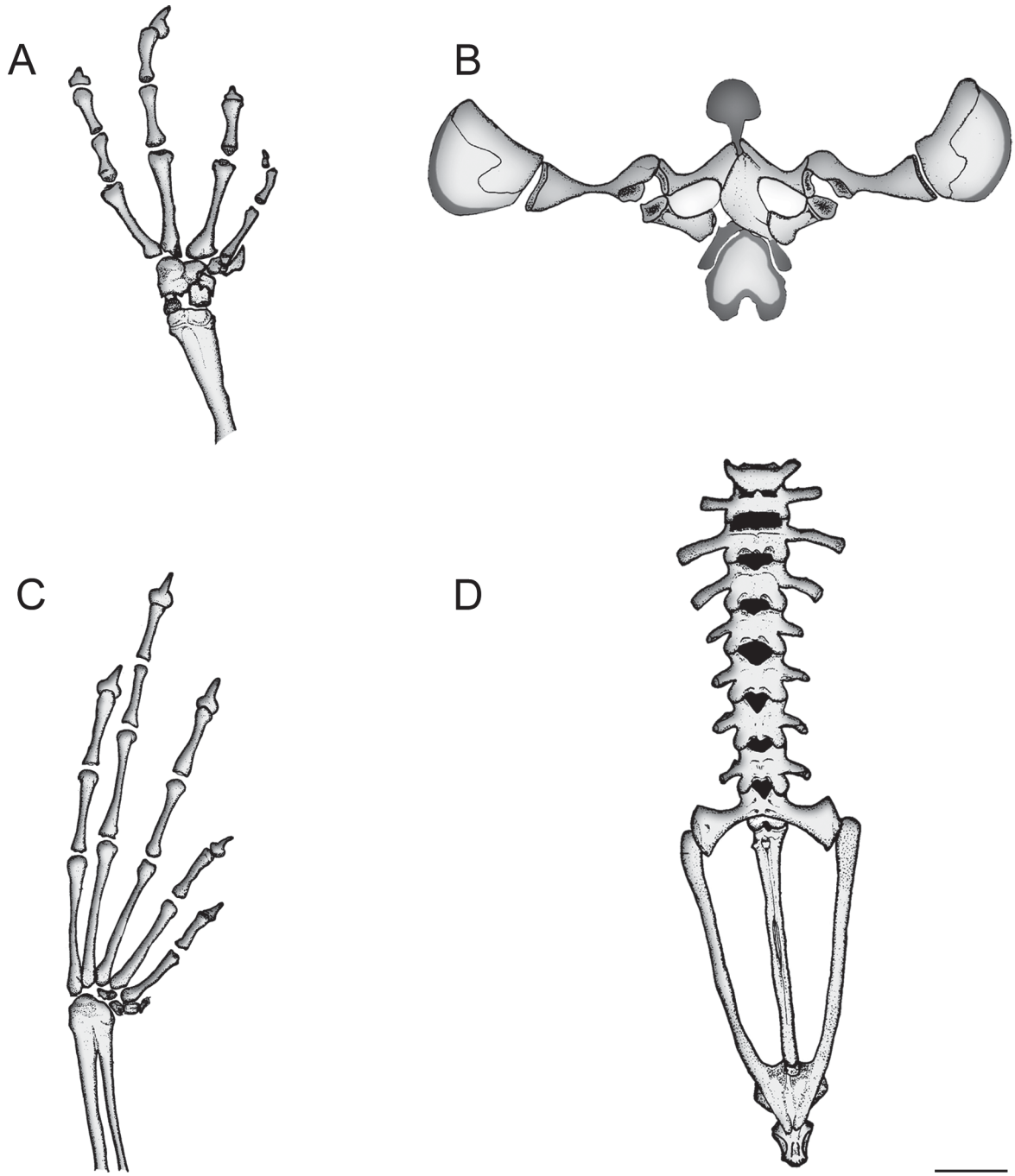

FIGURE 30.—Skeletal features of adult male *Hyloscirtus criptico* from Cuellaje, Provincia de Imbabura (QCAZ 10486, SVL = 61.2 mm). (A) ventral view of manus, (B) ventral view of pes, (C) ventral view of pectoral girdle, and (D) dorsal view of vertebral column and pelvic girdle. Cartilage is shown in dark gray. Scale = 0.5 cm. Drawings by Arturo Paredes-Recalde.

Paired exoccipitals are anterodorsally in contact with the prootic and the frontoparietal, and anteroventrally are synostotically fused to the posteroventral margin of the parasphenoid. The posterior margins of the exoccipitals form the posteromedial wall of the otic capsules, occipital condyles, and the margin of the foramen magnum. The tympanic annulus is cartilaginous and incomplete; its posterior region, at the level of the posterolateral zone of the crista parotica, possesses a process that is small in *Hyloscirtus criptico, H. pantostictus, H. psarolaimus, H. pacha,* and *H. staufferorum,* and elongated in *H. lindae* and *H. ptychodactylus.* Its orientation is parallel to the midline in all species. The stapes is long and cylindrical, with a wide pars interna plectri located lateral to the operculum and posterior to the fenestra ovalis; its pars media plectri extends in a slightly anterodorsal direction. In most of the skeletons, cartilaginous structures of the pars externa plectri are not evident, except in *H. ptychodactylus* and one female of *H. lindae*. The oval operculum, in lateral view, is completely ossified in all examined individuals; it is cone-shaped and is located at the level of the fenestra ovalis.

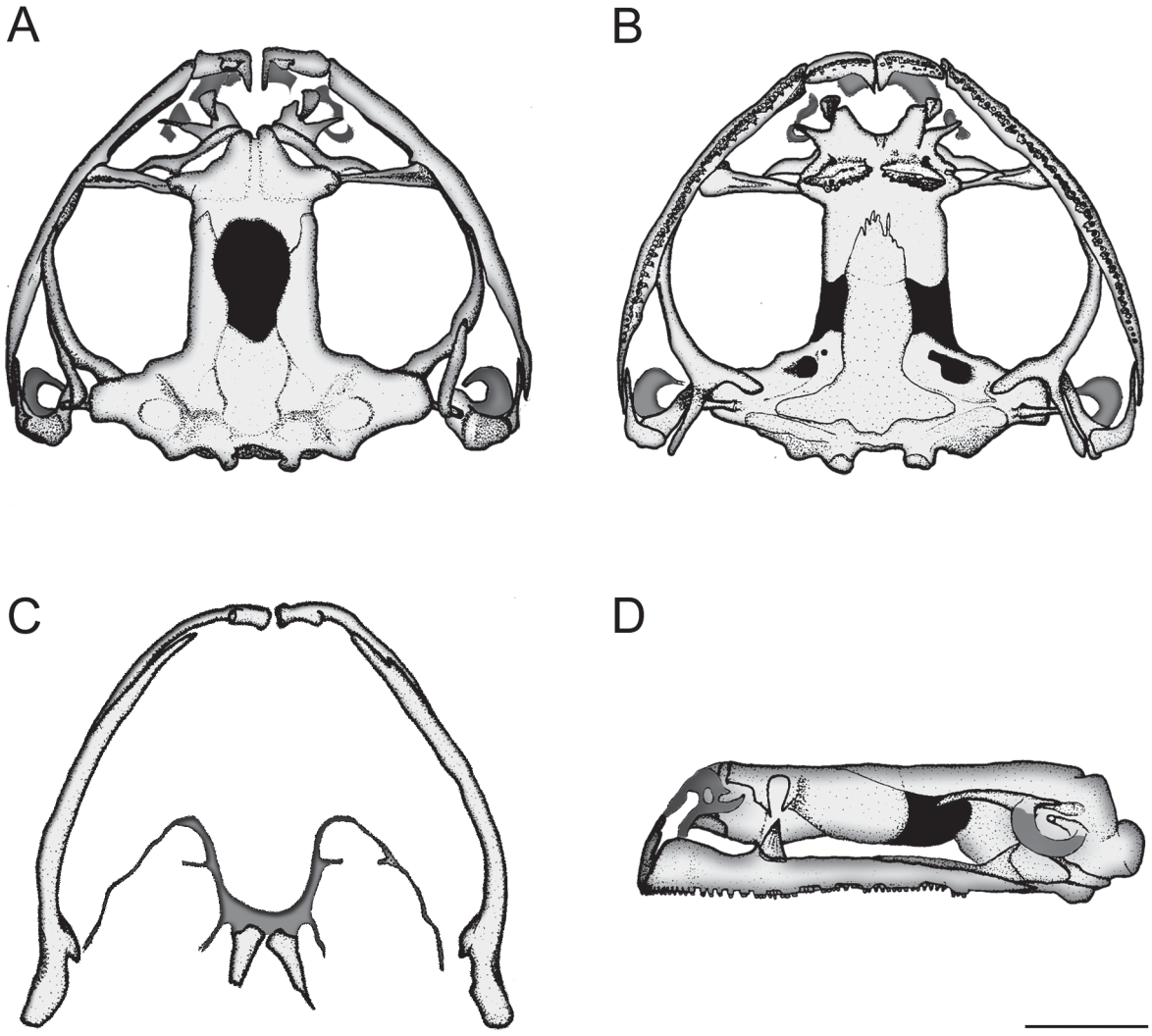

FIGURE 31.—Skull and hyobranchium of adult male *Hyloscirtus lindae* from Oyacachi, Provincia de Napo (QCAZ 10484, SVL = 61.0 mm). (A) dorsal view, (B) ventral view, (C) ventral view of mandible and hyobranchium, and (D) lateral view. Cartilage is shown in dark gray. Scale = 0.5 cm. Drawings by Arturo Paredes-Recalde.

Dermal bones include the nasals, frontoparietals, vomers, neopalatines, and parasphenoid.

The nasals are subtriangular, and separated at the midline. They have an elongated maxillary process that extends ventrolaterally towards the maxilla. The maxillary process ends in a tip and it is near (not reaching) the

pars facialis of the maxilla; the posteromedial edges of the nasals are in contact with the anterolateral margins of the sphenethmoid, posterior to them. Only in *Hyloscirtus ptychodactylus* and in one female of *H. pantostictus* are the nasals separated from the sphenethmoid.

The frontoparietals are paired and rectangular, covering the dorsolateral surface of the cranium from the anterior margin of the orbit to the level of the anterior margin of the exoccipitals. The presence of a medial articulation in the frontoparietals varies. *Hyloscirtus criptico, H. psarolaimus,* and *H. pacha* do not have a medial suture, whereas *H. lindae, H. pantostictus, H. ptychodactylus*, and *H. staufferorum* do. There are occipital grooves in the articulation zone with the prootic are present.

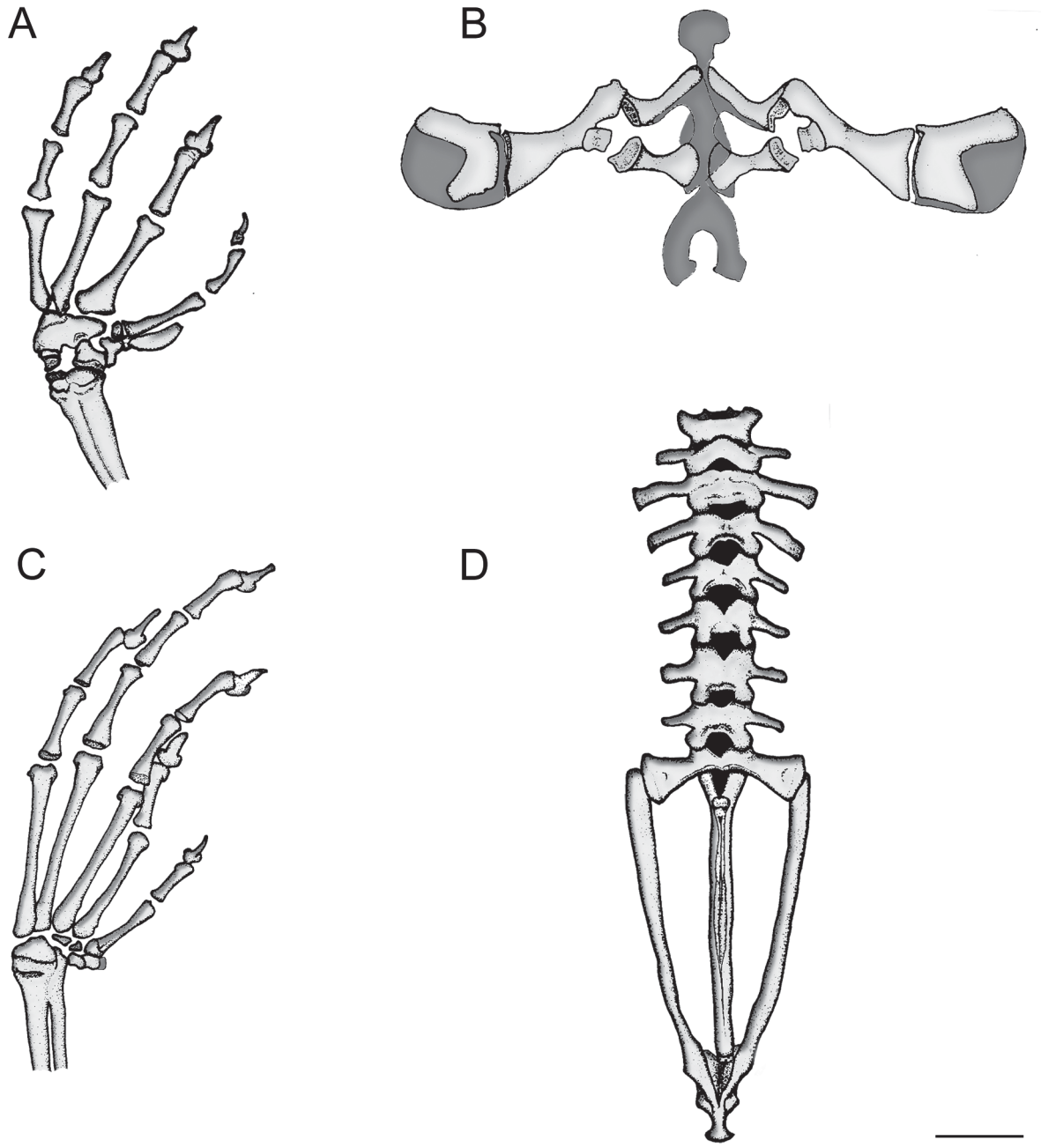

FIGURE 32.—Skeletal features of adult male *Hyloscirtus lindae* from Oyacachi, Provincia de Napo (QCAZ 10484, SVL = 61.0 mm). (A) ventral view of manus, (B) ventral view of pes, (C) ventral view of pectoral girdle, and (D) dorsal view of vertebral column and pelvic girdle. Cartilage is shown in dark gray. Scale = 0.5 cm. Drawings by Arturo Paredes-Recalde.

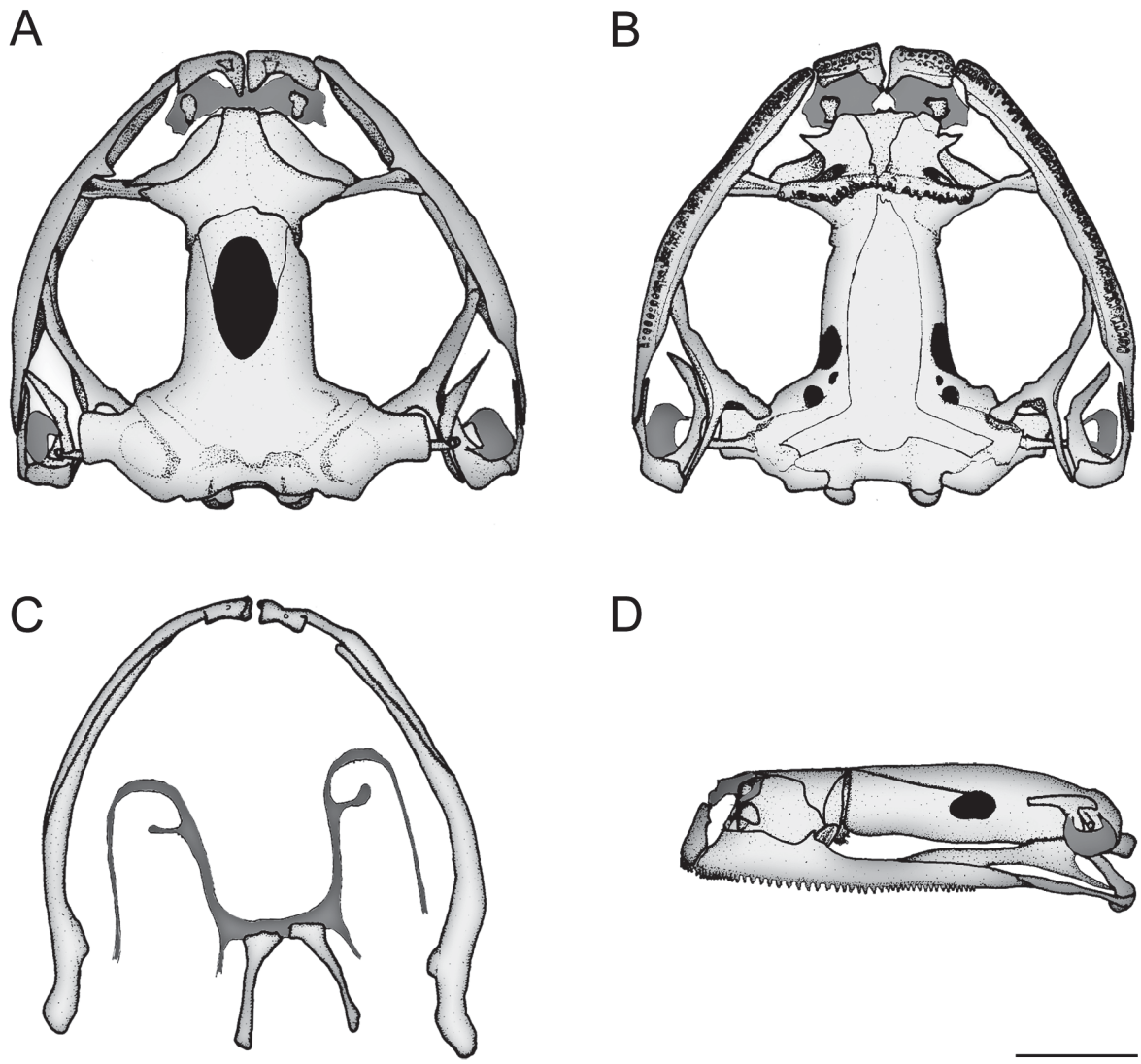

FIGURE 33.—Skull and hyobranchium of adult male *Hyloscirtus pacha* from 25.6 km East of borderline between Azuay and Morona Santiago, Provincia Morona Santiago (KU 217573, SVL = 61.9 mm). (A) dorsal view, (B) ventral view, (C) ventral view of mandible and hyobranchium, and (D) lateral view. Cartilage is shown in dark gray. Scale = 0.5 cm. Drawings by Arturo Paredes-Recalde.

The vomers are paired, triradiate, toothed, and irregular. They are jointed medially in *Hyloscirtus criptico* and *H. pacha*, and located below the sphenethmoid. The terminus of the anterior ramus is thin and pointed in *H. psarolaimus* and *H. staufferorum,* whereas it is wide and truncated in the other species. The orientation of the rami varies interspecifically in *H. criptico* and *H. staufferorum*, being oriented towards the medial portion of the premaxila; in *H. lindae, H. pantostictus, H. psarolaimus,* and *H. pacha* it is oriented towards the external portion of the premaxilla, and in *H. ptychodactylus* it points to the articulation between the maxilla and the premaxilla. The anterior ramus is shorter than the prechoanal ramus. Pre- and postchoanal rami are pointed and surround the medial, antero- and posteromedial borders of the choanae. The orientation of the prechoanal rami also varies, being horizontal in *H. pantostictus, H. pacha,* and *H. ptychodactylus,* forming an acute angle in relation to midline, whereas it points to the anterior portion of the maxilla in *H. criptico, H. lindae, H. psarolaimus,* and *H. staufferorum*. The postchoanal ramus is posterolaterally oriented in all species. The dorsal surface of the vomer is in contact with the parasphenoid ventral surface.

The neopalatine is an elongate, triangular bone that is located below the planum antorbitale, between the sphenethmoid and the maxilla. In *Hyloscirtus ptychodactylus* and *H. staufferorum* it is incompletely ossified. The maxillary half of the neopalatine is widest and its lateral border and has two vertices and the medial extreme is pointed. The neopalatine articulates with the inner face of the maxilla through its distal end, just behind the pars facialis of the maxilla. *Hyloscirtus criptico* and *H. psarolaimus* have a small non-prominent peak in the middle of the anterior margin of the neopalatine.

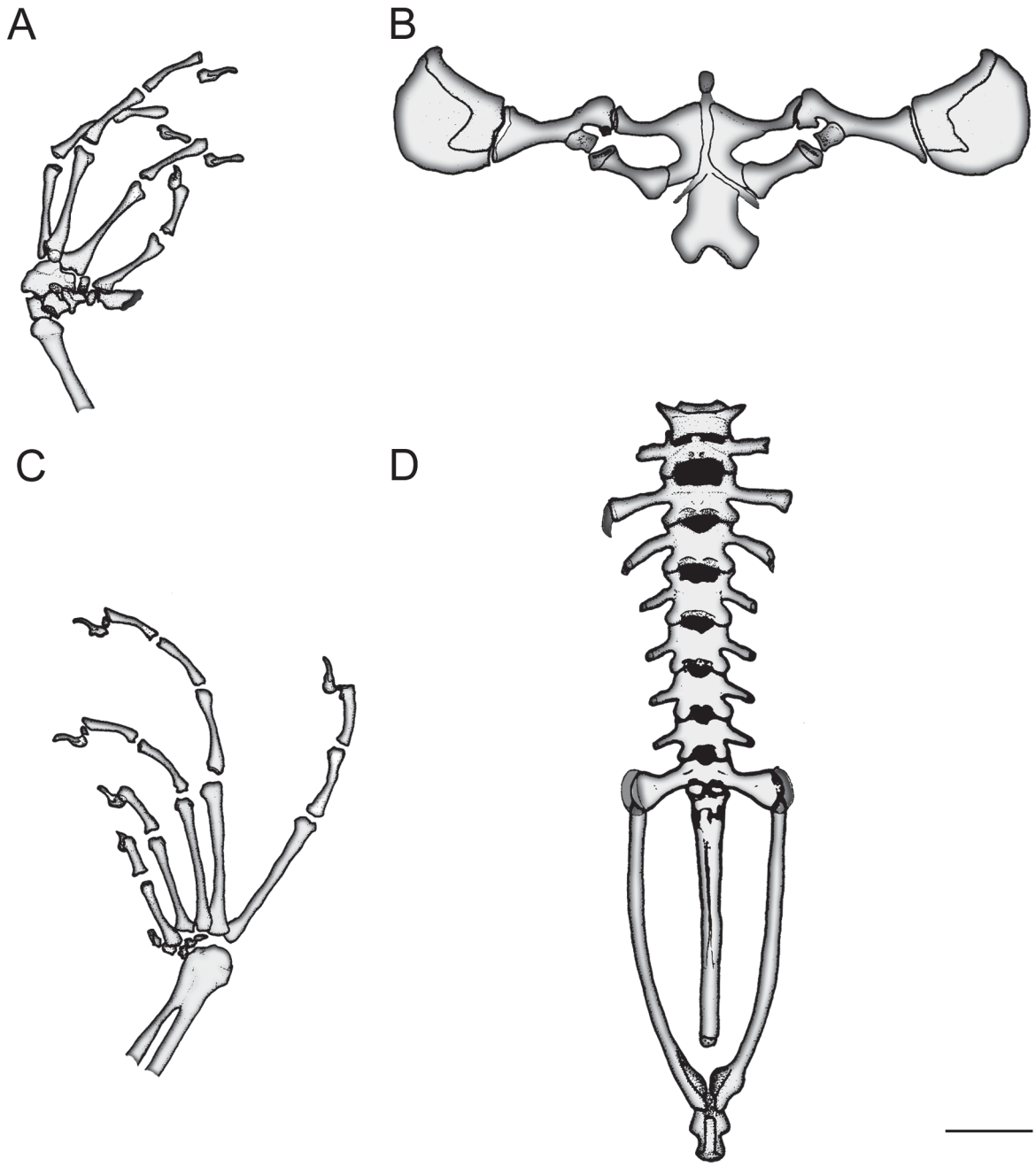

FIGURE 34.—Skeletal features of adult male *Hyloscirtus pacha* from 25.6 km East of borderline between Azuay and Morona Santiago, Provincia Morona Santiago (KU 217573, SVL = 61.9 mm). (A) ventral view of manus, (B) ventral view of pes, (C) ventral view of pectoral girdle, and (D) dorsal view of vertebral column and pelvic girdle. Cartilage is shown in dark gray. Scale = 0.5 cm. Drawings by Arturo Paredes-Recalde.

The parasphenoid has an inverted T-shape and invests the ventral surface of the neurocranium; it extends from a level at the anterior margin of the orbit toward the margin of the foramen magnum; its ventral surfaces are slightly rough. The cultriform process is cylindrical or bottle-shaped in ventral view, contacting with its anterior end the anterior portion of the sphenethmoid. There is interspecific variation in the anterior end of the cultriform process,

being cone-shaped in *Hyloscirtus pacha* and *H. staufferorum,* and serrate in the remaining species. The parasphenoid alae are oriented slightly posterolateral in relation to the cultriform process. The posterior margin of parasphenoid is nearly straight, except at the ventromedial zone, where variation was found. *Hyloscirtus criptico* has two broad processes in this margin; *H. lindae* and *H. pantostictus* have one broad and truncated process; *H. psarolaimus* present a V-shaped process; *H. pacha* and *H. staufferorum* have two broad and truncate processes; *H. ptychodactylus* presents a broad and truncated process with a small peak posteriorly oriented in the middle of the posterior margin of the process; processes are parallel to the midline in all the species. The distal margins of parasphenoid alae are in contact with the ventral portion of the otic capsule.

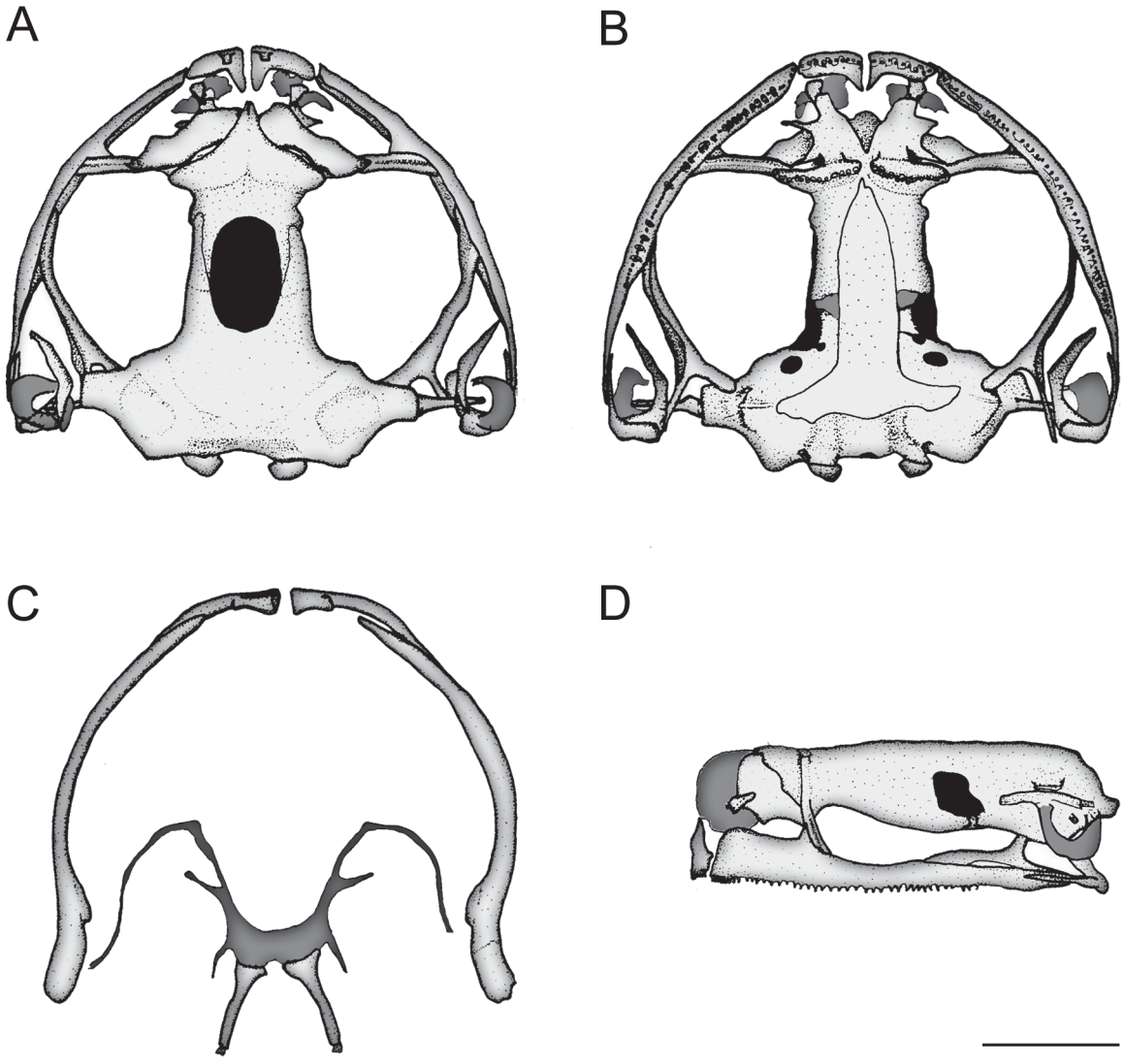

FIGURE 35.—Skull and hyobranchium of adult male *Hyloscirtus psarolaimus* from 26.2 km WSW Plan de Milagro, Provincia Morona Santiago (KU 202727, SVL = 58.9 mm). (A) dorsal view, (B) ventral view, (C) ventral view of mandible and hyobranchium, and (D) lateral view. Cartilage is shown in dark gray. Scale = 0.5 cm. Drawings by Arturo Paredes-Recalde.

The maxillary arcade is composed of the premaxilla, maxilla, and quadratojugal.

The paired premaxillae have a toothed pars dentalis at its anterior margin. All the species have a dorsal alary process (nasal process or pars dorsalis) and a biradiate pars palatina. There is variation in the length of the pars palatina lateral ramus in relation to the medial ramus; in *Hyloscirtus criptico*, *H. psarolaimus, H. pacha, H. ptychodactylus,* and *H. staufferorum,* the lateral ramus is more than twice the length of the medial ramus. In *H. lindae* and *H. pantostictus* the lateral ramus length is twice the length of the palatine process medial ramus. The terminal portion of the lateral ramus is truncate, square, and not in contact with the maxillae. The medial ramus of

the pars palatine is well developed, triangular and pointed; it has two crests parallel to its posterolateral border, forming the floor of a channel that goes from the medial border to the pars dentalis. This formation is more conspicuous in *H. criptico*. The premaxillary alary process projects dorsally forming a straight angle with the pars facialis in *H. larinopygion*, *H. pantostictus,* and *H. psarolaimus*, whereas in *H. lindae*, *H. pacha*, *H. ptychodactylus,* and *H. staufferorum* it is posterodorsally projected forming an acute angle with the pars facialis. The length of the alary process of the premaxilla is about the same as the pars dentalis in *H. criptico, H. psarolaimus,* and *H. pacha,* whereas the alary process is longer in *H. lindae, H. pantostictus, H. ptychodactylus,* and *H. staufferorum*.

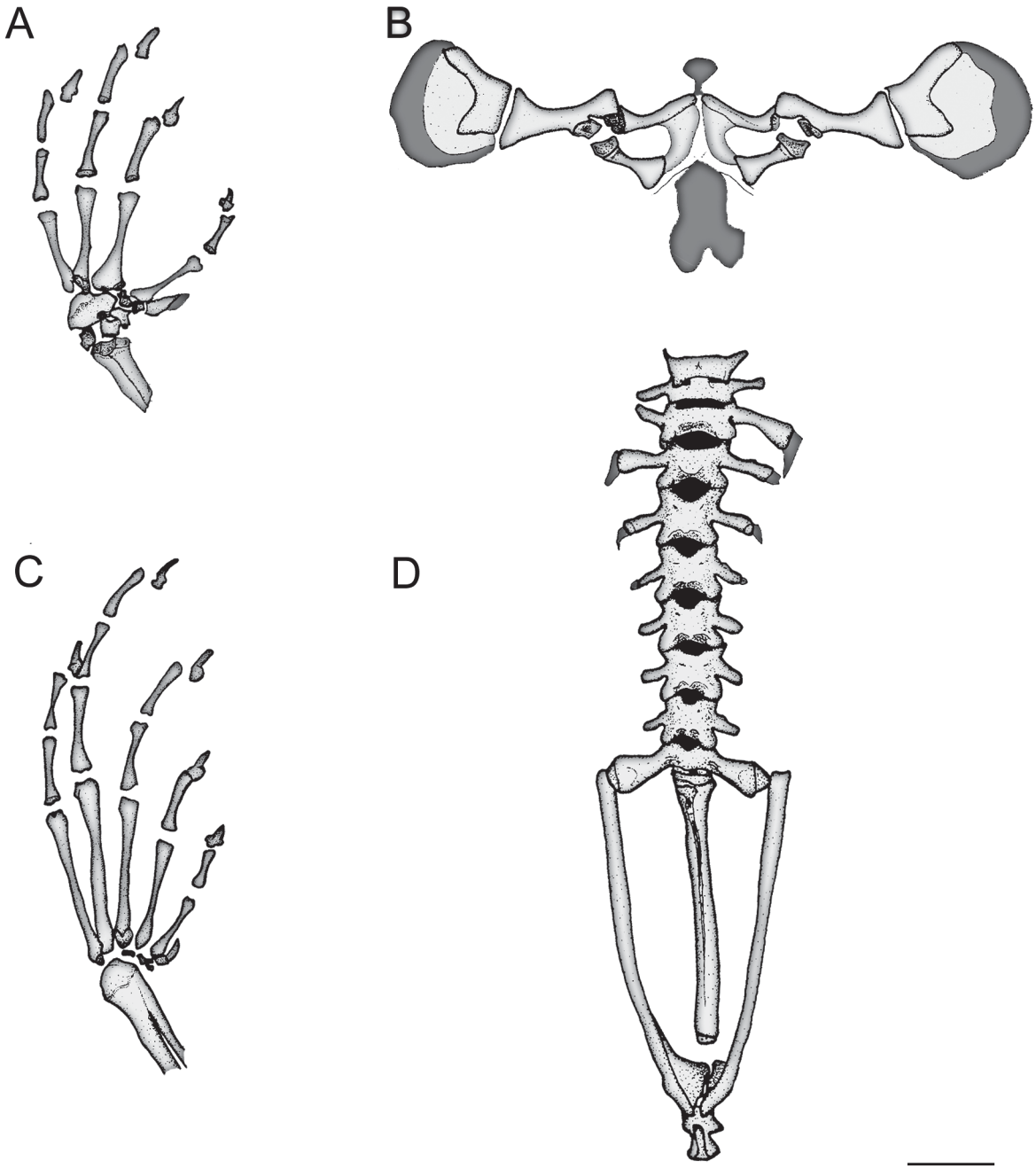

FIGURE 36.—Skeletal features of adult male *Hyloscirtus psarolaimus* from 26.2 km WSW Plan de Milagro, Provincia Morona Santiago (KU 202727, SVL = 58.9 mm). (A) ventral view of manus, (B) ventral view of pes, (C) ventral view of pectoral girdle, and (D) dorsal view of vertebral column and pelvic girdle. Cartilage is shown in dark gray. Scale = 0.5 cm. Drawings by Arturo Paredes-Recalde.

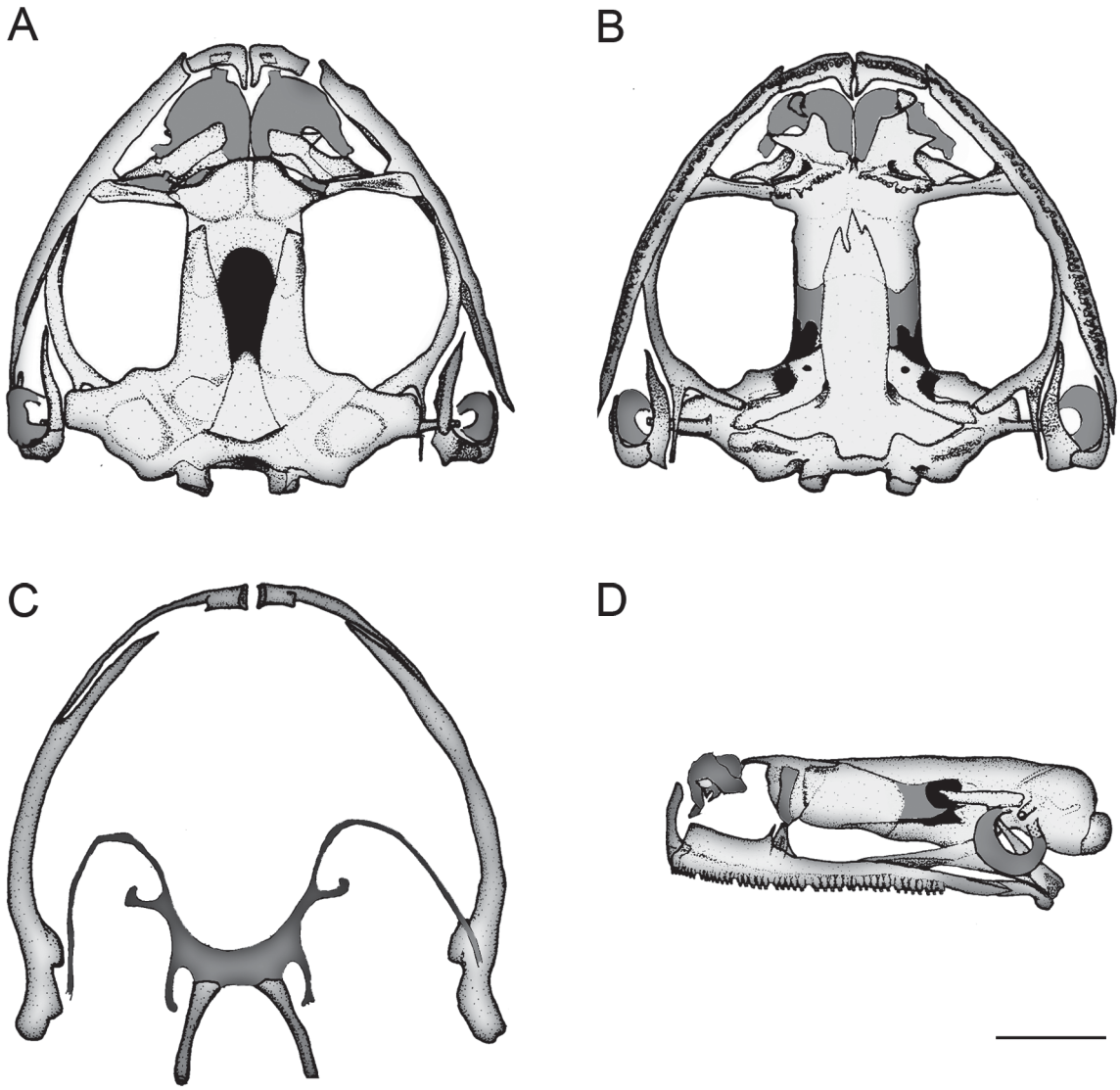

FIGURE 37.—Skull and hyobranchium of adult male *Hyloscirtus pantostictus* from Santa Bárbara, Provincia de Sucumbíos (QCAZ 10488, SVL = 62.7 mm). (A) dorsal view, (B) ventral view, (C) ventral view of mandible and hyobranchium, and (D) lateral view. Cartilage is shown in dark gray. Scale = 0.5 cm. Drawings by Arturo Paredes-Recalde.

The maxilla is an elongate, toothed bone located between the premaxilla and the quadratojugal. The pars palatina extends along the lingual margin of the maxilla; posteriorly this shelf articulates with the anterior ramus of the pterygoid. The maxilla is deepest anteriorly and bears a large, subtriangular-shaped pars facialis. The palatine process of the pars facialis almost contacts the nasal maxillary process in *Hyloscirtus criptico*, *H. pantostictus, H. psarolaimus, H. ptychodactylus,* and *H. staufferorum*, whereas the palatine process is separated from the nasal maxillary process in *H. lindae* and *H. pacha*. In lateral view the pars facialis of *H. criptico*, *H. pantostictus,* and *H. staufferorum* is perpendicular to the longitudinal axis of the pars palatine; in *H. lindae, H. psarolaimus, H. pacha,* and *H. ptychodactylus* it is oblique. In all the species the anterior border of the maxilla is truncated and it does not contact the premaxilla, whereas the posterior end is pointed and overlaps anterior ramus of the quadratojugal.

The quadratojugal is small and L-shaped and located below the ventral ramus of the squamosal; its posterior ramus articulates with the pars articularis of the palatoquadrate; the anterior ramus of the quadratojugal is projected towards the maxilla, articulating medially on its posterior border.

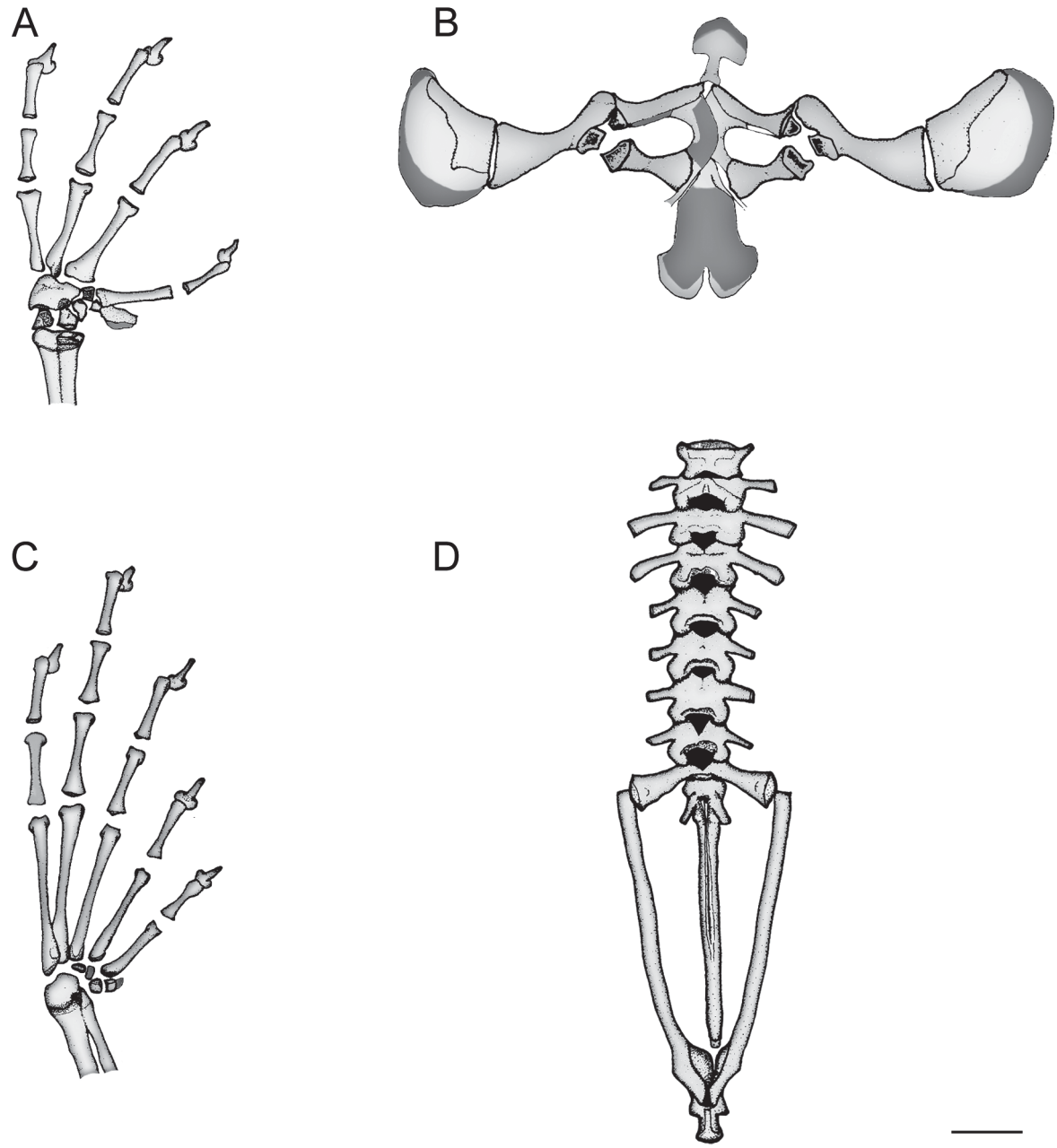

FIGURE 38.—Skeletal features of adult male *Hyloscirtus pantostictus* from Santa Bárbara, Provincia de Sucumbíos (QCAZ 10488, SVL = 62.7 mm). (A) ventral view of manus, (B) ventral view of pes, (C) ventral view of pectoral girdle, and (D) dorsal view of vertebral column and pelvic girdle. Cartilage is shown in dark gray. Scale = 0.5 cm. Drawings by Arturo Paredes-Recalde.

The suspensorium is composed of the squamosal, pterygoid, and palatoquadrate. The squamosal is a T-shaped bone with two dorsal rami (zygomatic and otic) and one ventral. The length of the otic ramus is variable; short in *Hyloscirtus lindae, H. pantostictus,* and *H. staufferorum*; slightly longer in *H. criptico, H. psarolaimus,* and *H. ptychodactylus*; and longest in *H. pacha*. In all the species the otic ramus is oriented towards the lateral margin of the prootic and does not contact its dorsolateral surface; the posterior margin of the otic ramus is irregular and has flanges and crests. The zygomatic ramus is prominent and triangular; its anterior end is pointed in all the species; in *H. criptico* and one female of *H. pantostictus* there is a triangular cartilaginous structure that overlaps its distal end. The ventral ramus extends posteroventrally and is oblique to the dorsal ramus. It is formed by a long arm that projects towards the ventral portion and then it changes its orientation laterally; its lower end is broad and invests the palatoquadrate.

The triradiate, paired pterygoid consists of anterior, medial, and posterior rami. The anterior ramus articulates with the posterior half of the maxilla. The medial ramus covers the prootic pseudobasal process without touching it

and the posterior ramus is oriented towards the palatoquadrate, but does not contact it at its terminal end. The ventrolateral surface of the pseudobasal process articulates with the pterygoid through the end of the medial ramus. *Hyloscirtus criptico*, *H. pantostictus*, *H. staufferorum,* and one female of *H. lindae* have the medial ramus border truncated, whereas in *H. psarolaimus*, *H. ptychodactylus,* and one male of *H. lindae,* the medial ramus is rounded. The palatoquadrate has no noticeable variation; it is a bony element that is held laterally by the ventral arm of the squamosal and medially and posteromedially by the posterior ramus of the pterygoid.

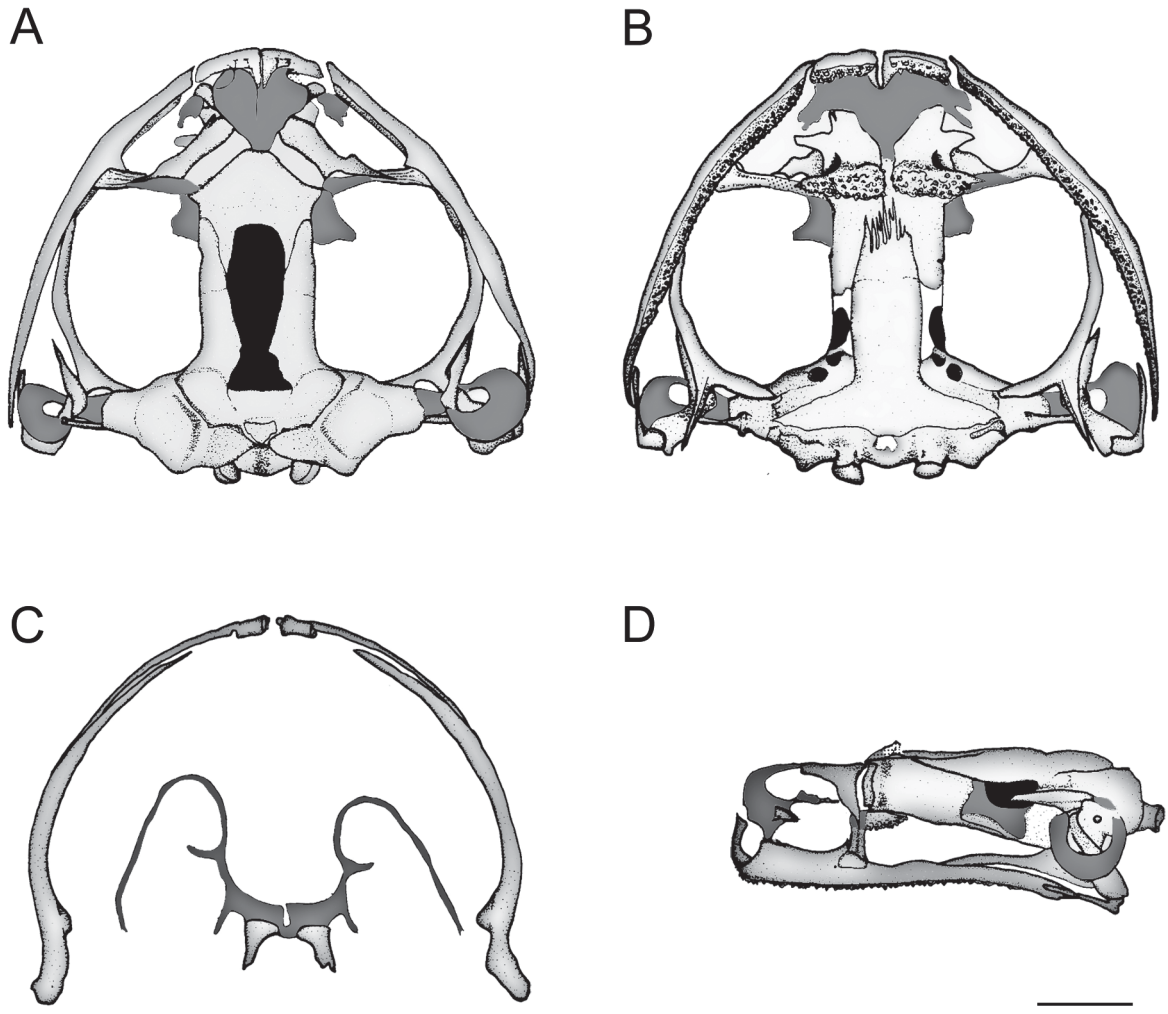

FIGURE 39.—Skull and hyobranchium of adult female *Hyloscirtus ptychodactylus* from Pilaló, Provincia Cotopaxi (QCAZ 2275, SVL = 67.8 mm). (A) dorsal view, (B) ventral view, (C) ventral view of mandible and hyobranchium, and (D) lateral view. Cartilage is shown in dark gray. Scale = 0.5 cm. Drawings by Arturo Paredes-Recalde.

The lower jaw is composed of four paired elements. Anteromedially the mentomeckelian bone bears a cartilaginous margin that forms a symphysis with the opposite medial margin. Posteriorly the dorsal portion of the mentomeckelian bone is fused to the dentary. In lateral view the dentary is an elongated bone that overlaps laterally the angulosplenial. It is located in the medial ventral side, from behind the mentomeckelian bone, to the posterior end of the jaw. Between the dentary and the angulosplenial a Meckel's cartilage extends along the jaw. The Meckel's cartilage is invested by the dentary anterodorsally and anterolaterally, and by the angulosplenial posteroventrally and posteromedially.

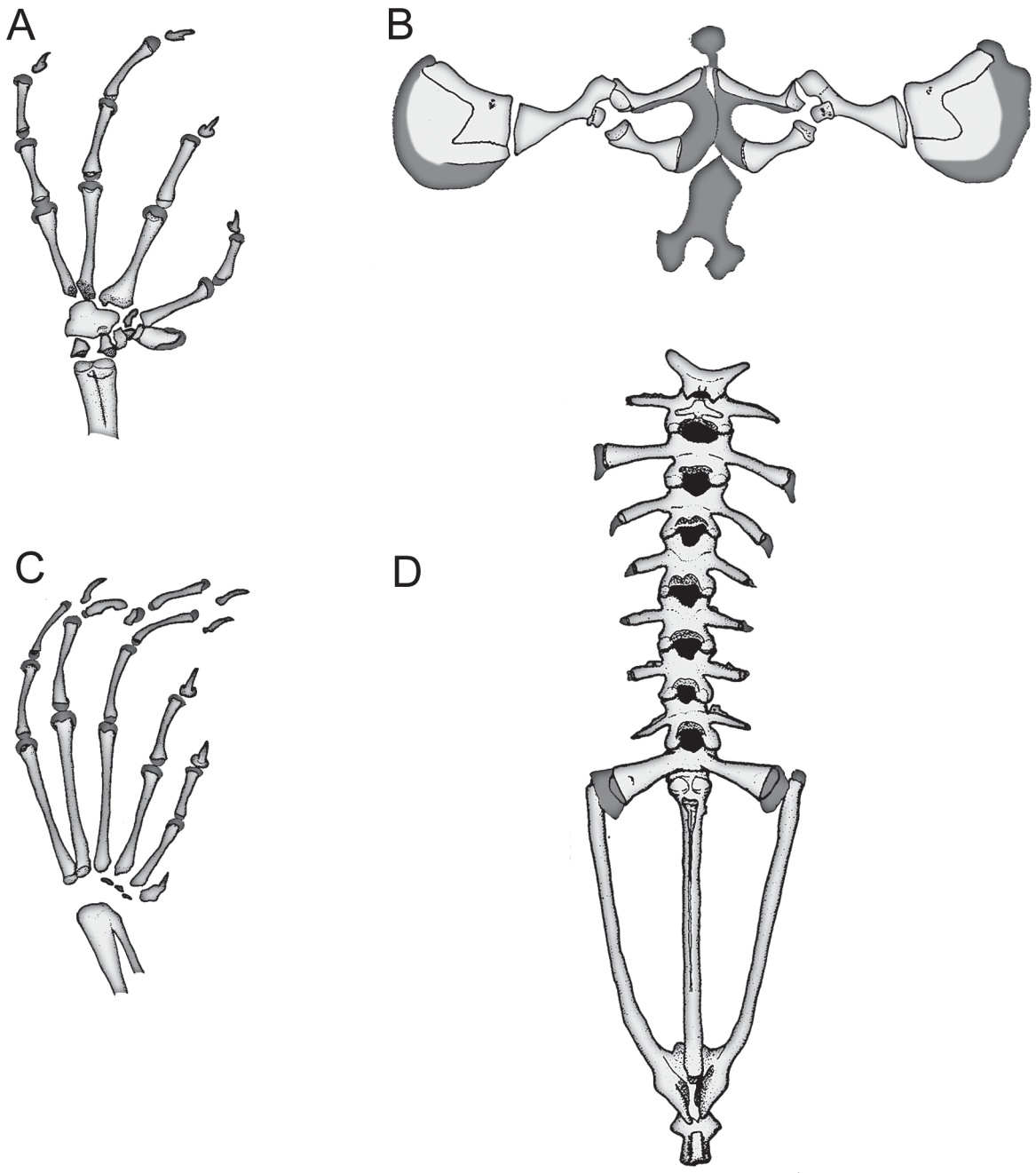

FIGURE 40.—Skeletal features of adult female *Hyloscirtus ptychodactylus* from Pilaló, Provincia Cotopaxi (QCAZ 2275, SVL = 67.8 mm). (A) ventral view of manus, (B) ventral view of pes, (C) ventral view of pectoral girdle, and (D) dorsal view of vertebral column and pelvic girdle. Cartilage is shown in dark gray. Scale = 0.5 cm. Drawings by Arturo Paredes-Recalde.

Hyobranchium. (Figs. 29C, 31C, 33C, 35C, 37C, 39C, 41C). The hyobranchium is composed of a cartilaginous plate, two hyalia, a pair of basally narrow alary processes, a pair of posterolateral processes, and two ossified posteromedial processes; it lacks a parahyoid and ossifications. The plate's configuration (= corpus) is broader than long. There is no ossification of the corpus, or of the anterior processes of the hyale. The hyale has a broad anterior portion that is folded laterally. The hyoglossal sinus is U-shaped and opened in *Hyloscirtus criptico*, *H. psarolaimus*, *H. pacha,* and one female of *H. lindae*; in the other species the hyoglossal sinus looks like a U. The anterolateral processes varies; in *H. criptico, H. pacha, H. pantostictus,* and *H. staufferorum* it is narrow basally, the processes are broader distally forming a disc; *H. lindae, H. psarolaimus,* and *H. ptychodactylus* have

rectangular processes with no distal expansions. Broad-based posterolateral processes are as long as the anterolateral processes; they are pointed in *H. criptico*, *H. lindae*, *H. pacha, H. psarolaimus,* and *H. staufferorum*; and truncate in *H. pantostictus* and *H. ptychodactylus*. The posteromedial processes are long and ossified with cartilaginous ends in all the species, with exception of one male of *H. pantostictus* that bears ossified ends. For *H. ptychodactylus* these data are not available due to damage of the posteromedial processes in their medial portion (probably caused by preparation). The posterior half of the posteromedial processes projects dorsally with a broad anterior end.

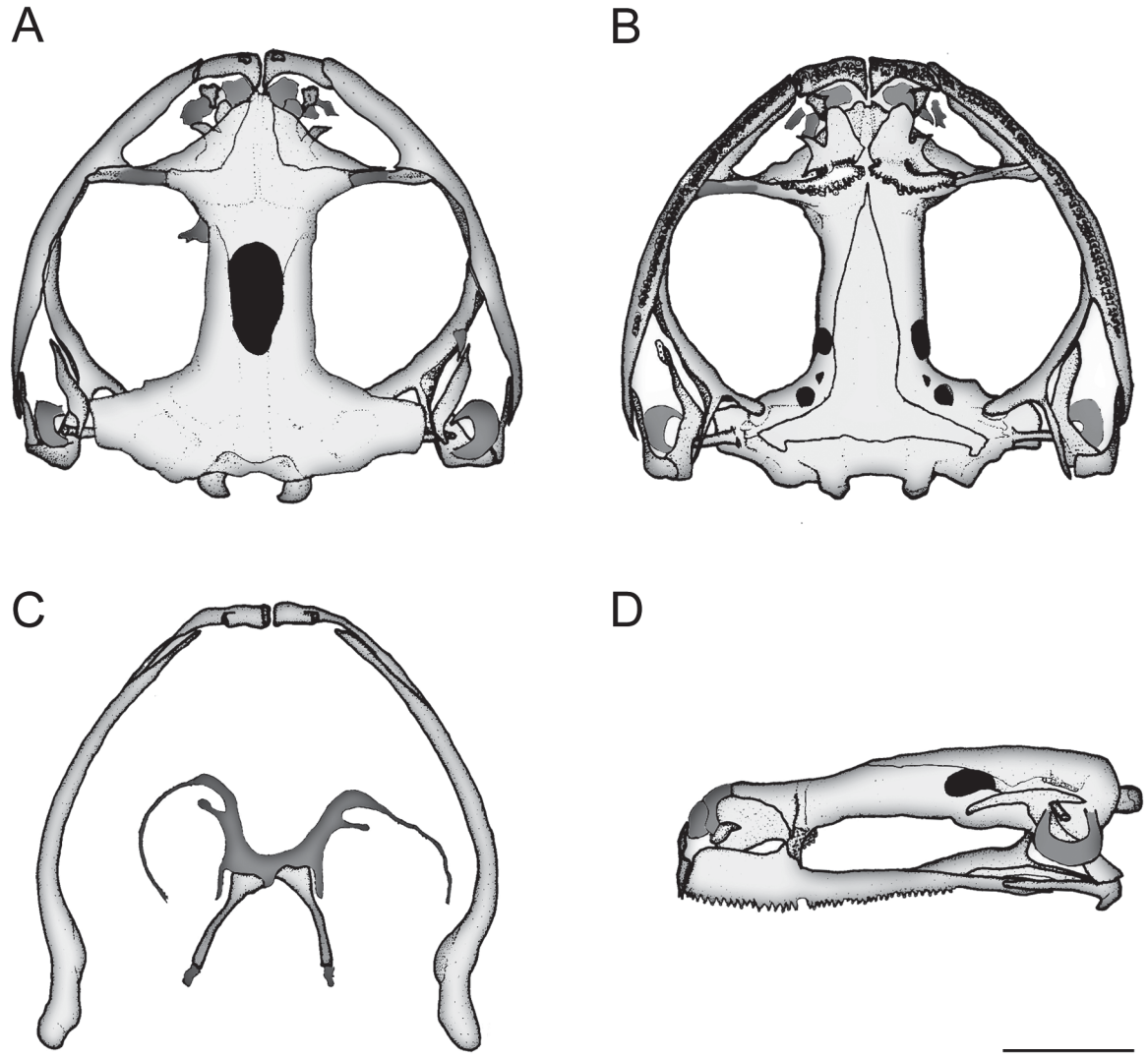

FIGURE 41.—Skull and hyobranchium of adult male *Hyloscirtus staufferorum* from Cordillera de los Guacamayos, Provincia de Napo (QCAZ 11146, SVL = 60.5 mm). (A) dorsal view, (B) ventral view, (C) ventral view of mandible and hyobranchium, and (D) lateral view. Cartilage is shown in dark gray. Scale = 0.5 cm. Drawings by Arturo Paredes-Recalde.

Pectoral girdle. (Figs. 30C, 32C, 34C, 36C, 38C, 40C, 42C). Each half of the pectoral girdle is composed by a suprascapula, scapula, and zonal area. Zonal elements are the clavicle, procoracoid, coracoid, and epicoracoid. Mineralization of the suprascapula varies from completely cartilaginous in *Hyloscirtus lindae* to completely mineralized in *H. criptico*, *H. pantostictus*, and *H. pacha*; intermediate stages are observed in *H. psarolaimus* and *H. staufferorum* that have cartilaginous margins. In *H. ptychodactylus* only the cleithrum is ossified. The suprascapula is fan-shaped; its internal margin is articulated with the external margin of the scapula. The cleithrum is well ossified and L-shaped (except in *H. lindae* where it is cartilaginous). The long arm of the cleithrum is located along the anterior margin of the suprascapula; the short arm is located along its medial border. There is no noticeable interspecific variation in the cleithrum.

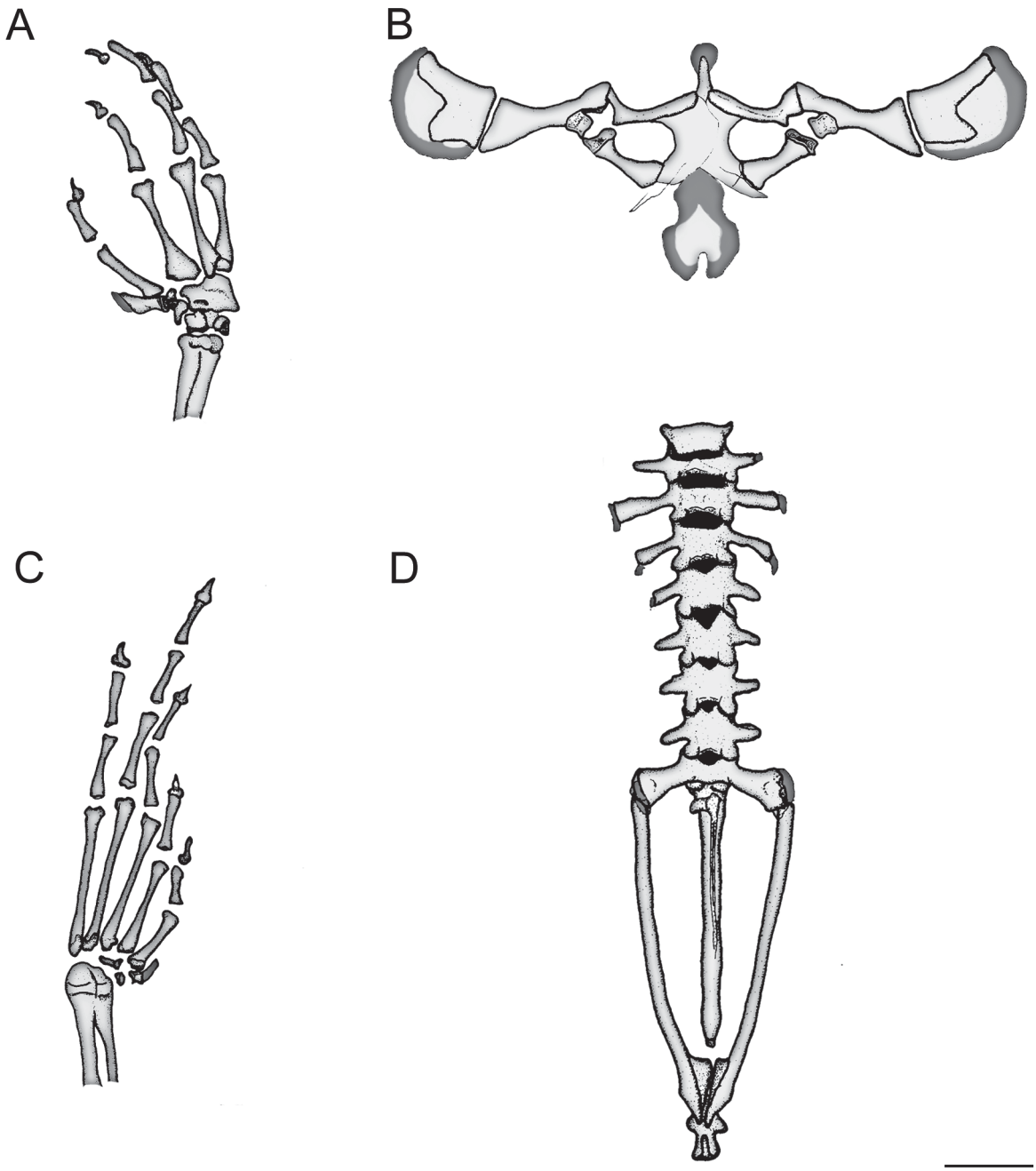

FIGURE 42.—Skeletal features of adult male *Hyloscirtus staufferorum* from Cordillera de los Guacamayos, Provincia de Napo (QCAZ 11146, SVL = 60.5 mm). (A) ventral view of manus, (B) ventral view of pes, (C) ventral view of pectoral girdle, and (D) dorsal view of vertebral column and pelvic girdle. Cartilage is shown in dark gray. Scale = 0.5 cm. Drawings by Arturo Paredes-Recalde.

The scapula is short and robust; its anteromedial end (pars acromialis) is in contact with the scapular margin of the clavicle and its posteromedial end (pars glenoidalis) is in contact with the external margin of the coracoid. There is no fusion of the scapula with the clavicle and the coracoid. The pars acromialis bears a square-shaped anterior end, whereas the pars glenoidalis has a square-shaped concave surface that forms the anterodorsal wall of the glenoid cavity. The pars acromialis is smaller than the pars glenoidalis. The prezonal element (= omosternum) is cartilaginous and has an expanded disc-shape with a short ramus in *Hyloscirtus criptico*; *H. staufferorum,* and *H. pacha* have the same shape but the ramus is ossified; in *H. lindae* and *H. pantostictus* the ramus is elongate and cartilaginous and the disc is circular; in *H. psarolaimus* and *H. ptychodactylus* the disc is oval, the ramus is elongated, and both are cartilaginous. The clavicle is oriented anteromedially; its distal end articulates with the pars acromialis of the scapula and the distal end of the coracoid. The anterior margins of the scapula and the clavicle are anteromedially oriented.

The pectoral girdle is arciferous (Griffiths 1959). The epicoracoid cartilages are mineralized at the midline, and their internal margins are cartilaginous. The right one overlaps the left one in *Hyloscirtus lindae*, *H. pacha*, *H. pantostictus*, *H. psarolaimus*, *H. ptychodactylus,* and *H. staufferorum*; whereas in *H. criptico* the overlap pattern is opposite. The only specimens with completely cartilaginous epicoracoids are *H. ptychodactylus* and one male of *H. lindae*. The epicoracoids are joined in its anteromediallly, forming the epicoracoid bridge. In all species the procoracoid cartilage is anteriorly located in relation to the medial end of the clavicles, also the limit between the procoracoid and the epicoracoid is easily distinguishable due to the marked mineralization of the latter. The medial margin of the pectoral fenestra is formed by the external margins of the epicoracoid.

The paired coracoid is a short bone oriented transversely; the medial margin is rounded, and its distal end is broad with a concavity that forms part of the glenoid cavity. The anterior margin of the coracoid forms the posterior margin of the pectoral fenestra.

The degree of mineralization of the sternum is variable: from completely cartilaginous in *Hyloscirtus ptychodactylus* and a male of *H. lindae,* to completely ossified in *H. criptico, H. pantostictus, H. psarolaimus, H. pacha, H. staufferorum,* and a female of *H. lindae*; it is composed of two regions, the mesosternum (anterior) and the xiphisternum (posterior).

Pelvic girdle. (Figs. 30D, 32D, 34D, 36D, 38D, 40D, 42D). The pelvic girdle is V-shaped in dorsal view; being composed of paired ilia, ischia, and pubes. The ilial shafts are cylindrical, lack crests, and have completely ossified tips anteriorly in *Hyloscirtus criptico*, *H. pantostictus,* and one male of *H. lindae*; in *H. psarolaimus, H. pacha, H. ptychodactylus, H. staufferorum,* and one female of *H. lindae* the anterior tips are cartilaginous. Each ilium extends anteriorly beneath the sacral diapophysis; the distal end of the ilium reaches the posterior outer margin of the sacral diapophysis. Posteriorly the ilia are united in a medial symphysis with the ischia and pubes. The pubis is ossified. The iliosacral articulation is Type IIB (*sensu* Emerson, 1979), and the sacral diapophyses are slightly expanded, rounded, and posterolaterally oriented. The ilium is attached to the sacral diapophysis by a transverse and thin ligament that inserts in its distal portion. There are no sesamoid bones at the anterior end of the ilium.

Vertebral column. (Figs. 30D, 32D, 34D, 36D, 38D, 40D, 42D). The vertebral column contains nine elements: the atlas complex is formed by the articulation of Presacrals I and II. There are six independent, trunk vertebrae (presacrals III to VIII), plus the sacrum and the coccyx. Vertebral centers are procoelus and the sacrum bears a bicondylar articulation with the coccyx. The holochordal centra are solid and cylindrical. The neural arches of Presacrals VI–VIII are slightly imbricate. There are no vertebral shields or ribs.

In the atlas complex, the two first presacrals are articulated, but not fused. Presacral II has one pair of transverse processes that are oriented anterolaterally, oblique to the midline. In Presacrals III–VIII there are transverse processes (parapophysis). The transverse processes of Presacral III are the longest; they are sub circular in cross-section, of equivalent width over their entire lengths. Only *Hyloscirtus lindae* has the terminal end of the transverse process regular and ossified. *Hyloscirtus criptico, H. ptychodactylus, H. princecharlesi* (on one side)*, H. staufferorum,* and one female of *H. pantostictus* have a small bony process in the anterior margin of Presacral VII. In all the examined skeletons the transverse processes of Presacral III are longer than the sacral diapophyses. Orientation of the transverse processes varies markedly. The processes of Presacral III are posteroventrally inclined in *H. criptico, H. lindae*, *H. psarolaimus, H. pantostictus,* and *H. ptychodactylus*; in *H. pacha* and *H. staufferorum* they are perpendicular to the long axis of the body. In all the species the transverse processes of Presacral IV are more inclined posteriorly. In the skeleton of *H. psarolaimus* there is a deformity in the number of vertebra and in the transverse processes of Presacrals III and IV. The transverse processes of Presacral V are parallel to the ones of Presacral IV. The processes of Presacral VI are parallel to the ones of Presacral V in *H. criptico, H. pacha, H. pantostictus, H. princecharlesi,* and *H. psarolaimus*, whereas in *H. lindae, H. ptychodactylus,* and *H. staufferorum* the transverse processes of Presacral VI are perpendicular to the long axis of the body. The transverse processes of Presacral VII are parallel to those of Presacral VI in *H. criptico*, *H. pacha,* and *H. psarolaimus*, whereas in *H. lindae, H. pantostictus, H. ptychodactylus,* and *H. staufferorum* the transverse processes of the Presacral VII are perpendicular to the long axis of the body. The transverse processes of Presacral VIII are nearly parallel to those of Presacral VII in *H. criptico*, *H. pacha, H. princecharlesi,* and *H. psarolaimus*, whereas in *H. lindae, H. pantostictus, H. ptychodactylus,* and *H. staufferorum* are perpendicular to the long axis of the body.

The anterior and posterior margins of the sacral diapophyses are nearly parallel to the transverse processes of Presacral VIII. The lateral margins of the transverse processes are completely ossified in *Hyloscirtus criptico, H. lindae, H. pantostictus,* and *H. psarolaimus*, whereas in *H. pacha, H. ptychodactylus,* and *H. staufferorum* they are cartilaginous. The sacrococcygeal bicondylar articulation is fused in *H. staufferorum, H. psarolaimus, H. lindae,*

and one male of *H. pantostictus*, whereas in *H. criptico, H. pacha, H. ptychodactylus,* and one female of *H. pantostictus* there is no fusion. The coccyx is elongate and sub cylindrical with a dorsal crest. The crest starts as a bony process on the anterodorsal region, and extends along the anterior three-fourths of its length. In lateral view the crest is uniform. There is little variation in process size among species, but in *H. pantostictus* it is more prominent than in the other species. *Hyloscirtus pantostictus, H. princecharlesi* (on one side), and *H. staufferorum* have one pair of short and thin lateral processes posterolaterally oriented at both sides of the process. The distal end of the coccyx is truncate and bears a cartilaginous process.

Forelimb. (Figs. 30A, 32A, 34A, 36A, 38A, 40A, 42A). The forelimb is composed of humerus, radioulna, carpal elements, four digits (II–V), and a prepollex. Cartilaginous intercalary elements are present between the phalanges. Torsion is absent in Digit II. The following carpal elements were observed: postaxial centrale (= radiale), ulnare, element Y, distal Carpal 2, and distal Carpal 3+4+5 fused into one bone. There are no evident sesamoid bones as part of the carpus. Terminal phalanges on the digits are claw-shaped. The phalangeal formula is 2-2-3-3. The prepollex bears two elements, one proximal and one distal. There is variation in degree of calcification of the prepollex; in *Hyloscirtus criptico* and one male of *H. lindae* is nearly completely calcified except for an external cartilaginous border; the rest of species and one female of *H. lindae* have a completely cartilaginous prepollex.

Hind limb. (Figs. 30B, 32B, 34B, 36B, 38B, 40B, 42B). The hind limb consists of a femur, tibiofibula, a reduced plantaris cartilage, tarsal elements, five metatarsals, five digits, and a prehallux. In all the skeletons the plantaris cartilage is small and appears as a triangular cartilaginous plate in ventral view. The tarsal elements include the tibiale (= calcaneum), fibulare (= astragalus), Tarsal 1, Tarsals 2+3 (fused), and centrale. There are no evident sesamoid or os sesamoid bones. The tibiale and the fibulare are separated medially, but are joined at their distal ends. Phalangeal formula of the pes is 2-2-3-4-3. The distal end of distal phalange of Toe I reaches the medial portion of proximal phalange of Toe II. There is variation in the degree of ossification of the prehallux; it is completely ossified in *Hyloscirtus criptico* and *H. lindae*, whereas in the rest of species ossification is incomplete. The prehallux is composed of one element (*H. lindae*) or two–three in the remaining species; the distal ones are smaller and have cartilaginous borders.

Calls

Hyloscirtus criptico. (Fig. 43D; Table 10). An individual of *H. criptico* (QCAZ 42149) was recorded at a stream nearby Cuellaje (2720 m, Provincia Imbabura) at 00:20h on 17 May 2009, at an air temperature of 13.4 ºC and 82% relative humidity, by Ítalo G. Tapia and Diego Almeida-Reinoso. Ten calls were analyzed. The call consists of an unpulsed single note of variable duration (181.0–200.0 ms). Calls were emitted at regular time intervals (766.0–991.0 ms) and clustered in bouts of variable number of calls (25.7 ± 6.1, range 19–31). A 4-min recording contained 3 bouts. These bouts had a duration of 19.6–30.3 s and a time interval of 42.6–111.6 s. The fundamental frequency coincides with the dominant frequency (1593.5–1636.5 Hz).

Hyloscirtus lindae. (Fig. 43A; Table 10). Two individuals of *H. lindae* (QCAZ 45346, MZUTI 707) were recorded. QCAZ 45346 was recorded at 11–12 km E of Papallacta (2600 m, Provincia de Napo) on 20 February 2010, by Juan F. Dueñas and Diego Almeida-Reinoso. The frog was located in a small stream within primary forest habitat. It was calling about 2 m from the ground, on a branch of *Chusquea* sp. The frog was calling nearby other calling males. MZUTI 707 was recorded at the Oyacachi-El Chaco trail (2500 m, Provincia de Napo) at 23:37h of 25 May 2012, at an air temperature of 11.5 ºC and 86% relative humidity, by Ítalo G. Tapia. The frog was located at the margin of a ravine. It was calling about 1.8 m from the ground; on a branch of *Chusquea* sp. Ten calls per specimen were analyzed. The call consists of a single periodic pulsed note. The call has variable duration (338.0–542.0 ms) and it is emitted at irregular time intervals (658.0–20860.0 ms). Number of pulses per call varied from 13.4 to 14.5. The fundamental frequency coincides with the dominant frequency (1464.3–1714.2 Hz).

Hyloscirtus pantostictus. (Fig. 43B; Table 10). An individual of *H. pantostictus* (QCAZ sc 31055) was recorded at Santa Bárbara (2800 m, Provincia Sucumbíos) at 00:59h of 29 September 2008, at an air temperature of 16 ºC, by Juan F. Dueñas and Ítalo G. Tapia. Ten calls were analyzed. Call consists of a short-pulsed note. The call has variable duration (336.0–433.0 ms) and it is emitted at irregular time intervals (8829.0–21215.0 ms). Number of pulses per call varied from 12 to 15. The fundamental frequency coincides with the dominant frequency (1550.4–1636.5 Hz).

Hyloscirtus psarolaimus. (Fig. 43C; Table 10). An individual of *H. psarolaimus* (QCAZ 46890) was recorded at a stream near the Río Mulatos (km 60, on the road between Salcedo and Tena, Provincia de Napo) at 20:00h of 17 November 2009, at an air temperature of 9.4 ºC, by Elicio E. Tapia. Calls were obtained from a specimen that was calling at the margin of a small waterfall, approximately 2.5 m from the ground on the dried branches of a thicket. Ten calls were analyzed. The call consists of a single periodic pulsed note of variable duration (166.0–203.0 ms) and it is emitted at irregular time intervals (1194.0–1585.0 ms). Number of pulses per call varied from 6 to 7. The fundamental frequency coincides with the dominant frequency (2304.1–2433.3 Hz).

Hyloscirtus pacha. (Fig. 43G; Table 10). Two individuals of *H. pacha* (one individual not collected, QCAZ 48237) were recorded at 8 km W Plan de Milagro (on road to Cuenca, 2152 m, Provincia Morona Santiago) on April 2010, by Elicio E. Tapia and Ronald Grefa. Five calling males were found along a transect of about 20 m in a creek with natural vegetation, which was close to a recently deforested zone and areas of pasture. The first male (no voucher) was recorded at 19:36h on 9 April 2010. It was calling close to another calling male at the margin of a ravine, on a branch at approximately 2 m from the ground. A second one (QCAZ 48237) was recorded at 22:15h on 12 April 2010. It was calling close to other calling males on a branch approximately 1 m from the ground at the margin of a small waterfall. Ten calls per specimen were analyzed. The call consists of an unpulsed single note of variable duration (154.0–188.0 ms). Calls were emitted at irregular time intervals (403.0–2485.0 ms), most of them clustered in bouts. A 2-min segment of a recording contained 4 bouts with a variable number of calls (6–9). These bouts lasted 5.7–8.0 s with time intervals of 4.5–37.4 s. The fundamental frequency coincides with the dominant frequency (1781.3–1902.8 Hz).

Hyloscirtus staufferorum. (Fig. 43E; Table 10). Three individuals of *H. staufferorum* (QCAZ 45962–63, and one individual not collected) were recorded nearby Santa Clara, at a stream at the headwaters of Río Challuwa Yacu in Reserva Comunitaria Ankaku (buffer zone of Llanganates National Park, Provincia de Pastaza) on 24 October 2009, by Elicio E. Tapia. Frogs began their calling at 18:10h along the stream, which was covered by dense vegetation. They were calling from mossy branches in between fallen branches. The cascading stream had an inclination of about 60 percent. The first specimen (QCAZ 45962) was recorded at 18:58h at an air temperature of 12 ºC. It was calling from a position close to five other calling males from a bush containing mosses and epiphytes ~2 m from the ground. The second individual (no voucher specimen collected) was recorded at 19:05h, as it was calling at the margin of a creek, on a branch at approximately 1.5 m above the ground. The third one (QCAZ 45963) was recorded at 19:43h and at an air temperature of 18.8 ºC. It was calling at the margin of a creek approximately 2 m from the ground and from a position close to other calling males. A playback was used in order to obtain these recordings. Ten calls per specimen were analyzed. The call consists of a single unpulsed note of variable duration (133.0–225.0 ms). Calls were emitted at irregular time intervals (482.0–621.0 ms) and clustered in bouts. A 2-min segment of a recording contained three bouts with a variable number of calls (21.0–57.0). These bouts lasted 15.1–39.6 s with time intervals of 5.4–11.0 s. The fundamental frequency coincides with the dominant frequency (1412.4–2012.0 Hz).

Comparisons: The call reported by Duellman and Coloma (1993) differs from the ones described herein in that note duration is shorter (about 75 ms) in the former, and the number of calls in each bout is smaller (9.7, range 4–17), the bout length is shorter (7.5 s, 3–13 s). Differences in physical parameters might be due to either geographic variation or a different ethological contexts (e.g., territorial class vs. advertisement calls). The differences found among calls require further analyses with more extensive sampling.

Hyloscirtus tapichalaca. (Fig. 43F; Table 10). An individual of *H. tapichalaca* (QCAZ 46887) was recorded at Reserva Tapichalaca (1637 m, Provincia Zamora Chinchipe) at 01:48h on 29 September 2009, at an air temperature of 10 ºC, by Elicio E. Tapia. The area was primary forest, on a steep slope of about 60% inclination, with abundant *Chusquea* sp., epiphytes and mosses. The collection site was at about five meters from the paved road, and there were at least three calling males in an area of about ten square meters. The frog was calling on a branch at the margin of a creek with a cascading stream of about 3 m width. The headwaters of the stream were located at about 400 m upslope the collecting site. Ten calls were analyzed. The call consists of a single unpulsed single note of variable duration (142.0–193.0 ms). Calls were emitted at irregular time intervals (680.0–1187.0 ms), most of them clustered in bouts. A 2-min segment of a recording contained 12 bouts with a variable number of calls (2.0–11.0). These bouts lasted 1.6–12.2 s with time intervals of 1.8–6.9 s. The fundamental frequency (732.1–904.4 Hz) does not coincide with the dominant frequency (1421.2–1507.3 Hz).

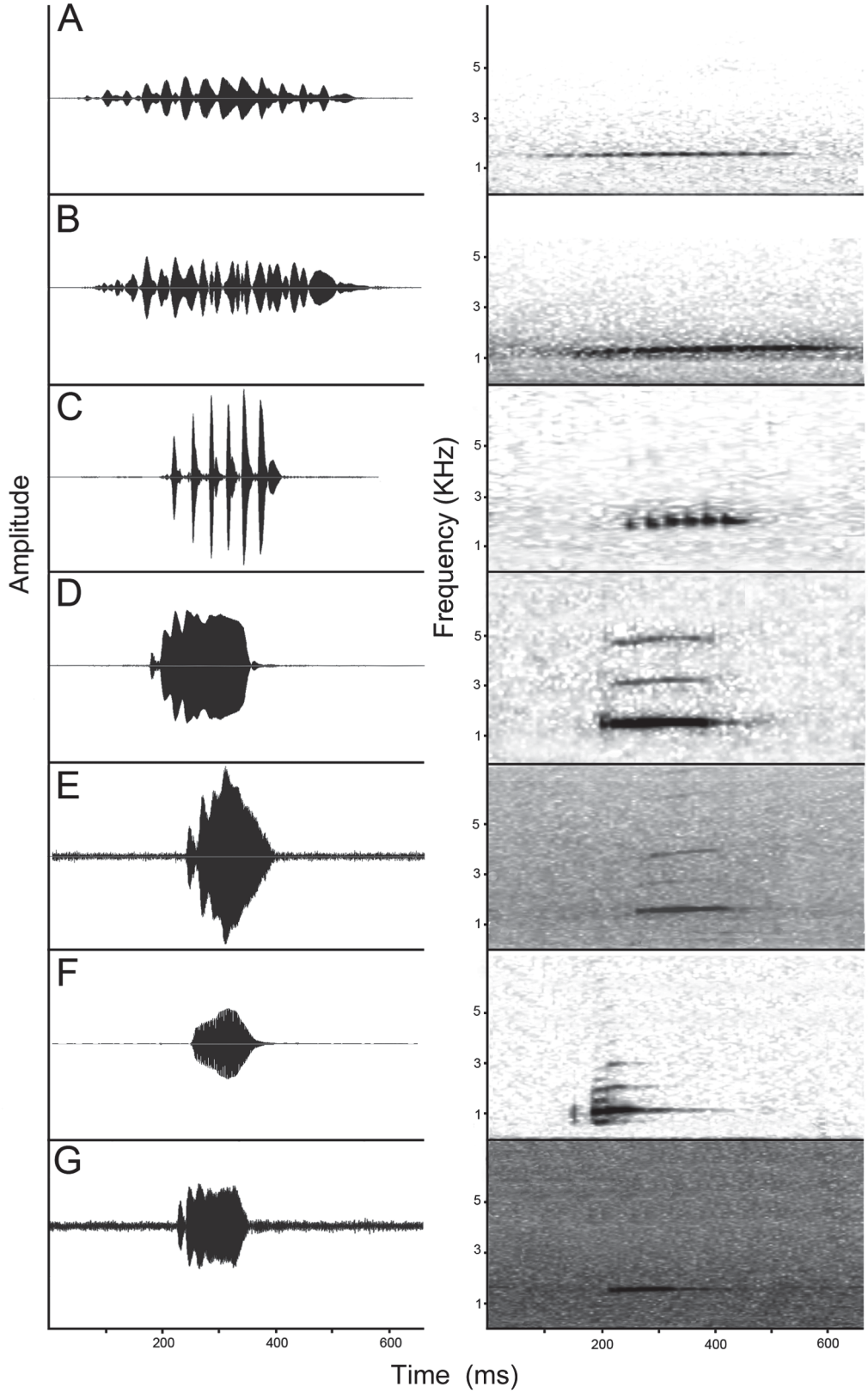

FIGURE 43.—Advertisement calls of species of the *Hyloscirtus larinopygion* group. Oscillograms (left) and spectrograms (right) of (A) *H. lindae,* QCAZ 45346, (B) *H. pantostictus*, QCAZ (sc 31055), (C) *H. psarolaimus,* QCAZ 46890, (D) *H. criptico,* QCAZ 42149, (E) *H. staufferorum,* QCAZ 45962, (F) *H. tapichalaca,* QCAZ 46887, and (G) *H. pacha* (no voucher). Time is given in miliseconds at the x-axis.

Comparisons: The call reported by Kizirian *et al.* (2003) is similar to the one described herein. Their statement that a recording of 31.5 seconds contained 565 notes is an error and refers to a recording of 31.5 minutes. A difference is that Kizirian *et al.* (2003) failed to distinguish the fundamental frequency (see their Figure 3) due to background noise. Dominant frequency is slightly lower (1378 Hz) in Kizirian *et al.* (2003).

TABLE 10. Descriptive statistics for call parameters of *Hyloscirtus criptico, H. lindae, H. pacha*, *H. pantostictus, H. psarolaimus, H. staufferorum,* and *H. tapichalaca* and Mean ± SD is given with range below. Sample sizes (n) and number of calls per individual are indicated. Temporal characters are given in miliseconds; spectral characters in Hertz.

	Hyloscirtus criptico	*Hyloscirtus lindae*		*Hyloscirtus pacha*	
	n = 1 10 calls/individual	n = 2 10 calls/individual		n = 2 10 calls/individual	
Pulses/call	1.0 –	14.6 ± 1.4 12.0–16.0	13.4 ± 1.35 11.0–15.0	1.0 –	1.0 –
Call length	188.5 ± 5.6 181.0–200.0	491.6 ± 41.0 417.0–542.0	397.8 ± 32.9 338.0–441.0	170.4 ± 11.1 154.0–188.0	184.7 ± 22.8 137.0–208.0
Calls/minute	31.0 –	36.0 –	6.0 –	13.0 –	33.0 –
Interval between calls	827.6 ± 70.2 766.0–991.0	1331.8 ± 669.2 658.0–2226.0	945.2 ± 8340.8 978.0–20860.0	1475.9 ± 578.4 792.0–2485.0	500.6–98.35 403.0–718.0
Rise time	78.2 ± 13.4 54.0–96.0	173.1 ± 49.8 118.0–257.0	187.9 ± 27.5 145.0–225.0	79.9 ± 32.4 28.0–121.0	58.3 ± 20.2 23.0–80.0
Call shape	414.5 ± 67.1 284.2–480.0	354.7 ± 106.8 257.2–507.9	475.0 ± 76.9 347.7–572.6	467.3 ± 181.7 155.6–30.6	315.8 ± 111.3 167.9–487.7
Fundamental frequency	1608.6 ± 14.5 1593.5–1636.5	1659.0 ± 22.4 1632.2–1714.2	1472.9 ± 27.2 1464.3–1550.4	1866.8 ± 30.6 1815.6–1902.8	1842.0 ± 30.9 1781.3–1886.7
Dominant Frequency	1608.6 ± 14.51 1593.5–1636.5	1659.0 ± 22.4 1632.2–1714.2	1472.9 ± 27.2 1464.3–1550.4	1866.8 ± 30.6 1815.6–1902.8	1842.0 ± 30.9 1781.3–1886.7

TABLE 10. Continued.

	Hyloscirtus pantostictus	*Hyloscirtus psarolaimus*	*Hyloscirtus staufferorum*		
	n = 1 10 calls/individual	n = 1 10 calls/individual	n = 3 10 calls/individual		
Pulses/call	14.3 ± 0.9 12.0–15.0	6.5 ± 0.5 6.0–7.0	1.0 –	1.0 –	1.0 –
Call length	394.6 ± 34.7 336.0–433.0	185.2 ± 14.6 166.0–203.0	195.8 ± 18.7 166.0–225.0	187.8 ± 31.2 144.0–224.0	154.5 ± 10.7 133.0–165.0
Calls/minute	3.5 ± 0.5 3.0–4.0	18.0 –	81.0 –	67.0 –	76.0 –
Interval between calls	16399.6 ± 4812.4 8829.0–21215.0	1370.5 ± 156.0 1194.0–1585.0	528.4 ± 13.3 510.0–549.0	555.8 ± 60.0 480.0–641.0	541.4 ± 47.5 482.0–621.0
Rise time	193.5 ± 4 0.8 139.0–265.0	122.3 ± 22.2 68.0–152.0	56.1 ± 10.1 47.0–80.0	26.3 ± 6.4 16.0–42.0	55.7 ± 7.2 45.0–68.0
Call shape	495.0 ± 118.4 343.2–719.30	664.3 ± 125.3 343.4–775.5	289.9 ± 63.5 208.9–396.0	145.8 ± 17.0 72.4–247.1	360.9 ± 43.2 314.5–433.1
Fundamental frequency	1569.5 ± 38.0 1550.4–1636.5	2402.0± 41.3 2304.1–2433.3	1960.3 ± 29.5 1893.1–1997.4	1438.6 ± 46.30 1412.4–1465.1	1954.2 ± 27.8 1923.6–2012.0
Dominant Frequency	1569.5 ± 38.0 1550.4–1636.5	2401.9 ± 41.3 2304.1–2433.3	1960.3 ± 29.5 1893.1–1997.4	1438.6 ± 46.30 1412.4–1465.1	1954.2 ± 27.8 1923.6–2012.0

TABLE 10. Continued.

	Hyloscirtus tapichalaca n = 1 10 calls/individual
Pulses/call	1.0 –
Call length	159.1 ± 16.3 142.0–193.0
Calls/minute	36.0 –
Interval between calls	833.8 ± 144.2 680.0–1187.0
Rise time	49.8 ± 7.8 38.0–60.0
Call shape	208.9 ± 17.0 185.0–236.0
Fundamental frequency	792.4 ± 46.3 732.1–904.4
Dominant Frequency	1468.6 ± 24.4 1421.2–1507.3

Discussion

Systematics

Relationships among the three *Hyloscirtus* species groups (*H. bogotensis, H. larinopygion,* and *H. armatus*) are congruent with most previous hypotheses (Duellman *et al.* 1997, Faivovich *et al.* 2005; Wiens *et al.* 2010) based on morphological and/or molecular data, but it is incongruent with groups (A and B) proposed by Sánchez (2010) based on larval morphological features. The *H. bogotensis* group, initially proposed by Duellman (1970), has high support, but the molecular analyses presented herein only includes four (out of 16) species. Therefore, fully testing its monophyly will require an expanded data set. According to Paredes-Recalde (1999) and Kizirian *et al.* (2003), the *H. larinopygion* group could not be diagnosed exclusive of the *H. armata* group, but Faivovich *et al.* (2005) and Wiens *et al.* (2010) found support for the recognition of both groups. The sister relationship of the two species currently included in the *H. armatus* clade is well supported by Wiens *et al.* (2010) and in our analyses. Although the monophyly of the *H. larinopygion* group and its position as sister taxon of the *H. armatus* group are well supported under MP criteria, they have low support in the Bayesian majority-rule consensus tree. Also the *H. larinopygion* and *H. armatus* groups are not sister taxa in our ML analyses. Thus, further testing is desirable including more species and loci of the *H. bogotensis* group. However, these same relationships among the groups (*H. armatus* as sister taxa of *H. larinopygion*) are strongly supported in ML analyses of mitochondrial and nuclear data by Wiens *et al.* (2010). The incongruence between our hypothesis and Groups A and B of *Hyloscirtus* proposed by Sánchez (2010) stems from his allocation of *H. pantostictus* in Group B (mislabeled as Group A in his Table 1), which was based on the number of upper and lower tooth rows (4/6) provided in the description of tadpoles given by Duellman and Hillis (1990). In our description of larvae of *H. pantostictus* LTRF varied from 4(4)/5(1) to 6(4–6)/7(1); also it has one simple triangular fleshy projection on the inner margin of naris, the anterior jaw sheath is narrow and has small serrations (Fig. 15). Therefore, given these revised data, this species actually fits well with Group A of Sánchez. Thus, if *H. pantostictus* is moved to Group A, the incongruence between our findings and those of Sánchez disappears. Therefore, species in Group A correspond with *Hyloscirtus,* whereas placement of species of Group B within *Hyloscirtus* needs further analyses because none of them have been included in other molecular phylogenetic analyses of *Hyloscirtus*. Species of Group B might belong to a derived subclade within the *H. bogotensis* group (defined by the larval features described by Sánchez) or they might belong to a clade outside of *Hyloscirtus.*

The only unambiguous morphological synapomorphy for *Hyloscirtus*, proposed by Sánchez (2010), is the bag over the vent tube that covers developing hindlimbs in larvae. This synapomorphy is present in all species studied, and up to date no observation of the same structure has been found on other hylids. Other morphological characters that currently are putative synapomorphies of *Hyloscirtus* and the three ingroup clades need to be re-evaluated. Their character states require further analysis. For example, given our phylogenetic hypothesis (Fig. 3), the presence of a shelf on the larval upper jaw, which was hypothesized as a synapomorphy of the *H. armatus* group (Duellman *et al.* 1997), could be a synapomorphy of *Hyloscirtus* group. Similarly, the hypertrophied forearms, hypothesized to be a synapomorphy of the *H. armatus* group (Duellman *et al.* 1997), are also present in *H. tapichalaca* and might be either a convergent or a shared derived feature from their common ancestor.

The *Hyloscirtus larinopygion* group was found to be composed of *H. tapichalaca* plus two major, well-supported clades: Clade A, consisting of *H. larinopygion, H. lindae,* and *H. pantostictus*; and Clade B, consisting of *H. criptico, H. pacha, H. princecharlesi, H. psarolaimus, H. ptychodactylus, H. staufferorum,* and *H. tigrinus*. Their phylogenetic relationships are congruent under the different phylogenetic inference criteria. Nonetheless, the position of *H. larinopygion* in Clade A under the MP analyses requires further testing, adding more characters and species. The problematical assignment of *H. tapichalaca* to a species clade in Hylidae (Kizirian *et al.* 2003, Faivovich *et al.* 2004) was resolved by Faivovich *et al.* (2005) and Wiens *et al.* (2010), whom showed strong support for placing this species inside the *H. larinopygion* group. Thus, some of the conflicting morphological features (e.g., phenetic similarity in several features with members of the *Hypsiboas pulchellus* group) can be interpreted as homoplasy.

The phylogenetic relationships of the *Hyloscirtus larinopygion* group, depicted in our analyses (Fig. 3), are considerably different from those of Duellman and Hillis (1990) (based on allozymes) and of Paredes-Recalde (1999) (based on osteology and external morphology). The incongruence can be explained by the low number of sampled taxa in the first case and by the paucity of character data in both. The tree of Wiens *et al.* (2010) is also different, because it shows strong support for placing *H. tapichalaca* as the sister species of *H. lindae* This may be due to more limited sampling of taxa or greater sampling of characters in that study. Phenetic similarity in color patterns and distribution of *Hyloscirtus sarampiona* (from the western versant of Cordillera Occidental of the Andes of Colombia) may suggest a close relationship to *H. princecharlesi* whereas *H. caucanus* (from the eastern versant of the Cordillera Central of the Andes in Colombia) may be closely related to *H. pantostictus* or *H. lindae* (note: neither *H. sarampiona* nor *H. caucanus* were included in our or previous molecular analyses). Nonetheless, these speculations need to be confirmed by pending, combined analyses of molecular and morphological data, with the inclusion of *H. caucanus*, *H. sarampiona,* and species yet to be discovered.

The discovery of additional new species in the *Hyloscirtus larinopygion* group is to be expected, especially in the Andes of Colombia, where further collecting and taxonomic work is needed. Collecting species in this group may require intense search efforts in appropriate habitats throughout the year. Raising tadpoles and DNA analyses of their tissues is critical when adults are not found. Otherwise their diversity at any given sites may be understimated. For example, after extensive field work by experienced herpetologists for more than two decades at the Santa Bárbara site, adults of only a single species were collected. However, the collection of tadpoles has now revealed the existence of four species at this site (this study).

Color patterns revealed by our description of ontogenetic changes may prove useful in assessing phylogenetic relationships; in addition, some of them may represent synapomorphies for certain clades. For example, the unique dental formula of *Hyloscirtus lindae* and *H. pantostictus* may be a share-derived feature of both. The bright green-yellow colors of frogs after metamorphosis is a unique feature of a least three species (*H. princecharlesi, H ptychodactylus,* and *H. tigrinus*) in Clade B. It could also be interesting to trace the evolution of these characters on a molecular phylogeny.

The calls described herein (Fig. 43) and by previous authors show interesting features that differ among species. For example, some species have pulsed calls (*Hyloscirtus lindae, H. pantostictus, H. psarolaimus*), whereas in others the calls are unpulsed (*H. criptico, H. staufferorum, H. tapichalaca*, *H. pacha*). Also, the call of *H. tapichalaca* is very distinctive from the other species, as the dominant frequency does not coincide with the fundamental frequency. The calls of sister species (*H. pacha* and *H. staufferorum*; *H. lindae* and *H. pantostictus*) show remarkable similarity in temporal and frequency characteristics. Additionally, the calls of sympatric sister species (*H. pantostictus* and *H. lindae*) have very similar calls, contrary to expectations of reinforcement of call differentiation, which would occur under a prezygotic reproductive mechanisms of isolation (Gerhardt and Huber

2002). However, our call recordings of both species were not at the same site. Therefore, it is possible that the differences in calls may be greater in sympatry, and this should be addressed in future studies. The distribution of these features in the phylogeny needs to be mapped and included in future analyses of behavioral evolution. Another interesting feature of most *Hyloscirtus* calls is that they can be heard from long distances (e.g., the call of *H. staufferorum* was heard from ~500 m from the calling site; Elicio E. Tapia pers. obs. October 2009). Call amplitude has not been measured or described for any of these species, and its variation deserves further attention in future acoustical studies.

Genetic distances and speciation

Diversity and speciation in Andean frogs is a subject of active research (Guayasamin *et al.* 2008, Santos *et al.* 2009, Páez-Vacas *et al.* 2010, Guayasamin *et al.* 2010, Páez *et al.* 2011) and these studies are revealing interesting patterns that are also supported by our results from *Hyloscirtus*. Levels of molecular diversity are not necessarily linked to genetic differentiation and morphologically cryptic species are being commonly revealed in many taxa by either large genetic distances or by the non-monophyly of populations previously considered a single one species (Páez-Vacas *et al.* 2010, Guayasamin *et al.* 2010). In contrast, species that are well differentiated morphologically sometimes have low genetic divergence, at least in mitochondrial genes (Guayasamin *et al.* 2010). The latter is the case for several sister taxa of the *Hyloscirtus larinopygion* group, in which we found relatively low genetic distances. Divergence of 3% in the mitochondrial 16S rRNA gene has been suggested as an operable threshold for the consideration of lineages as possible species, to be confirmed by an integrative approach (Fouquet *et al.* 2007, Vieites *et al.* 2009). Nonetheless, recent studies of mitochondrial genome divergence among described species can be lower than the 3%-threshold (e.g. Schick *et al.* 2010, Zimkus and Schick 2010, Lötters *et al.* 2011, Guayasamin *et al.* 2010, Páez-Moscoso *et al.* 2011). Our study fits the pattern emerging from these studies. For example, genetic divergence between sympatric sister species *H. pantostictus* and *H. lindae* is 1.5% (both of them occur at Santa Bárbara, Provincia de Sucumbíos). Genetic divergence is 1.8% between the sister species *H. pacha* and *H. staufferorum,* which occur at different latitudes in the eastern Andean Cordillera. Genetic divergence is 1.3% between the sister species *H. princecharlesi* and *H. ptychodactylus* from the western Andean Cordillera (which occur at different latitudes and are separated by 167 km airline; Fig. 9). In contrast, genetic divergence within species ranges from 0.9% between populations of *Hyloscirtus lindae* from the eastern Andean Cordillera (at different latitudes, separated by 122 km airline; Fig. 9), to 0.4% between populations of *H. psarolaimus* from the eastern Andean Cordillera (at different latitudes, separated by 189 km airline; Fig. 9), to 0.2% between populations of *H. criptico* from the western Andean Cordillera (at different latitudes, separated by 71 km airline; Fig. 9).

Regarding modes of speciation (see Lynch and Duellman 1997), the structure of our phylogeny and the geographic distribution of sister taxa suggests a mostly allopatric speciation pattern, probably facilitated by the uplift of the Andes and its linearity. The Andes is a long mountain range fragmented by several transverse valleys, and these valleys are thought to promote allopatric divergence by limiting contact among otherwise contiguous populations (Graves 1988). Allopatric speciation, promoted by the linearity of the Andes, may have caused the splits between *Hyloscirtus ptychodactylus* and *H. princecharlesi*, and also the split between *H. pacha* and *H. staufferorum*. The uplift of the Andes that separated taxa at the western versant of Cordillera Occidental and eastern versant of Cordillera Oriental is the most likely mechanism for the speciation event that separated *H. criptico* from the clade formed by *H. pacha* and *H. staufferorum*, as well as the split between *H. larinopygion* from the *H. lindae* + *H. pantostictus* clade. In contrast, a sympatric mode of speciation might explain the overlapping distribution of the sympatric *H. lindae* and *H. pantostictus.* However, these species may have speciated allopatrically and later came into secondary contact.

Timing of species origin

Molecular clock calibrations and dating are a matter of debate and results should be interpreted with caution. Parham *et al.* (2012) alert that the lack of rigorous protocols for assigning calibrations based on fossils raises serious questions about the credibility of these age estimates. Consequently, an explicit justification of both

phylogenetic and chronological age assessments is necessary for all fossils used for calibration. Faivovich *et al.* (2005) reviewed the scant hylid fossil information and the problems associated with it. Smith *et al.* (2005) and Wiens *et al.* (2011) provided information on fossils used to calibrate hylid phylogenies.

Our chronogram is a rough approximation of divergence time frames. Nonetheless, the estimation of the age for *Hyloscirtus* goes back to the Eocene and coincides with results of Wiens *et al.* (2011), whom estimated the age of *Hyloscirtu*s in 64.0 MYA. Our estimation of the most recent ancestor of *Hyloscirtus* is at minimum 52.2 MYA (based on fossil calibration), and 61 MYA (using *Pseudacris* substitution rate). The most recent ancestor of the *H. larinopygion* group originated during the Middle-Late Eocene (at minimum 40.9 MYA). Then, a decline of diversification occurred for a period of about 21 MYA, and our results might suggest a rapid radiation of *Hyloscirtus* starting in the Miocene into the Pliocene, from at least 14.2 MYA to the most recent divergence between sister taxa occurred at least 2.6 MYA. However, explicit tests for rapid diversification are needed to compare this Pliocene-Miocene *Hyloscirtus* radiation to other hylid clades. Between 8.5 and 13 MYA, the two major lineages of the *H. larinopygion* group appeared. Similar patterns of complex and explosive radiation since the Miocene have been found in dendrobatid frogs (Santos *et al.* 2009).

According to our dating of most recent speciation events in the *Hyloscirtus larinopygion* group, the hypothesis of speciation being promoted by alternate compression and expansion of cloud forest during the Quaternary (Duellman, 1982) is not supported. Speciation among these frogs occurred mostly prior (~2.6–51.2 MYA) to the Quaternary glacial periods (~2.6 MYA to date). Dating of the most recent speciation events for other Andean clades, such as *Gastrotheca* (Wiens 2011), for which hypotheses of radiation associated to Quaternary events have been proposed (see references in Duellman 1999, Faivovich *et al.* 2005) suggests that these speciation events were also mostly prior to the Quaternary. Nonetheless, the climatic Quaternary events and Holocene habitat fragmentation (caused by humans) may have played an important role in current population differentiation.

Acknowledgments

Specimens of new species and tissues of species of the *Hyloscirtus larinopygion* group used in this study are the result of fieldwork that was supported from personal funds of authors and mostly by grants from: Secretaría Nacional de Ciencia y Tecnología del Ecuador issued to Pontificia Universidad Católica del Ecuador (Luis A. Coloma, P. I., in 2008–2010; throughout the project "Inventario y caracterización genética y morfológica de la diversidad de anfibios, reptiles y aves de los Andes del Ecuador", PIC-08-0000470), Wikiri SA to Centro Jambatu (in 2011–2012), and the Saint Louis Zoo to Centro Jambatu (Luis A. Coloma, P. I., in 2011–2012; throughout the project "Providing sustainability to the Jambatu Center and ex situ conservation program of amphibians in risk of extinction"). Fieldwork at Reserva Las Gralarias was partially supported by Centro para la Investigación de la Biodiversidad y Cambio Climático (BioCamb) of the Universidad Tecnológica Indoamérica and SOS-IUCN program. Fieldwork along the Oyacachi-Chaco trail was supported by a Dimensions of Biodiversity grant from the National Science Foundation (DEB-1046408). Juan M. Guayasamin and Carl Hutter thank Reserva Las Gralarias (www.reservalasgralarias.com) and Las Gralarias Foundation (www. lasgralarias-foundation.org) for providing lodging and accommodation; they also thank Henry Imba and Timothy Kell for help in the field. We thank Taran Grant and Mauricio Rivera for making available specimens loaned from QCAZ, and William E. Duellman for a loan of specimens deposited at the Museum of Natural History of the University of Kansas. We thank María Eugenia Ordóñez and Charles Barnes, whom did DNA extraction and amplification as part of the SENACYT project. We are indebted to many field companions, who also provided assistance and logistic support during field trips (they are indicated in the collection data of specimens). We are greatly indebted to Ítalo G. Tapia, who enthusiastically helped on tadpole photography, recordings of calls, collection of specimens, and in curatorial matters. Pablo A. Menéndez-Guerrero helped with geographic calculations and the distribution map. Centro Jambatu researchers are especially indebted to Jeff Bonner, Eric Miller, and Mark Wanner (of Saint Louis Zoo), Giovanni Onore (of Fundación Otonga,), María Dolores Guarderas (of Wikiri S.A), and Kevin Zippel, and Ron Gagliardo (of Amphibian Ark) for their commitment and sustained support to CJ research and conservation program of Ecuadorian amphibians. Kevin Zippel, Ron Gagliardo, and Madeleine Groves (of Royal Botanic Gardens) generously invested efforts in getting permission from HRH Charles (Prince of Wales) to use his name in the etymology of one of the new species. Research, collection and rearing tadpoles were done under permits of the

Ecuadorian Ministerio de Ambiente: FAU-001-DNB/VS, 008-09-IC-FAU-DNB/MA, 2009-011-FAU-DPAP-MA (issued to PUCE), 09-2011-FAU-DPAP-MA, 003-11 IC-FAU-DNB/MA (issued to Centro Jambatu), and 14-2011-IC-FAU-DPAP-MA and 56-IC-FAU/FLO-DPN/MA (issued to Universidad Tecnológica Indoamérica). We are also grateful to John J. Wiens, William E. Duellman, Joseph Mendelson III, and an anonymous reviewer, whom graciously reviewed this manuscript and provided helpful suggestions for its improvement. We thank the Chief editor of Zootaxa (Zhi-Qiang Zhang) for supporting the open access of this paper and for providing gratuitous reprints. This article is part of the systematics component of the program for research of native amphibians of the Centro Jambatu´s strategic plan for the conservation of the Ecuadorian amphibians in risk of extinction.

References

Altig, R. & Johnston, G.F. (1989) Guilds of anuran larvae: relationships among developmental modes, morphologies, and habitats. *Herpetological Monographs,* 81–109.

Altig, R. & McDiarmid, R.W. (1999) Body Plan: development and morphology. *In:* R.W. McDiarmid & R. Altig (Eds.), *Tadpoles.* The University of Chicago Press, Chicago, E.U.A., pp. 295–335.

Ardila-Robayo, M.C., Ruiz-Carranza P.M. & Roa-Trujillo, S.H. (1993) Una nueva especie de *Hyla* del grupo *larinopygion* (Amphibia: Anura: Hylidae) del sur de la Cordillera Central de Colombia. *Revista de la Academia Colombiana de Ciencias Exactas, Físicas y Naturales,* 18, 71, 559–566.

Ayarzagüena, J. & Señaris J.C. (1994 "1993") Dos nuevas especies de *Hyla* (Anura; Hylidae) para las Cumbres Tepuyanas del Estado Amazonas, Venezuela. *Memoria. Sociedad de Ciencias Naturales La Salle. Caracas,* 53, 127–146.

Barnet, SL., Cover, Jr., J, &Wright, K.M. (2001) Chapter 5. Amphibian husbandry and housing. *In:* Wright, K.M. & Whitaker, B.R. (Eds.), *Amphibian medicine and captive husbandry.* Krieger Publishing Company, Malabar, Florida, USA, pp. 35–61.

Brandley, M.C, Schmitz, A. & Reeder, T. (2005) Partitioned Bayesian analyses, partition choice, and the phylogenetic relationships of scincid lizards. *Systematic Biology*, 54(3), 373–390.

Bolívar W., Coloma, L.A., Ron, S., & Renjifo, J.M. (2004) *Hyloscirtus larinopygion.* In: IUCN 2011. IUCN Red List of Threatened Species. Version 2011.2. Available from http://www.iucnredlist.org (accessed 13 April 2012)

Boulenger, G.A. (1902) Descriptions of new batrachians and reptiles from the Andes of Peru and Bolivia. *Annals and Magazine of Natural History,* 7, 10, 394–402.

Boulenger, G.A. (1908) Descriptions of new batrachians and reptiles discoverd by Mr. M.G. Palmer in south-western Colombia. *Annals and Magazine of Natural History,* 8, 2, 515–522.

Bustamante, M.R., Ron, S.R. & Coloma, L.A. (2005) Cambios en la diversidad en siete comunidades de anuros en los Andes de Ecuador. *Biotropica,* 37, 180–189.

Castillo-Trenn, P. (2004) Description of the tadpole of *Colostethus kingsburyi* (Anura: Dendrobatidae) from Ecuador. *Journal of Herpetology,* 38, 600–606.

Charif, R.A., Clark, C.W. & Fristrup, K.M. (2004) *Raven 1.2. User's Manual.* Cornell Laboratory of Ornithology, Ithaca, New York, 191 pp.

Cochran, D.M., & Goin, C.J. (1970) Frogs of Colombia. *Bulletin of the United States National Museum,* 288, 1–655.

Coloma, L.A., Lötters, S., Duellman, W.E. & Miranda-Leiva, A. (2007) A taxonomic revision of *Atelopus pachydermus*, and description of two new (extinct?) species of *Atelopus* from Ecuador (Anura : Bufonidae). *Zootaxa,* 1557, 1–32.

Coloma, L. A., Duellman, W. E., Almendáriz, A., Ron, S., Terán-Valdez, A. & Guayasamin, J. M. (2010) Five new (extinct?) species of *Atelopus* (Anura: Bufonidae) from Andean Colombia, Ecuador, and Peru. *Zootaxa,* 2574, 1–54.

Darst, C.R. & Cannatella, D.C. (2004) Novel relationships among hyloid frogs inferred from 12S and 16S mitochondrial DNA sequences. *Molecular Phylogenetics and Evolution,* 31 (2), 462–475.

Dingerkus, G. & Uhler, L.D. (1977) Enzyme clearing of alcian blue stained whole small vertebrates for demonstration of cartilage. *Stain Technology,* 52, 229–232.

Drummond, A.J. & Rambaut, A. (2007) BEAST: Bayesian evolutionary analysis by sampling trees. *BMC Evolutionary Biology,* 7, 214.

Duellman, W.E. (1970) Hylid frogs of Middle America. *Monographs of the Museum of Natural History, University of Kansas,* 1–2, 1–753.

Duellman, W.E. (1972) A review of the neotropical frogs of the *Hyla bogotensis* group. *Occasional Papers of the Museum of Natural History, University of Kansas,* 11, 1–31.

Duellman, W.E. (1973) Descriptions of new hylid frogs from Colombia and Ecuador. *Herpetologica,* 29, 3, 219–227.

Duellman, W.E. (1979) The herpetofauna of the Andes: Patterns of distribution, origins, differentiation, and present communities. *In:* W.E. Duellman (Ed.), *The South American herpetofauna: Its origin, evolution, and dispersal.* Monographs of the Museum of Natural History, The University of Kansas, Lawrence, pp. 371–459.

Duellman, W.E. (1981) Three new species of centrolenid frogs from the Pacific versant of Ecuador and Colombia. *Occasional Papers of the Museum of Natural History, University of Kansas,* 88, 1–9.

Duellman, W.E. (1982) Compresión climática cuaternaria en los Andes. Efectos sobre la especiación. *Actas VIII Congreso*

Latinoamericano de Zoología, Mérida, Tomo I, 177–201.
Duellman, W.E. (1999) Distribution patterns of amphibians in South America. *In:* W.E. Duellman (Ed.), *Patterns of distribution of amphibians. A global perspective:* Baltimore: The Johns Hopkins University Press, pp. 255–328.
Duellman, W.E. & Altig, R. (1978) New species of tree frogs (family Hylidae) from the Andes of Colombia and Ecuador. *Herpetologica,* 34, 177–185.
Duellman, W.E. & Berger, T.J. (1982) A new species of Andean treefrog (Hylidae). *Herpetologica,* 38, 456–460.
Duellman, W.E. & Burrowes, P.A. (1989) New species of frogs, *Centrolenella,* from the Pacific versant of Ecuador and southern Colombia. *Occasional Papers of the Museum of Natural History, University of Kansas,* 132, 1–14.
Duellman, W.E. & Coloma, L.A. (1993) *Hyla staufferorum,* a new species of treefrog in the *Hyla larinopygion* group from the cloud forests of Ecuador. *Occasional Papers of the Museum of Natural History, The University of Kansas,* 161, 1–11.
Duellman, W.E. & Hillis, D.M. (1990) Systematics of frogs of the *Hyla larinopygion* group. *Occasional Papers of the Museum of Natural History, The University of Kansas,* 134, 1–23.
Duellman, W.E. & Trueb, L. (1986) *Biology of Amphibians.* New York: McGraw-Hill, 670 pp.
Duellman, W.E., De la Riva, I. & Wild, E.R. (1997) Frogs of the *Hyla armata* and *Hyla pulchella* groups in the Andes of South America, with definitions and analyses of phylogenetic relationships of Andean groups of *Hyla*. *Scientific Papers of the Natural History Museum, The University of Kansas,* 3, 1–41.
Dunn, E.R. (1931) New frogs from Panama and Costa Rica. *Occasional Papers of the Boston Society of Natural History,* 5, 385–401.
Elmer, K.R. & Cannatella, D.C. (2008) Three new species of leaflitter frogs from the upper Amazon forests: cryptic diversity within *Pristimantis "ockendeni"* (Anura: Strabomantidae) in Ecuador. *Zootaxa,* 1784, 11−38.
Emerson, S.B. (1979) The ilio-sacral articulation in frogs: form and function. *Biological Journal of the Linnean Society,* 11, 153–168.
Fabrezi, M. & Alberch, P. (1996) The carpal elements of anurans. *Herpetologica,* 52, 188–204.
Faivovich, J., Garcia, P.C., Ananias, F., Lanari, L., Basso, N.G. & Wheeler, W.C. (2004) A molecular perspective on the phylogeny of the *Hyla pulchella* species group (Anura, Hylidae). *Molecular Phylogenetics and Evolution,* 32, 938–950.
Faivovich, J., Haddad, C.F.B, García P.C.A., Frost, D.R. & Campbell, J.A. (2005) Systematic review of the frog family Hylidae, with special reference to Hylinae: phylogenetic analysis and taxonomic revision. *Bulletin of the American Museum of Natural History,* 294, 1–240.
Fouquet, A., Gilles, A., Vences, M., Marty, C, Blanc, M. & Gemmell, N.J. (2007) Underestimation of species richness in Neotropical frogs revealed by mtDNA analyses. *PLoS ONE 2,* e1109.
Frost, D.R. (2011) Amphibian Species of the World: an Online Reference. Version 5.5 (31 January, 2011). Available from http://research.amnh.org/vz/herpetology/amphibia/ American Museum of Natural History, New York, USA. American Museum of Natural History, New York, USA (accessed 1 June 2012)
Funk, C.W., Caminer, M. & Ron, S. (2011) High levels of cryptic species diversity uncovered in Amazonian frogs. *Proceedings of the Royal Society,* doi:10.1098/rspb.2011.1653.
Gerhardt, H.C. & Huber, F. (2002) *Acoustic communication in insects and anurans.* Chicago: The University of Chicago Press, 531 pp.
Goebel, A.M., Donnelly, J.M. & Atz, M.E. (1999) PCR primers and amplification methods for 12s ribosomal DNA, the control region, cytochrome oxidase I, and cytochrome b in bufonids and other frogs, and an overview of PCR primers which have amplified DNA in amphibians successfully. *Molecular Phylogenetics and Evolution,* 11, 163–199.
Goin, C.J. (1961) Three new centrolenid frogs from Ecuador. *Zoologischer Anzeiger,* 166, 95–104.
Gosner, K.L. (1960) A simplified table for staging anuran embryos and larvae with notes on identification. *Herpetologica,* 16, 183–190.
Graves, G.R. (1988) Linearity of geographic range and its possible effect on the population structure of Andean birds. *Auk,* 105, 47–52.
Griffiths, I. (1959) The phylogenetic status of the Sooglossinae. *Annals and Magazine of Natural History,* 13, ii, 626–640.
Guayasamin, J.M., Castroviejo-Fisher, S., Ayarzagüena, J., Trueb, L. & Vilà, C. (2008) Phylogenetic relationships of glassfrogs (Centrolenidae) based on mitochondrial and nuclear genes. Molecular Phylogenetics and Evolution, 48, 574–595.
Guayasamin, J.M., Bonaccorso, E., Duellman, W.E. & Coloma, L.A. (2010) Genetic differentiation in the nearly extinct harlequin toads (Bufonidae: *Atelopus*), with emphasis on the *Atelopus ignescens* and *A. bomolochos* species complexes. *Zootaxa,* 55–68.
Guindon, S. & Gascuel, O. (2003) A simple, fast, and accurate algorithm to estimate large phylogenies by maximum likelihood. *Systematic Biology,* 52, 696–704.
Hijmans, R.J., Cameron, S.E., Parra, J.L., Jones, P.G. & Jarvis, A. (2005) Very high resolution interpolated climate surfaces for global land areas. *International Journal of Climatology,* 25, 1965–1978.
Huelsenbeck, J.P. & Ronquist, F. (2001) MRBAYES: Bayesian inference of phylogeny. *Bioinformatics,* 17, 754–755.
Hutter, C.R. & Guayasamin, J.M. (2012) A new cryptic species of glassfrog (Centrolenidae: *Nymphargus*) from Reserva Las Gralarias, Ecuador. *Zootaxa,* 3257, 1–21.
Iturralde-Vinent, M.A. & MacPhee, R. (1999) Paleogeography of the Caribbean region: implications for Cenozoic biogeography. *Bulletin of the American Museum of Natural History,* 238, 1–95.
IUCN. (2001) Red list categories: version 3.1. Gland UICN Species Survival Comission.

Jarrín-V, P. & Kunz, T.H. (2008) Taxonomic history of the genus *Anoura* (Chiroptera: Phyllostomidae) with insights into the challenges of morphological species delimitation. *Acta Chiropterologica,* 10, 257–269.

Kass R.E., & Raftery, A.E. (1995) Bayes factors. *Journal of the American Statistical Association,* 90, 773–795.

Kizirian, D., Coloma, L.A. & Paredes-Recalde, A. (2003) A new treefrog (Hylidae: *Hyla*) from southern Ecuador and a description of its antipredator behavior. *Herpetologica,* 59, 339–349.

La Marca, E., Lips, K.R., Lötters, S., Puschendorf, R., Ibáñez, R., Rueda-Almonacid, J.V., Schulte, R., Marty, C., Castro, F., Manzanilla-Puppo, J., García-Pérez, J.E., Bolaños, F., Chaves, G., Pounds, J.A., Toral, E. & Young, B.E. (2005) Catastrophic population declines and extinctions in Neotropical harlequin frogs (Bufonidae: *Atelopus*). *Biotropica,* 37, 190–201.

Larkin, M.A., Blackshields, G., Brown, N.P., Chenna, R., McGettigan, P.A., McWilliam, H., Valentin, F., Wallace, I.M., Wilm, A., Lopez, R., Thompson, J.D., Gibson, T.J. & Higgins, D.G. (2007) Clustal W and Clustal X version 2.0. *Bioinformatics,* 23, 2947–2948.

Lemmon, E.M., Lemmon, A.R. & Cannatella D.C. (2007) Geological and climatic forces driving speciation in the continentally distributed trilling chorus frogs (*Pseudacris*). *Evolution,* 61, 2086–2103.

Leviton, A.E., Gibbs, Jr., R.H., Heal, E. & Dawson, C.E. (1985) Standars in herpetology and ichtyology: Part 1. Standard symbolic codes for institutional resource collections in Herpetology and Ichthyology. *Copeia,* 1985, 802–832.

Littlejohn, M.J. (2001) Patterns of differentiation in temporal properties of acoustic signals of anurans. *In:* Ryan, M. J. (Ed.) *Anuran Communication.* Smithsonian Institution Press, Washington, DC, USA. Pp. 102–120.

Lötters, S., Reichle, S., Faivovich, J. & Bain R.H. (2005) The stream-dwelling tadpole of *Hyloscirtus charazani* (Anura: Hylidae) from Andean Bolivia. *Studies on Neotropical Fauna and Environment,* 40, 181–185.

Lötters, S., van der Meijden, A., Coloma, L.A., Boistel, R., Cloetens, P., Ernst, R., Lehr, E. & Veith, M. (2011) Assessing the molecular phylogeny of a near extinct group of vertebrates: the Neotropical harlequin frogs (Bufonidae; *Atelopus*). *Systematics and Biodiversity,* 9, 45–57.

Lynch, J.D. & Duellman, W.E. (1997) Frogs of the genus *Eleutherodactylus* in western Ecuador. *University of Kansas Natural History Museum, Special Publication,* 23, 1–236.

Luo, A., Qiao, H., Zhang, Y., Shi, W., Ho, S., Xu, W., Zhang, A. & Zhu, C. (2010) Performance of criteria for selecting evolutionary models in phylogenetics: a comprehensive study based on simulated datasets. *BMC Evolutionary Biology,* 10, 242.

Maddison, W.P. & Maddison, D.R. (2010) Mesquite: a modular system for evolutionary analysis. Version 2.73. Available at http://mesquiteproject.org.

Melin, D.E. (1941) Contributions to the knowledge of the Amphibia of South America. *Göteborgs Kungl. Vetenskaps-och Vitterhets-samhälles. Handlingar. Serien B, Matematiska och Naturvetenskapliga Skrifter,* 1, 1–71.

Merino-Viteri, A. (2001) Análisis de posibles causas de las disminuciones de poblaciones de anfibios en los Andes del Ecuador. Tesis de Licenciatura. Pontificia Universidad Católica del Ecuador, Quito, Ecuador, 66 pp.

Merino-Viteri, A., Coloma, L.A. & Almendáriz, A. (2005) Los *Telmatobius* (Leptodactylidae) de los Andes del Ecuador y su declive poblacional. *In* Lavilla, E.O. & De la Riva, I. (Eds.), *Estudios sobre las ranas andinas de los géneros* Telmatobius *y* Batrachophrynus *(Anura: Leptodactylidae).* Asociación Herpetológica Española, Monografías de Herpetología 7, Valencia, España, pp. 9–37.

Montezuma, M.F. & Mueses-Cisneros, J.J. (2009) Notes on geographic distribution. Amphibia, Anura, Hylidae, *Hyloscirtus tigrinus:* Distribution extension, first department record, Cauca and Huila, Colombia. *Check List,* 5, 2, 243–245.

Mueses-Cisneros, J.J. & Anganoy-Criollo M.A. (2008) Una nueva especie del *grupo Hyloscirtus larinopygion* (Amphibia: Anura: Hylidae) del Suroccidente de Colombia. *Papéis Avulsos de Zoología,* 48, 15, 129–138.

Mueses-Cisneros, J.J. & Perdomo-Castillo, I.V. (2011) *Hyloscirtus tigrinus* Mueses-Cisneros y Anganoy-Criollo, 2008: una especie amenazada, con comentarios sobre su distribución geográfica e historia natural. *Herpetotropicos,* 5, 2, 93–103.

Myers, C.W. & Duellman, W.E. (1982) A new species of *Hyla* from Cerro Colorado, and other tree frog records and geographical notes from western Panama. *American Museum Novitates,* 2752, 1–32.

Padial, J.M., Miralles, A., De la Riva, I. & Vences, M. (2010) The integrative future of taxonomy. *Frontiers in Zoology*, 2010, 7, 16.

Páez-Moscoso, D.J., Guayasamin, J.M. & Yánez-Muñoz, M.H. (2011) A new species of Andean toad (Bufonidae, *Osornophryne*) discovered using molecular and morphological data, with a taxonomic key for the genus. *Zookeys,* 108, 73–97.

Páez-Vacas, M., Coloma, L.A. & Santos, J.C. (2010) Systematics of the *Hyloxalus bocagei* complex (Anura: Dendrobatidae), description of two new cryptic species, and recognition of *H. maculosus*. *Zootaxa,* 2711, 1–75.

Paredes-Recalde, A. (1999) Osteología y relaciones filogenéticas del grupo *Hyla larinopygion* (Anura, Hylidae). Tesis de Licenciatura, Pontificia Universidad Católica del Ecuador, Quito, Ecuador, 146 pp.

Parham, J.F., Donoghue, P.C.J., Bell, C.J., Calway, T.D., Head, J.J., Holroyd, P.A., Inoue, J.G., Irmis, R.B., Joyce, W.G., Ksepka, D.T., Patané, J.S.L., Smith, N.D., Tarver, J.E., van Tuinen, M., Yang, Z., Angielczyk, K.D., Greenwood, J.M., Hipsley, C.A., Jacobs, L., Makovicky, P.J., Müller, J., Smith, K.T., Theodor, J.M., Warnock, R.C.M., & Benton, M.J. (2012) Best practices for justifying fossil calibrations. *Systematic Biology,* 61, 346–359.

Peters, W.C.H. (1882) Den namen der Batrachiergattung *Hylonomus* in *Hyloscirtus* zu ändern und legte zwei neue Arten von Schlangen, *Microsoma notatum,* und *Liophis ygraecum*. *Sitzungsberichte der Gesellschaft naturforschender Freunde zu*

Berlin, 1882, 127–129.
Posada, D. (2008) jModelTest: phylogenetic model averaging. *Molecular Biology and Evolution,* 25, 1253–1256.
Pounds, J.A., Bustamante, M.R., Coloma, L.A., Consuegra, J.A., Fogden, M.P., Foster, P.N., La Marca, E., Masters, K.L., Merino-Viteri, A., Puschendorf, R., Ron, S.R., Sánchez-Azofeifa, G.A., Still, C.J. & Young, B.E. (2006) Widespread amphibian extinctions from epidemic disease driven by global warming. *Nature,* 439, 161–7.
Quiguango, M.A. (1997) Diversidad y abundancia relativa de la herepetofauna en San Venancio (Cuellaje), zona de amortiguamiento de la Reserva Ecológica Cotacachi-Cayapas, Imbabura, Ecuador. *In:* Mena, P.A., Soldi, A., Alarcón, R., Chiriboga C., & Suárez, L. (eds.) *Estudios Biológicos para la Conservación. Diversidad, Ecología y Etnobiología.* Ecociencia, Quito, pp. 195–209.
Ronquist, F. & Huelsenbeck, J.P. (2003) MRBAYES 3: Bayesian phylogenetic inference under mixed models. *Bioinformatics,* 19, 1572–1574.
Ruiz-Carranza, P.M. & Lynch, J.D. (1982) Dos nuevas especies de *Hyla* (Amphibia: Anura) de Colombia, con aportes al conocimiento de *Hyla bogotensis. Caldasia,*13, 647–671.
Sánchez, D.A. (2010) Larval development and synapomorphies for species groups of *Hyloscirtus. Copeia,* 2010, 351–363.
Santos, J.C., Coloma, L.A., Summers, K., Caldwell, J.P., Ree, R. & Cannatella, D.C. (2009) Amazonian amphibian diversity is primarily derived from Late Miocene Andean lineages. *PLOS Biology,* 7, 1–14.
Sambrook, J., Fritsch, E.F. & Maniatis, T. (1989) *Molecular Cloning: A Laboratory Manual, second ed.* Cold Spring Harbor Laboratory Press, Cold Spring Harbor, New York, USA. 3v., ill.
Savage, J.M. & Heyer, W.R. (1967) Variation and distribution of the tree-frog genus *Phyllomedusa* in Costa Rica, Central America. *Beitrage zur Neotropischen Fauna,* 5, 111–131.
Schick, S., Zimkus, B.M., Channing, A., Köhler, J. & Lötters, S. (2010) Systematics of 'Little Brown Frogs' from East Africa: recognition of *Phrynobatrachus scheffleri* and description of a new species from the Kakamega Forest, Kenya (Amphibia: Phrynobatrachidae). *Salamandra*, 46, 24–36.
Smith, S.A., Stephens, P.R. & Wiens J.J. (2005) Replicate patterns of species richness, historical biogeography, and phylogeny in Holarctic treefrogs. *Evolution,* 59, 2433–2450.
Swofford, D.L. (2009). Phylogenetic Analysis Using Parsimony (*and other methods) ver. 4.0a109. Sinauer Associates, Sunderland, Massachusetts.
Toral, E., Feinsinger, P. & Crump, M.L. (2002) Frogs and a cloud-forest edge in Ecuador. *Conservation Biology,* 16, 735–743.
Trueb, L. (1993) Patterns of cranial diversity among Lissamphibia. *In:* J. Hanken & B. K. Hall (Eds.), *The Skull. Patterns of Structural and Systematic Diversity.* The University of Chicago Press, Chicago, pp. 255–343.
Valencia, R., Cerón, C., Palacios, W. & Sierra, R. (1999) Las formaciones naturales de la Sierra del Ecuador. *In:* R. Sierra (Ed.), *Propuesta preliminar de un sistema de clasificación de vegetación para el Ecuador continental.* Proyecto INEFAN/GEF-BIRF y Ecociencia, Quito, pp. 79–108.
Vieites, D.R., Wollenberg, K.C., Andreone, F., Köhler, J., Glaw, F. & Vences, M. (2009) Vast underestimation of Madagascar's biodiversity evidenced by an integrative amphibian inventory. *Proceedings of the National Academy of Sciences USA*, 106, 8267–8272.
Wiens, J.J. (2007) Species delimitation: new approaches for discovering diversity. *Systematic Biology,* 56, 875–878.
Wiens, J.J. (2011) Re-evolution of lost mandibular teeth in frogs after more than 200 million years, and re-evaluating dollo's law. *Evolution,* 65, 1283–1296.
Wiens, J.J., Fetzner, J.W., Parkinson, C.L., & Reeder T.W. (2005) Hylid frog phylogeny and sampling strategies for speciose clades. *Systematic Biology,* 54, 719–748.
Wiens, J.J., Graham, C. H., Moen, D. S., Smith, S.A. & Reeder, T.W. (2006) Evolutionary and ecological causes of the latitudinal diversity gradient in hylid frogs: treefrog trees unearth the roots of high tropical diversity. *American Naturalist,* 168, 579–596.
Wiens, J.J., Kuczynski, C.A., Hua, X. & Moen, D.S. (2010) An expanded phylogeny of treefrogs (Hylidae) based on nuclear and mitochondrial sequence data. *Molecular Phylogenetics and Evolution,* 55, 871–882.
Wiens, J.J., Pyron R.A. & Moen, D.S. (2011) Phylogenetic origins of local-scale diversity patterns and the causes of Amazonian megadiversity. *Ecology Letters,* 14, 643–652.
Yánez-Muñoz, M.H. & Meza-Ramos, P. (2006) Generando información para conservar a *Colostethus delatorreae* (Anura: Dendrobatidae): una especie de rana nodriza críticamente amenazada en los Andes ecuatorianos. *Boletín Especies Amenazadas UICN,* 6, 1–3.
Zimkus, B.M. & Schick, S. (2010) Light at the end of the tunnel: Insights into the molecular systematics of East African puddle frogs (Anura: Phrynobatrachidae). *Systematics and Biodiversity,* 8, 39–47.
Zwickle, D.J. (2006) Genetic algorithm approaches for the phylogenetic analysis of large biological sequence datasets under the maximum likelihood criterion. Ph.D. dissertation, University of Texas, Austin, TX.